

Identification and Characterization of Proteins interacting with metabotropic Glutamate Receptor subtype 8

Dissertation

zur Erlangung des Doktorgrades
der Naturwissenschaften

vorgelegt beim Fachbereich
Biochemie, Chemie und Pharmazie
der Johann Wolfgang Goethe-Universität
in Frankfurt am Main

von

Zhongshu Tang

aus Anhui (China)

Frankfurt 2005

Die vorliegende Arbeit wurde in der Abteilung Neurochemie am Max-Planck Institut für Hirnforschung in Frankfurt am Main unter Anleitung von Prof. Heinrich Betz durchgeführt und vom Fachbereich Biochemie, Chemie und Pharmazie der Johann Wolfgang Goethe-Universität in Frankfurt am Main als Dissertation angenommen.

Dekan: Prof. Harald Schwalbe
Gutachter: Prof. Ernst Bamberg
Prof. Heinrich Betz

Datum der Disputation:

Identifikation und Charakterisierung intrazellulärer Interaktionspartner des metabotropen Glutamatrezeptors mGluR8

Zusammenfassung

Glutamat ist einer der wichtigsten exzitatorischen Neurotransmitter im Gehirn. Glutamatrezeptoren werden in zwei verschiedene Klassen unterteilt: ionotrope (iGluRs) und metabotrope Glutamatrezeptoren (mGluRs). Die iGluRs bilden einen Ionenkanal und sind postsynaptisch lokalisiert. Dagegen zählen mGluRs zur Familie der G-Protein gekoppelten Rezeptoren (GPCRs) und sind sowohl post- als auch präsynaptisch zu finden. mGluRs spielen eine Rolle bei der Regulation der Transmitterfreisetzung, der Kurz- und Langzeit-Modulation von synaptischer Transmission, der neuronalen Entwicklung und der synaptischen Plastizität. Mittlerweile sind acht verschiedene mGluR-Isoformen in Säugerzellen identifiziert worden, die in drei Gruppen eingeteilt werden. Gruppe I Rezeptoren (mGluR1 und 5) sind hauptsächlich postsynaptisch lokalisiert und aktivieren die Phospholipase C. Gruppe II (mGluR2 und 3) und Gruppe III (mGluR4, 6, 7 und 8) Rezeptoren sind hauptsächlich präsynaptisch zu finden und inhibieren die Adenylat-Zyklase.

Es existieren drei mGluR8-Isoformen (a, b und c), wobei sich mGluR8a von mGluR8b nur in den letzten 16 Aminosäuren unterscheidet. Bei mGluR8c scheint es sich um eine sekretierte Isoform zu handeln, die nur aus der N-terminalen Region des gesamten Proteins besteht. Obwohl bereits pharmakologische Studien an mGluR8 durchgeführt wurden und auch eine mGluR8-“Knockout“-Maus generiert wurde, ist nur wenig über die Funktion dieses Rezeptors bekannt. Deshalb wurden in der vorliegenden Arbeit “Hefe-Zwei-Hybrid“-Untersuchungen mittels des “DupLexA yeast two-hybrid“-Systems durchgeführt. Dabei dienten die C-terminale Domänen (CTDs) von mGluR8a und mGluR8b als “Köder” zum Durchsuchen einer adaptierten Rattenhirn-cDNA-Bibliothek, die verschiedene offene Leseraster beinhaltet. In Hefezellen, in denen es zu einer Interaktion zwischen “Köder”- und einem der “Beute”-Proteine kommt, wird die Expression von speziellen Reportergenen (Leu und LacZ) aktiviert und somit eine Selektion der positiven Klone ermöglicht. Es wurden für mGluR8a 6×10^8 Hefezellen und für mGluR8b $8,4 \times 10^4$ Hefezellen analysiert, wovon 1385 bzw. 934 Klone Leucin-auxotroph waren und LacZ exprimierten. Mittels

DNA-Sequenzierung konnten ca. 30 Proteine als potenzielle Interaktionspartner identifiziert werden, die in drei Klassen eingeteilt wurden. Die erste Gruppe beinhaltet Sumoylierungsproteine. Bei der Sumoylierung wird das SUMO-Protein (Small ubiquitin related modifier) kovalent an einen Lysinrest des Substrates gebunden. Für den Sumoylierungsprozess sind drei Enzyme notwendig: das aktivierende Enzym E1, das konjugierende Enzym E2 und die Ligase E3. Durch die „Hefe-zwei-Hybrid“-Analyse wurden fünf Proteine identifiziert, die mit der Sumoylierung in Verbindung stehen: Pias1, Piasx β und ube2a, die während der Untersuchungen als häufigste Interaktionspartner auftraten, und SUMO-1 und Piasy, die nur als Interaktoren für mGluR8b identifiziert wurden. Bei SUMO-1 handelt es sich um E1-, bei ube2 um E2- und bei Pias1, Piasx β und Piasy um E3-Enzyme. Die zweite Klasse der potenziellen Interaktionspartner umfasst apoptotische Proteine: Hipk3 und Fas-related Protein. Alle zusätzlich identifizierten Kandidaten sind in Gruppe 3 zusammengefasst. In der vorliegenden Arbeit wurde die Interaktion mit Sumoylierungs-Proteinen näher analysiert.

Um Interaktionen zwischen den identifizierten Proteinen und mGluR8 zu bestätigen, wurde ein Hefe-Paarungs-Experiment durchgeführt. Hierzu wurden haploide RFY206 Zellen (MATa), die das „Köder“-Protein exprimierten, wurden mit haploiden EGY48 Zellen (MAT α), die das „Beute“-und ein Reporterprotein koexprimierten, verwendet. Kultiviert man solche Hefezelltypen entgegengesetzten „Matingtyps“ miteinander, so können sie miteinander fusionieren und dadurch eine diploide Zelle bilden. Da in diesem experimentellen Ansatz alle Zellen, die die fünf Sumoylierungsproteine exprimierten, Leucin-auxotroph waren und LacZ-Expression aufwiesen, wurden diese Proteine als Interaktionspartner sowohl für mGluR8a als auch für mGluR8b eingestuft (siehe Tabelle 7). Mittels dieses Ansatzes konnten Piasy und SUMO-1, die mit der „Hefe-Zwei-Hybrid“-Untersuchung nur als potenzielle Interaktoren des C-Terminus von mGluR8b identifiziert worden waren, auch als mögliche Bindungspartner des C-Terminus von mGluR8a nachgewiesen werden.

Um die Ergebnisse der „Hefe-Zwei-Hybrid“-Analyse zu bestätigen, wurden GST(Glutathion-S-Transferase)-Pull-down-Experimente angewandt. Dazu wurden GST-Fusionsproteine des C-Terminus von mGluR8a (GST-mGluR8a-C) und des C-Terminus von mGluR8b (GST-mGluR8b-C) in *E. coli* exprimiert und anschließend an einer Glutathion-Sepharose-Matrix, an die GST spezifisch bindet, immobilisiert. Die

potenziellen Interaktionspartner ube2, Pias1 und Piasy wurden dagegen als MBP(myelin basic protein)-Fusionsproteine in Bakterien exprimiert. Nachdem die Interaktoren mit den immobilisierten GST-C-Termini inkubiert worden waren, wurde die Sepharose-Matrix gewaschen, um nichtgebundene Moleküle zu entfernen, und anschließend mit SDS-Probenpuffer versetzt, um die gebundenen Proteine zu eluieren. Danach wurden die erhaltenen Proben mittels SDS-PAGE aufgetrennt und schließlich durch ein Western-Blotting analysiert, wobei ein Antikörper, der spezifisch MBP erkennt, verwendet wurde. Die Ergebnisse zeigten, dass MBP-Pias1 mit GST-mGluR8b-C und, in vergleichsweise geringerem Maße, mit GST-mGluR8a-C aufgereinigt werden konnte. Eine deutlich schwächere Interaktion konnte zwischen dem MBP-Fusionsprotein des C-Terminus von Piasy und den beiden C-Termini der mGluR8-Isoformen detektiert werden. Dagegen konnte für MBP-ube2a keine Bindung an die beiden C-Termini gezeigt werden. Als Negativkontrolle wurde immobilisiertes GST mit MBP und auch mit den MBP-Fusionsproteinen inkubiert, wobei in allen Fällen keine Interaktion festgestellt werden konnte.

Zusätzlich wurden die potenziellen Interaktionspartner (Pias1, ube2a und SUMO-1) als GFP („green fluorescent protein“)-, YFP („yellow fluorescent protein“)- und CFP („cyan fluorescent protein“)-Fusionsproteine in Säugerzellen (HEK 293) exprimiert. Diese wurden anschließend ebenfalls in einem GST-Pulldown-Experiment mit immobilisiertem GST-mGluR8a-C bzw. GST-mGluR8b-C inkubiert. Dabei konnte die starke Interaktion zwischen GST-mGluR8a-C und Pias1 bestätigt werden, wogegen nur eine sehr schwache Bindung von ube2a und SUMO1 an die GST-Fusionsproteine detektiert werden konnte. Diese Ergebnisse zeigen, dass von den untersuchten möglichen Interaktoren Pias1 die stärkste Bindung an mGluR8 aufweist.

Im Anschluss an diese Untersuchungen wurde überprüft, ob Pias1 auch an weitere präsynaptisch lokalisierte mGluRs der Gruppen II und III binden kann, oder ob diese Interaktion spezifisch für mGluR8 ist. Hierzu wurden binäre „Hefe-Zwei-Hybrid“-Analysen durchgeführt. Die so erhaltenen Daten weisen darauf hin, dass zwar auch eine Affinität für andere Gruppe III mGluRs besteht, die Interaktion mit mGluR8 jedoch deutlich stärker ist. Dagegen konnte keine Bindung von Pias1 an die Gruppe II mGluRs mGluR2-C und mGluR3-C aufgezeigt werden. Zur Bestätigung dieser Daten erfolgten anschließend GST-Pulldown-Analysen mit GFP-Pias, das in Säugerzellen exprimiert worden war, und den GST-Fusionsproteinen der C-Termini der bereits

genannten mGluRs. Als Negativkontrollen wurden immobilisiertes GST mit GFP-Pias1 bzw. GFP mit GST-mGluR7a-C inkubiert, wobei keine Interaktionen erhalten wurden. In diesen Pulldown-Experimenten konnte für alle Gruppe III mGluRs eine Bindung an Pias1 nachgewiesen werden. Aus diesen Ergebnissen lässt sich schließen, dass alle C-Termini der Gruppe III mGluRs mit Pias1 interagieren können.

Um die Domänen von mGluR7a-C und mGluR8a-C, die mit Pias1 interagieren, zu identifizieren, wurden je zwei Fragmente der C-terminalen Domänen der beiden Rezeptoren als GST-Fusionsproteine exprimiert und in einem GST-Pulldown-Experiment mit CFP-Pias1 inkubiert. Starke Interaktion konnten zwischen Pias1 und den Trunkationen mGluR7a-N38 bzw. mGluR8a-C44 nachgewiesen werden. Diese beiden Domänen überlappen in 17 Aminosäuren, wobei nur die sechs letzten, die das Sumoylierungsmotif enthalten, identisch sind. Diese Ergebnisse weisen darauf hin, dass diese Aminosäurereste wichtig für die Bindung der Gruppe III mGluRs an Pias1 sind.

Im Folgenden wurde untersucht, ob mGluRa-C *in vivo* sumoyliert wird. Da bei der Sumoylierung SUMO-1 kovalent an die Aminogruppe eines Lysinrestes des Substratproteins gebunden wird, erfolgt eine detektierbare Größenveränderung desselben. Für die *in vivo*-Sumoylierungs-Analyse wurden GFP-mGluR8a-c, YFP-ube2a und CFP-SUMO-1 in HEK 293 Zellen koexprimiert. Der Zellextrakt der transfizierten Zellen wurde durch SDS-PAGE aufgetrennt und anschließend mittels Western Blotting mit einem Antikörper, der spezifisch den C-Terminus von mGluR8 erkennt, analysiert. Dabei wurde für ca. 1% des exprimierten mGluR8a-C-Proteins eine Erhöhung des Molekulargewichtes um ungefähr 40 kDa gefunden, was genau der Addition eines GFP-SUMO-1 Moleküls entspricht. Zusätzlich konnte eine Proteinbande des gleichen Molekulargewichtes mit einem Antikörper, der spezifisch SUMO-1 erkennt, nachgewiesen werden, was bestätigt, dass es sich bei dieser Bande tatsächlich um das sumoylierte mGluR8a-C-Protein handelte. Um den Lysinrest (K) in mGluR8 zu identifizieren, an dem die Sumoylierung erfolgt, wurden drei Lysine, die in mGluR8a und mGluR8b konserviert sind, substituiert: K882, das sich innerhalb eines konservierten Sumoylierungsmotives befindet, und K868 und K 872, die nahe dieser Konsensussequenz lokalisiert sind. Dazu wurden verschiedene Mutanten hergestellt, in denen ein oder mehrere dieser Aminosäurerest(e) durch Argininreste (R) ersetzt wurden (KR-Mutanten). Diese wurden anschließend in einem Sumoylierungsexperiment auf ihre Modifizierbarkeit hin untersucht. Die

Punktmutante mGluR8a-C-K882R und die Mutante, in der alle drei Lysinreste substituiert worden waren, konnte nicht sumoyliert werden, während für mGluR8a-C-Proteine mit Einzel- oder Doppelmutationen der Lysine K868 und K872 eine Sumoylierung weiterhin nachweisbar war. Daraus lässt sich schließen, dass in mGluR8a-C spezifisch der Lysinrest 882 sumoyliert wird.

Zusammengefasst konnte in der vorliegenden Arbeit konnte die E3-Ligase Pias1, die wichtig für den Prozess der Sumoylierung ist, als Interaktionspartner von mGluR8 und anderer Gruppe III mGluRs identifiziert werden. Weiterhin konnte gezeigt werden, dass diese Interaktion funktionell bedeutsam ist, da der C-Terminus von mGluR8 *in vivo* spezifisch am Lysinrest 882 durch Sumoylierung modifiziert wird. In weiterführenden Experimenten gilt es nun zu untersuchen, ob auch der intakte Rezeptor *in vivo* durch Sumoylierung modifiziert wird.

Identifikation und Charakterisierung intrazellulärer Interaktionspartner des metabotropen Glutamatrezeptors mGluR8

Die presynaptischen metabotropen Glutamat-Rezeptoren der Gruppe III (mGluRs) spielen eine zentrale Rolle in der Regulation presynaptischer Aktivität über G-Protein-Effekte auf Ionenkanäle und signalübertragende Enzyme. Wie alle G-Protein-gekoppelten Rezeptoren der Klasse C hat auch mGluR8 eine verlängerte intrazelluläre C-terminale Domäne (CTD), die vermutlich die Modulation nachgeordneter Signale erlaubt. In einem Hefe-Zwei-Hybrid-Screen einer cDNA-Bibliothek aus adultem Rattenhirn, in welchem CTDs vom mGluR8a und 8b (mGluR8-C) als "Köder" verwendet wurden, konnten neben anderen Proteinen verschiedene Komponenten der Sumoylierungskaskade (ube2a, sumo-1, Pias1, Pias α , Piasx β) als Interaktionspartner identifiziert werden. Bindungsexperimente mit rekombinanten GST-Fusionsproteinen bestätigten, daß Pias1 nicht nur mit mGluR8-C, sondern mit allen Gruppe III mGluR CTDs interagiert. Die Pias1-Bindung an mGluR8-C benötigt eine N-terminal des Sumoylierungs-Konsensusmotivs liegende Region und wird nicht beeinträchtigt durch Arginin-Austausch des innerhalb dieser Region liegenden, konservierten Lysin-Restes K882.

Kotransfektionsexperimente mit fluoreszenzmarkiertem mGluR8a-C, Sumo1 und Enzymen der Sumoylierungskaskade in HEK293-Zellen zeigten, daß mGluR8a-C *in vivo* sumoyliert werden kann. Der Arginin-Austausch des Lysin-Restes K882, jedoch nicht Austausch von anderen konservierten Lysin-Resten innerhalb der CTD-Domäne, verhinderte die *in vivo* Sumoylierung. Unsere Ergebnisse deuten darauf hin, daß die posttranslationale Sumoylierung einen neuen Mechanismus der Gruppe III mGluR Regulation darstellt.

Schlüsselwörter: Metabotrope Glutamat-Rezeptoren, Pias1, Sumoylierung, Hefe-Zwei-Hybrid, Ubiquitin konjugierendes Enzym 9, Sumo-1

ABSTRACT

Group III presynaptic metabotropic glutamate receptors (mGluRs) play a central role in regulating presynaptic activity through G-protein effects on ion channels and signal transducing enzymes. Like all Class C G-protein coupled receptors, mGluR8 has an extended intracellular C-terminal domain (CTD) presumed to allow for modulation of downstream signaling. To elucidate the function and modulation of mGluR8, yeast two-hybrid screens of an adult rat brain cDNA library were performed with the CTDs of mGluR8a and 8b (mGluR8-C) as baits. Different components of the sumoylation cascade (ube2a, sumo-1, Pias1, Pias γ and Pias β) and some other proteins were identified as mGluR8 interacting proteins. Binding assays using recombinant GST-fusion proteins confirmed that Pias1 interacts not only with mGluR8-C, but all group III mGluR CTDs. Pias1 binding to mGluR8-C required a region N-terminally to a consensus sumoylation motif and was not affected by arginine substitution of the conserved lysine K882 within this motif. Co-transfection of fluorescently tagged mGluR8a-C, sumo-1 and enzymes of the sumoylation cascade into HEK 293 cells showed that mGluR8a-C can be sumoylated in cells. Arginine substitution of lysine K882 within the consensus sumoylation motif, but not of other conserved lysines within the CTD, abolished *in vivo* sumoylation. The results are consistent with post-translational sumoylation providing a novel mechanism of group III mGluR regulation.

Keywords: Metabotropic glutamate receptor, Pias1, sumoylation, yeast two-hybrid, ubiquitin conjugating enzyme 9, sumo-1

Published result of this work:

Tang Z, El Far O, Betz H, Scheschonka A (2005) PIAS1 interaction and sumoylation of metabotropic glutamate receptor 8. J Biol Chem 280: 38153-38159

ABBREVIATIONS

AA	amino acid
APPBP1	amyloid beta precursor protein-binding protein 1
ATP	adenosine-triphosphate
bp	base pair
BSA	bovine serum albumin
CFP	cyan fluorescent protein
cGMP	cyclic guanosine monophosphate
CMV	cytomegalovirus
CtBP	C-terminal binding protein of adenovirus E1A
CTD	carboxyl terminal domain
Da	dalton
DMEM	dulbecco's modified essential medium
DMSO	dimethylsulfoxide
DNA	deoxyribonucleic acid
dNTP	deoxyribonucleoside-5'-triphosphate
DTT	dithiothreitol
EDTA	ethylenediamine tetra acetic acid
EGTA	ethylene glycol-bis(β -aminoethyl ether)-N,N,N',N'-tetraacetic acid
FCS	fetal calf serum
g	gram
Gal	galactose
GFP	green fluorescent protein
Glc	glucose
GLUT	glucose transporter
GPCR	G-protein coupled receptor
GPI	glycosyl phosphatidylinositol
GST	glutathione-S-transferase
HECT	homologous to E6AP carboxyl terminus
HEK293	human embryonic kidney 293 cells
HPLC	high performance liquid chromatography
hr	hour
HRP	horseradish peroxidase- β -d-thiogalactopyranoside
-HUWL	medium short of histidine (H), uracil (U), tryptophan (W) and leucine (L)
L	liter
Ig	immunoglobulin
IPTG	isopropyl- β -thiogalactopyranoside
L-AP4	l(+)-2-amino-4-phosphonobutyric acid
LB	luria bertani
LiAc	lithium acetate
MBP	maltose binding protein
min	minute
mg	milligram
mGluR	metabotropic glutamate receptor
Nedd8	neural precursor cell expressed, developmentally down-regulated 8
NaOAc	sodium acetate

OD	optical density
PAGE	polyacrylamide gel electrophoresis
PBS	phosphate buffered saline
PCR	polymerase chain reaction
PEG	polyethylene glycol
Pias	protein inhibitor of activated STATs (signal transduction and activator of transcription)
Raf	raffinose
RanBP2	ran binding protein 2
RanGAP1	ran GTPase-activating protein
RING	really interesting new gene
RNA	ribonucleic acid
rpm	revolutions per minute
RT	room temperature
SAF	serum amyloid A activating factor
SAP domain	SAF-A/B acinus and Pias domain
SBM	sumo-binding motif
SD	synthetic dropout medium
SDS	sodium dodecyl sulphate
s	second
Siah	seven in absentia homolog
sumo	small ubiquitin related modifier
TE	Tris-EDTA buffer
TEMED	N,N,N',N'-tetramethylethylenediamin
Tris	tris-hydroxymethyl-aminomethane
ubc	ubiquitin conjugating enzyme
Ubl	ubiquitin-like modifier
UbL	ubiquitin-like domain
UV	ultraviolet
v/v	volume to volume
w/v	weight to volume
X-Gal	5-bromo-4-chloro-3-indolyl-beta-D-galactopyranoside
YFP	yellow fluorescent protein.
YPD	yeast growing medium containing 1% (m/v) yeast extract, 2% (m/v), peptone and 2% (m/v) dextrose.

CONTENT

1	INTRODUCTION.....	3
2	MATERIALS AND METHODS.....	10
2.1	Chemicals.....	10
2.2	Kits.....	10
2.3	Oligonucleotides.....	10
2.4	DNA Constructs.....	10
2.5	Yeast Two-Hybrid.....	12
2.5.1	Materials for Yeast Two-hybrid.....	12
2.5.2	Small-scale Yeast Transformation.....	13
2.5.3	Large-scale Yeast Transformation.....	14
2.5.4	Filter Assay.....	14
2.5.5	Screen under Selective Conditions.....	14
2.5.6	Yeast Mating.....	15
2.5.7	Isolation of Plasmid DNA from Yeast Cells.....	15
2.5.8	Amplification of Prey Fragments by PCR.....	15
2.6	DNA Sequencing.....	16
2.7	Preparation of Competent Bacterial Cells for Electroporation.....	17
2.8	Preparation of Heat-Shock Competent Bacterial Cells.....	17
2.9	Transformation of DNA into E. coli Cells by Heat Shock.....	17
2.10	Protein Expression in E. coli Cells.....	18
2.11	Transfection of DNA into HEK 293 Cells.....	18
2.12	Sumo-1 Conjugation <i>in vivo</i>	19
2.13	GST-Pulldown.....	19
2.14	Western Blot.....	20
3	RESULTS.....	22
3.1	Yeast Two-Hybrid Screens with the Tail Regions of mGluR8a and mGluR8b.....	22
3.1.1	Test of the Baits' Ability to Enter the Nucleus and Bind LexA Operator.....	22
3.1.2	Test for Autoactivation of the Bait Constructs.....	24
3.1.3	General Description of the Screening Procedure.....	25
3.1.4	Results of the Yeast Two-Hybrid Screens.....	27
3.2	Yeast Mating Confirms that Sumoylation Proteins Interact with mGluR8a/b.....	28

3.2.1	Segregation of Bait Plasmids from Yeast and Test for Autoactivation of the Prey Proteins	29
3.2.2	Yeast Mating Results	30
3.3	Pias1 is the Primary Interaction Partner for mGluR8.....	31
3.3.1	Isolation of Prey Plasmids from Yeast Cells.....	31
3.3.2	Construction and Expression of MBP Fusion Proteins	32
3.3.3	GST Pulldown Assay.....	33
3.4	Pias1 Interacts with All Group III mGluRs	35
3.5	Mapping of the Pias1 Binding Domain of mGluR7a-C and mGluR8a-C	36
3.6	<i>In vivo</i> Sumoylation of mGluR8a-C.....	38
3.6.1	<i>in vivo</i> Sumoylation of mGluR8a.....	38
3.6.2	mGluR8a-C Is Sumoylated on Lysine 882	42
3.7	Yeast Two-Hybrid Screen with the C-terminal tail of mGluR4b	44
3.8	Database Search for Genomic mGluR4b Sequences.....	47
4	DISCUSSION AND PROSPECTS.....	49
4.1	Prediction of Full-length mGluR8 Sumoylation	49
4.2	Interacting Motifs of mGluRs and Pias1	50
4.3	Possible Functions of mGluR Sumoylation.....	51
4.3.1	Alternative 1: Sumoylation Antagonizes other Modifications.....	51
4.3.2	Alternative 2: Sumoylation Interferes with Other Binding Proteins...	52
4.4	Pias 1 may function as an Adaptor in the Sumoylation of mGluR8	53
4.5	Other Candidates	55
4.5.1	Faf1 and Hipk3.....	55
4.5.2	PKAi	55
5	REFERENCES.....	56
	ACKNOWLEDGEMENTS.....	61
	CURRICULUM VITAE	62
	APPENDIX I: GENERATION AND VERIFICATION OF CONSTRUCTS.....	64
	APPENDIX II: REVIEW	74

1 INTRODUCTION

Glutamate, a major excitatory neurotransmitter in the brain, exerts its effects through two distinct classes of receptors, the ionotropic (NMDA, AMPA and kainate) and metabotropic glutamate receptors (mGluRs) (Conn and Pin, 1997). As shown in Figure 1, ionotropic glutamate receptors localize at postsynaptic density sites and mediate quick responses upon glutamate binding. mGluRs are distributed in perisynaptic areas (both pre- and postsynaptically), coupled to G-proteins and contain seven-transmembrane domains. They are structurally distinct from family A and B G-protein coupled receptors (GPCRs), as they possess a large extracellular ligand binding domain and an extended intracellular C-terminus and therefore were defined as a new family of GPCRs (Conn and Pin, 1997; Sachdev et al., 2001). mGluRs have been implicated in the regulation of transmitter release, short and long term modulation of synaptic transmission, neuronal development and synaptic plasticity (Nakanishi, 1994; Nakanishi et al., 1994; Pin and Duvoisin, 1995; Conn and Pin, 1997; Nakanishi et al., 1998).

At least eight different mGluR isoforms have been identified and are classified into three subgroups based on sequence homology, downstream effectors and agonist specificity. Group I receptors (mGluR1 and 5) are positively coupled to phospholipase C, whereas group II (mGluR2 and 3) and group III (mGluR4, 6, 7 and 8) receptors typically inhibit activated adenylate cyclase activity (Conn and Pin, 1997). Group I mGluRs are mainly located around postsynaptic density, and involved in synaptic plasticity including LTP and LTD (long-term potentiation and depression) (Aiba et al. 1994a, b. Lu et al. 1997). Group II and III mGluRs are distributed mainly around presynaptic active zone, with differently regional distributions and different functions in the brain. One of the group II receptors, mGluR2, has also been found to be linked to LTD (Yokoi et al. 1996). Another group II receptor, mGluR3, is widely expressed in glial cells and related to neurotrophin release from the glial cells (Ciccarelli et al. 1999). Apart from mGluR6, which is found both pre- and postsynaptically but only in the retina, group III mGluRs are mostly localized presynaptically throughout the brain. mGluR4, 7 and 8 differ in their distributions in the brain and affinities to Glu and other agonists and antagonists (Shigemoto et al., 1997; Conn and Pin, 1997).

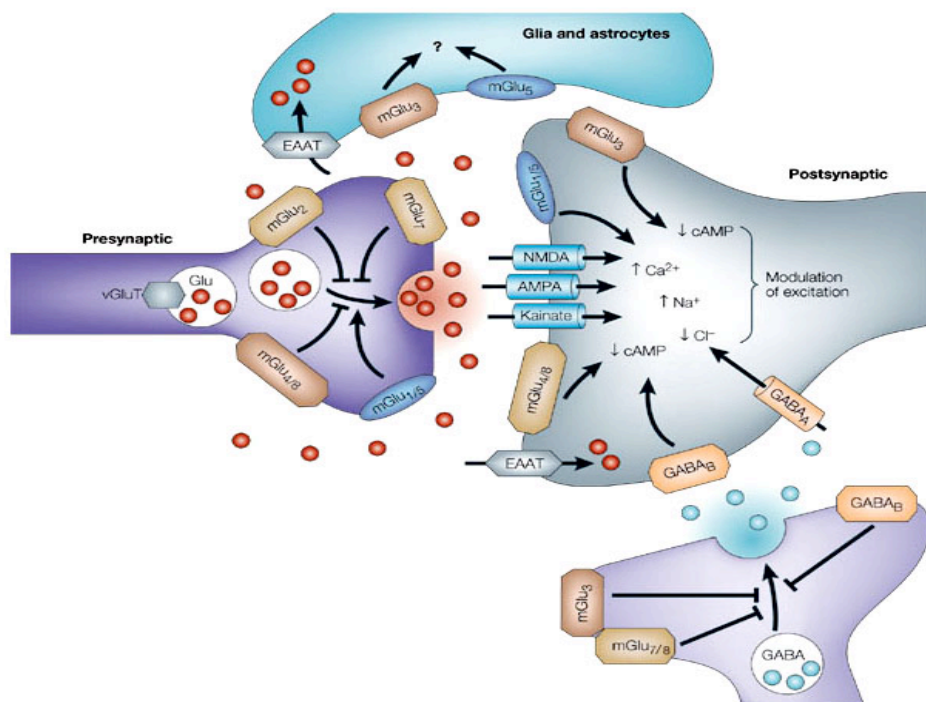


Figure 1. Hypothetical synapse illustrating the general synaptic localization and function of glutamatergic receptors and transporters. The ionotropic glutamate receptors (NMDA, kainate and AMPA subtypes) largely function to mediate fast receptor transmission, but also mediate the changes required for neuronal plasticity. The vesicular transporters (vGluT1 and vGluT2) load glutamate into vesicles presynaptically. The glial, astrocyte and postsynaptic glutamate transporters EAATs (excitatory amino-acid transporters) are thought to mediate the uptake of glutamate and therefore termination of synaptic transmission. The metabotropic glutamate receptor 1-8 have a diverse synaptic localization and function pre- and postsynaptically to modulate neurotransmitter release and postsynaptic excitability, respectively. This figure is taken from Swanson et al. (2005).

Many group- and subtype-specific mGluR agonists and antagonists have been found and applied to both basic research and clinical treatment of anxiety disorders in human (Conn and Pin, 1997; Swanson et al., 2005). For all mGluRs except for mGluR3, mice deficient for single mGluR genes have been studied. The classification, characterization and knockout phenotypes of all known mGluRs are listed in table 1.

Table 1. Classification and characterization of mGluRs

Receptor family	Coupling	Transduction	Key localization and actions	Group/subtype-selective pharmacological agents	Knockout Phenotype (References)
Group I					
mGluR 1	Excitatory Gq-coupled	PLC	Enriched postsynaptically at glutamatergic synapses. Indicated in synaptic plasticity, including long-term potentiation /depression (LTP/LTD). Cerebellar localization in granular cell and parallel fibre layers.	Agonists: DHPG, 1S,3R-ACPD, quisqualate Antagonist: LY393675 Allosteric antagonist: LY367385	Viable but show characteristic cerebellar symptoms such as ataxic gait and intention tremor. The anatomy of the cerebellum and hippocampus is normal. LTD is clearly deficient in cerebellum and LTP is substantially reduced in hippocampus. A moderate level of impairment is observed in context-specific associative learning (Aiba et al., 1994a; Aiba et al., 1994b).
mGluR 5	Excitatory Gq-coupled	PLC	Most often postsynaptic at glutamatergic synapses, also found in glial cells. High expression in several forebrain regions including hippocampus and amygdala. Implicated in synaptic plasticity, especially some forms of cortical and hippocampal LTD.	Agonists: DHPG, 1S,3R-ACPD, quisqualate, CHPG Allosteric antagonist: MPEP	Weight is significantly less than littermate controls. The gross anatomy and development of CNS is normal. LTP was significantly reduced in the NMDA receptor dependent pathways such as the CA1 region and dentate gyrus. The mutant mice were also impaired in the acquisition and use of spatial information in both the Morris water maze and the fear-conditioning test (Lu et al., 1997; Bradbury et al., 2005).
Group II					
mGluR 2	Inhibitory Gi/Go -	AC	Localization largely presynaptic on glutamatergic and other	Agonists: DCG-IV, 2R,4R-APDC, 1S,3R-ACPD,	No histological changes and no alterations in basal synaptic transmission, paired-pulse facilitation, or tetanus-induced

	coupled		neurotransmitter synapses. High expression in forebrain regions including hippocampus and amygdala; also in certain layers within the cortex and cerebellum. Linked to hippocampal LTD and regulation on medial perforant path.	LY354740, LY379268 Antagonist: LY341495 Potentiator: 4-MPPTS (LY487379), 4-APPES, CBiPES	long-term potentiation (LTP) at the mossy fiber-CA3 synapses. Long-term depression (LTD) induced by low-frequency stimulation, however, was almost fully abolished (Yokoi et al., 1996).
mGluR 3	Inhibitory Gi/Go - coupled	AC	Widely expressed in glial cells but also discrete localization both pre- and postsynaptic on glutamatergic and other neurotransmitter synapses. Expression within forebrain regions including hippocampus and thalamus. Linked to neurotrophin release from glial cells.	Agonists: DCG-IV, 2R,4R-APDC, 1S,3R-ACPD, LY354740, LY379268 Antagonist: LY341495	No report.
Group III					
mGluR 4	Inhibitory Gi/Go - coupled	AC	Localization both pre- and postsynaptic on glutamatergic and other neurotransmitter synapses. Presynaptic in cerebellar parallel fibres and linked to cerebellar plasticity and motor learning.	Agonists: L-SOP, ACPT-1, L-AP4 Antagonist: MSOP, MAP4, CPPG	No gross motor behaviour abnormalities. Deficient on the rotating rod motor-learning test, suggesting the KO mice may have an impaired ability to learn complex motor tasks. Paired-pulse facilitation and post-tetanic potentiation were impaired. In contrast, long-term depression (LTD) was not impaired. Resistant to absence seizures induced by GABAAR antagonists.

					(Pekhletski et al., 1996; Snead et al., 2000)
mGluR 6	Inhibitory Gi/Go - coupled	AC	Expression confirmed only in retinal bipolar ON cells.	Agonists: L-SOP, L-AP4 Glutamate-site antagonist: MSOP, MAP4	No obvious changes in retinal cell organization or in the projection of optic fibers to the brain. The homozygous mutant mice showed a loss of ON responses but unchanged OFF responses to light (Masu et al., 1995).
mGluR 7	Inhibitory Gi/Go - coupled	AC	Localization both pre- and postsynaptic on glutamatergic and other neurotransmitter synapses in limbic and cortical regions. Has lower affinity for glutamate than other mGluR subtypes and only presynaptic inhibitory mGluR localized to active zone of synapses. Thought to serve a classical autoreceptor function.	Agonists: L-SOP, L-AP4 Antagonist: MSOP, MAP4, LY341495 (100-fold lower affinity than group II)	Significantly reduced levels in immediate postshock and delayed freezing responses. The knockout mice were normal in pain sensitivity and locomotor activity. In conditioned taste aversion (CTA) experiments, the KO mice failed to associate between the taste and the negative reinforcer in CTA experiments. Again, the knockout mice showed no abnormalities in taste preference and in the sensitivity to LiCl toxicity (Masugi et al., 1999). Increased susceptibility to pentylentetrazole-induced seizures (Sansig et al., 2001).
mGluR 8	Inhibitory Gi/Go - coupled	AC	Localization largely presynaptic on glutamatergic and other neurotransmitter synapses. High expression in forebrain regions including hippocampus and amygdala. Linked to regulation of lateral perforant path.	Agonists: L-SOP, L-AP4, (S)3,4-DCPG Antagonist: MSOP, MAP4	Blunted response to novelty and increased anxiety-like behaviors. Increased c-Fos expression in thalamus centromedial nucleus, and overweight (Linden et al., 2002; Linden et al., 2003b; Duvoisin et al., 2005).

The table is modified from Swanson *et al.* (2005).

First mGluR8a was cloned from mice (Duvoisin et al., 1995), and two alternatively spliced forms of mGluR8, designated HmGluR8b and HmGluR8c, were cloned from a human fetal brain cDNA library (Malherbe et al., 1999). The HmGluR8b and c receptors differ from a HmGluR8a by out-of-frame insertions, which result in substitution of the last 16 amino acids in the C-terminus of HmGluR8a with 16 different amino acids in HmGluR8b, and termination of the polypeptide before the putative seven transmembrane domains of HmGluR8c. Thus, the predicted HmGluR8c protein is 501 amino acids long and could represent a secreted isoform.

RT-PCR, Northern blot and in situ hybridization studies showed that both HmGluR8a and b are expressed with similar abundance in fetal and adult brains. In situ hybridization revealed prominent mGluR8 mRNA expression in olfactory bulb, pontine gray, lateral reticular nucleus of the thalamus, and piriform cortex. Less abundant expression was detected in cerebral cortex, hippocampus, cerebellum and mammillary body (Duvoisin et al., 1995; Saugstad et al., 1997). In the lateral reticular and ambiguous nucleus, only mGluR8a mRNA is found (Corti et al., 1998). The in situ hybridization results indicate that HmGluR8c is predominantly expressed in glial cells in the human brain (Malherbe et al., 1999). mGluR8 is also expressed in the enteric nervous system (Liu et al., 1997), pineal gland (Moriyama et al., 2000) and glucagon-secreting α -cells and intrapancreatic neurons in the pancreas islet (Tong et al., 2002). Rat microglia also expresses mGluR8 mRNA and receptor protein, together with mGluR4 and mGluR6, but not mGluR7 (Taylor et al., 2003). Immunocytochemical data demonstrate that mGlu8 receptors are mainly located presynaptically (Shigemoto et al., 1997), but in the retina they are also found post-synaptically (Koulen and Brandstatter, 2002). Recently it was found that mGluR8 is not only expressed in glutamatergic but also GABAergic synapses in periaqueductal gray matter (Marabese et al., 2005).

mGluR8 KO mice with deletion of both mGluR8a and mGluR8b have been generated (Linden et al., 2002; Duvoisin et al., 2005). The overall morphology of mGluR8 KO mice is normal. No differences in comparison to wild type animals were observed in eye reflexes, auditory reflexes, respiratory rate, body temperature, salivation, urination, defecation, skin color or irritability. Similarly, no differences were observed in stance, limb strength, placing, grasping, righting, tail pinch, and tail-flick latency (Linden et al.,

2002). But mGluR8 KO mice exhibit increased anxiety-related behaviour in the elevated plus maze test (Linden et al., 2002), and this increase is accompanied by increased c-FOS expression in the centromedial nucleus of the thalamus (Linden et al., 2003b). The mGluR8 KO mice are also slightly overweight and mildly insulin resistant (Duvoisin et al., 2005).

Despite numerous pharmacological *in vivo* studies and the generation of mGluR8 knockout mice (Thomas et al., 2001; Potheary et al., 2002; Linden et al., 2003a; Schmid and Fendt, 2005), still little is known about the function of this receptor. The aim of this study is to find intracellular proteins that may regulate mGluR8 function. Yeast two-hybrid screens were performed with baits corresponding to the intracellular C-terminal domains of both mGluR8a and mGluR8b. About 30 candidate interacting proteins were identified, including proteins related to sumoylation: sumo-1, an E2 protein ube2a, and three E3 proteins Pias1, Piasx β and Pias γ . Sumoylation is a type of modification in which the sumo protein is covalently conjugated onto a Lys residue of a substrate, and is catalysed by three enzymes: activating enzyme E1, conjugating enzyme E2 and ligase E3. Sumoylation has been shown to modify a large number of proteins with important roles in many cellular processes including gene expression, chromatin structure, signal transduction, and maintenance of the genome (Gill, 2004). A review on sumoylation is attached as Appendix I1. The interaction between Pias1 and group III mGluRs was verified by binary yeast two-hybrid assays and GST pulldown. *In vivo* sumoylation assays including mutations of the receptor proved that the mGluR8a-C protein could be sumoylated at K882. While ubiquitination of GPCRs is a well-documented phenomenon (Marchese and Benovic, 2004) and appears to play a role in group I mGluR degradation (Moriyoshi et al., 2004), the related but functionally distinct sumoylation cascade has not yet been linked to any plasma membrane receptor. Thus, the results of this thesis represent the first evidence for sumo-conjugation of a GPCR.

2 MATERIALS AND METHODS

2.1 Chemicals

All chemicals, unless otherwise stated, were ordered from the following companies: Roche Diagnostics, Eppendorf, Fluka, Gibco-BRL, Merck, Sigma and Roth. Solutions were prepared with Milli-Q water (Millipore).

Restriction enzymes were ordered from Roche Diagnostics or New England Biolabs.

2.2 Kits

Preparations of plasmid DNA, purifications of DNA from either PCR products or agarose gels, and substitutions of lysine to arginine of mGluR8a-C constructs were performed according to the protocols provided with the following kits.

- QIAprep Spin Miniprep Kit (QIAGEN).
- QIAGEN Plasmid Midi Kit (QIAGEN).
- QIAGEN Plasmid Maxi Kit (QIAGEN).
- QiaQuick PCR Purification Kit (QIAGEN).
- Perfectprep Gel Cleanup Kit (Eppendorf).
- QuikChange Site-Directed Mutagenesis Kit (Stratagene).

2.3 Oligonucleotides

Oligonucleotides (Table 2) were ordered from the company MWG, delivered as lyophilized pellets and dissolved in HPLC water to a final concentration of 100 pmol/ μ l.

2.4 DNA Constructs

The constructs listed in Table 3 were generated by cloning the fragments from either other plasmids or PCR products, or by using site-directed mutagenesis (Stratagene). The constructs were checked by DNA sequencing, restriction digestions, or Western blotting for proteins expressed in either bacterial or mammalian cells (Appendix I).

Table 2. List of primers for PCR or sequencing reactions

Primer names	Sequence (5'---3')
Aos1EcoRIATGHis, s	CGGAATTCCATGGGCAGCAGCCATCATC
Aos1-XbaI-end, as	GCTCTAGATCAGTTTTCCTTGCCTGGAGATG
DsRed2-C1-seq-1132, s	CTGGTGGAGTTCAAGT C
Lib-1, library cloning, s-1	CTTGCTGAGTGGAGATGCCTCC
Lib-2, library cloning, as	CTGGCAAGGTAGACAAGCCGAC
Lib-3, library cloning, s-2	TTATGATGTGCCAGATTATGC
m4b truncate B1, as	GCGTCTGACTCAAAAAGAGTTGGTGGATGAAG C
m4b truncate F2, s	GCGAATTCCACCACGTTGCAAAAAGAG
m4b, as	GCGTCTGACTCAGAGACCATCACCAAACA
m4b, s	GCGAATCCCATATTTTTCCATTCTGCTC C
m8 EcoRI-ATG, 56, s	GCGAATTCAATGGTATGCGAGGGAAAGC G
m8 K882R, as	GACTCTCACAGAGTTCAGATCTCACCTCGCCATTTG
m8 K882R, s	CAAATGGCGAGGTGAGATCTGAACTCTGTGAGAGTC
m8K868-872R, as	GGTCTGTCATTTCCCTTTGGATCAGTCTGCTTTGCA TGGTAG
m8K868-872R, s	CTACCATGCAAAGCAGACTGATCCAAAGGGGAAATG ACAGACC
m8N24Sall, 54, a s	TGCGGTCTGACTCAGCTTTGCATGGTAGCAGCTGTG
m8seq-end, 2596, s	CATCCAGAGCAGAATGTTC
m8seq-start, 232, as	CATGAACAGGAAAAAGACC
m8tailEcoRI, 57, s	GGAATTCATCCAGAGCAGAATGTTCAAAAAC
m8tailSall, 52, as	TGCGGTCTGACTCAGATCGAATGATTACTGTAGCTG
m8tC44EcoRI, 57, s	GGAATTCATGCAAAGCAAAGTATCCAAAAG
mGluR8aK868R, 64, as	CCCTTTTGGATCAGTCTGCTTTGCATGGT A G
mGluR8aK868R, 64, s	CTACCATGCAAAGCAGACTGATCCAAAAG G G
mGluR8aK872R, 64, as	GGTCTGTCATTTCCCTTTGGATCAGTTTGC
mGluR8aK872R, 64, s	GCAAAGTATCCAAAGGGGAAATGACAGACC
Myc-m8-2, as	GGATGGAATGGGCATACTCGAGGTCTCCTCGCTGA TCAGCTTCTGCTCTTGGCTGTGAGTTC
Myc-m8-2, s	GAACTCACAGCCAAGAGCAGAAGCTGATCAGCGAG GAGGACCTCGAGTATGCCATTCCATCC
pQE seq	AAACAAATAGGGGTTCC
SGT truncate B1, as	GCCTCGAGTCACTCAGCTGAGTCCTCCTCA G
SGT truncate B2, as	GCCTCGAGTCAAGGTTGGACTTGTACGT G
SGT truncate B3, as	GCCTCGAGTCACTCTTGCTGCTCCTCGT G
SGT truncate F1, s	GCGAATTCGACAACAGGAAGCGCCTGG
SGT truncate F2, s	GCGAATTCGACAGCGCCTTAAAACAGAA G
SGT truncate F3, s	GCGAATTCGACACGTACAAGTCCAACCT C
SUMO1ΔC4HindIII, 60, as	CCCAAGCTTACCCCCGTTTGTTCCTGATAAAC
SUMO-HindIII, as	CCCAAGCTTCTAAACCGTCGAGTGACCCC C
ube2iclone-BamHI, rat, 60C, s	CGGGATCCATGTCTGGGGATTGCCCTCAGC
ube2iclone-HindIII, 60C, as	CCCAAGCTTATGAGGGGGCAAACCTTCTCGC

Table 3. List of DNA constructs

constructs	inserts	5' site	3' site
pcDNA3-His-aos1	PCR product via pET28aHIS-aos1	EcoRI	Xho I
pEGFP-C1-sumo1	PCR product via pJG4-5-ubl1 (rat brain library)	BamHI/Bgl II	HindIII
pEGFP-C1-ube2i	PCR product via pJG4-5-ube2a (rat brain library)	BamHI/Bgl II	HindIII
pEGFP-C2 mGluR8a-C44	PCR product	EcoRI	Sal I
pEGFP-C2 Pias1	mouse pias1	Bgl II	HindIII
pEGFP-C2-8a-N24	PCR product	EcoRI	Sal I
pEGFP-mGluR8a-C-K868&872R	site-directed mutagenesis		
pEGFP-mGluR8a-C-K872R	site-directed mutagenesis		
pEGFP-mGluR8a-C-K882R	mGluR8a-CT-K882R		
pEGFP-mGluR8a-C-K868R	site-directed mutagenesis		
pEYFP-C1-sumo1	PCR product via pJG4-5-ubl1 (rat brain library)	BamHI/Bgl II	HindIII
pEYFP-C1-ube2i	PCR product via pJG4-5-ube2i (rat brain library)	BamHI/Bgl II	HindIII
pGEX5X-1-mGluR8a-C-K882R	site-directed mutagenesis		
pMAL-c2-Pias1	mouse pias1	BamHI	HindIII
pMAL-c2-ube2i	ube2i (rat brain library)		
pMAL-c2-Piasy (fragment)	Piasy (rat brain library)		

2.5 Yeast Two-Hybrid

The following protocols describe the two-hybrid screen for proteins interacting with mGluR-8a-C. The screens for mGluR8b-C and mGluR4b-C were performed in the same way.

2.5.1 Materials for Yeast Two-hybrid

Yeast strains

EGY48: MAT α *trp1 his3 ura3 leu2::6 LexAop-LEU2*

RFY206: MAT α *trp1 Δ ::hisG his3 Δ 200 ura3-52 lys2 Δ 201 leu2-3* (mating strain)

Reporter gene (LacZ) plasmids

pSH18-34 URA3, Amp^r, 8 ops-LacZ

pJK101 URA3, Amp^r, GAL1-2 op-LacZ (used in repression assay for nuclear transport)

Bait plasmid

PGilda: *HIS3*, Amp^r, inducible GAL1 promoter, expresses *LexA(1-202)* as DNA binding domain followed by a polylinker for making bait fusion protein.

Target plasmid

pJG4-5: *TRP1*, Amp^r, inducible GAL1 promoter, expresses *B42-HA tag* as a transcriptional activation domain followed by a polylinker for making target fusion protein expression libraries.

Medium

All media were prepared according to the User's Manual (OriGene Tech. Inc. Version 1.2).

2.5.2 Small-scale Yeast Transformation

Yeast cells from a single clone were cultured in 200 ml of YPD medium with shaking at 250 rpm until OD₆₀₀ reached 0.8-0.9. After pelleting twice and resuspending first in 50 ml of TE buffer and then in 1 ml TE/LiAc solution, 2 μ g of each plasmid DNA and 2 mg of herring testis carrier DNA were added to 0.1 ml of the yeast suspension and mixed well by vortexing, followed by addition of 0.6 ml of sterile PEG/LiAc and vortexing at high speed for 10 sec. The mixture was incubated for 30 min at 30°C with shaking at 200 rpm, and then mixed gently with 70 μ l of DMSO. After 15 min heat shock in a 42°C water bath, the cells were chilled in ice-water mixture for 2 min, then pelleted, diluted with TE buffer and spread on SD/Glc/-UH agar plates. The plates were incubated at 30°C for about three days until the clones grew up to 0.5 mm in diameter.

YPD: 10 g/L Yeast extract, 20 g/L Peptone, 20 g/L Dextrose (Glucose).

TE: Tris-HCl (0.01 M, pH 7.5)- EDTA (1 mM).

TE/LiAc: 0.1 M LiAc(lithium acetate) in TE.

PEG/LiAc: 40% (w/v) PEG 4000 (polyethylene glycol, MW 3,350) in TE/LiAc.

SD medium: Minimal Synthetic Dropout medium. Comprised of a nitrogen base, a carbon source (glucose or galactose), and a DO* supplement without some of histidine (-H), tryptophan (-W), uracil (-U) and Leucine (-L). (*DO: Dropout supplement; a mixture of specific amino acids and nucleosides used to supplement SD base to make SD medium; DO solutions are missing one or more of the nutrients required by untransformed yeast to grow on SD medium).

2.5.3 Large-scale Yeast Transformation

1000 ml of YPD medium were used to dilute a 150 ml overnight culture of EGY48/pSH18-34/pGilda-mGluR8a-C in SD/Glc/-UH medium, and incubated at 30 °C for about 6 hr until OD₆₀₀ had reached 0.8-1.0. The cells were then pelleted and resuspended three times, in H₂O for the first two times and 20 ml TE/LiAc at last, followed by mixture with 2.5 mg cDNA library (Origene) and 20 mg denatured carrier DNA. The mixture was transferred to a 500 ml glass flask containing 150 ml PEG/LiAc, and incubated at 30 °C with shaking at 200 rpm. After 30 min, 17.5 ml DMSO were added and mixed gently. The cells were heat-shocked for 15 min at 42 °C with gentle shaking every 2-3 minutes and then chilled for 5 min in an ice-water mixture. At last, the cells were pelleted, resuspended in 16 ml TE buffer and spread on SD/Glc/-UHW plates. The plates were incubated at 30 °C for three to four days until the clones grew up to 0.5 mm in diameter.

2.5.4 Filter Assay

Yeast clones were streaked on one plate, grown for two days, imprinted on a piece of nitrocellulose membrane and frozen in liquid nitrogen. The membrane was placed on a Whatman filter paper soaked with X-Gal. The time scale of the color change was recorded.

2.5.5 Screen under Selective Conditions

Cotransformant yeast cells that had been stored at -70 °C were put on ice for about 30 min for recovery, then diluted in TE buffer and incubated for 4 hr at 30 °C with rotation.

The cells were spread on SD/Gal/Raf/-UHWL/X-Gal plates and incubated at 30 °C for three days. Blue colonies were streaked on fresh SD/Gal/Raf/-UHWL/X-Gal plates.

2.5.6 Yeast Mating

EGY48 and RFY206 yeast cells with different plasmids were added into the same tube with 0.5 ml YPD medium and incubated for 6 hr at 30°C on a rotator set at 150 rpm. The cells were pelleted, spread on plates and incubated for 3–5 days at 30°C in order to allow diploid cells to form visible colonies.

2.5.7 Isolation of Plasmid DNA from Yeast Cells

5 ml of yeast cell suspension were pelleted and lysed by vortexing for 2 min in 200 μ l of yeast lysis solution, mixed with 300 mg glass beads (0.25-0.5 μ m in diameter) and 200 μ l PCI (Phenol/Chloroform/Isoamyl alcohol 25/24/1 (v/v/v)). After centrifugation at 14,000 rpm for 5 min, the DNA in the upper phase was precipitated by mixing with 1/10 volume of 3 M NaOAc (sodium acetate, pH 5.2), then 2.5 times volumes of absolute ethanol, followed by centrifugation for 5 min at 14,000 rpm. The pellet was washed with 70% (v/v) ethanol, dried with SpeedVac vacuum and redissolved in 20 μ l H₂O.

Yeast lysis solution

Triton X-100, 2% (v/v)

SDS, 1% (w/v)

NaCl, 0.1 M

EDTA, 1.0 mM

Tris, 0.01 M, pH 8.0

2.5.8 Amplification of Prey Fragments by PCR

Yeast cells were lysed by alternate freeze-thawing in liquid nitrogen and water for three times, and used for standard PCR reactions to amplify the inserts in the prey plasmids.

PCR mixture included:

Lysed yeast cells in H₂O 20 μ l

10 x PCR buffer	5	μ l
Primer Lib-1, s	0.5	μ l
Primer Lib-2, as	0.5	μ l
dNTP mixture (10 mM)	1	μ l
MgCl ₂ (50 mM)	1.5	μ l
H ₂ O	21.25	μ l
Taq polymerase	0.25	μ l
Total volume	50	μ l

Cycling was set as:

Stage	Step	Temperature (°C)	Time (min)	Number of cycles
I	1	94	5	1
II	1	94	1	30
	2	58	1	
	3	72	2.5	
III	1	72	10	1
Hold		4		

2.6 DNA Sequencing

PCR products purified with QIAquick PCR Purification kit (Qiagen), or plasmid DNA purified with Qiagen kits (see 2.14), were used as templates in sequencing reactions. Reaction mixture:

4 μ l Seq.mix (Amersham Bioscience)

5 pmol. lib-3 primer, s

DNA (10 ng DNA for per 100 bp DNA length)

HPLC water up to 10 μ l total volume.

PCR condition:

Step	Temperature (°C)	Time (sec)	Number of cycles
1	95	20	25
2	50	15	
3	60	60	
Hold	4		

PCR products were purified on AutoSeq G-50 columns (Amersham Pharmacia) and analyzed by MegaBACE sequencer.

2.7 Preparation of Competent Bacterial Cells for Electroporation

A primary culture of XL-1 blue was made in 50 ml LB medium, and incubated overnight at 37 °C and 250 rpm. Then 1 L of pre-warmed LB medium was added and incubated until OD₆₀₀ reached 0.5 to 0.6. The bacterial cells were pelleted 3 times and resuspended with 250 ml ice-cold water, 50 ml then 5 ml of 10% (v/v) glycerol. 50 µl aliquots of the bacteria were prepared, frozen in liquid nitrogen and stored at -70 °C.

2.8 Preparation of Heat-Shock Competent Bacterial Cells

1 ml overnight culture of either XL-1 or BL-21 cells was diluted in 50 ml medium A and incubated at 37 °C with shaking until OD₆₀₀ reached 0.3 to 0.5. The cells were cooled down on ice for 10 min, then pelleted and resuspended in 0.5 ml ice-cold medium A. 2.5 ml ice-cold solution B was added and mixed gently. 100 µl aliquots were made and stored at -70 °C after quick freezing in liquid nitrogen.

Medium A

LB medium supplemented with 10 mM MgSO₄ and 0.2% (w/v) glucose, sterile filtered and stored at 4 °C.

Solution B

Glycerol (36%, w/v)

24% (m/v) PEG (Polyethylene glycol. MW 7500)

0.012 M MgSO₄

In LB medium.

2.9 Transformation of DNA into E. coli Cells by Heat Shock

1 µl of plasmid DNA or up to 10 µl of ligation mixture were added to an aliquot of competent cells and incubated on ice for about 10 minutes after gentle mixture by flicking. The competent cells were heat-shocked at 42 °C for 60 s, then stored on ice for 2 min, followed by addition of 1

ml LB medium and incubation at 37 °C for 1 hr on a shaker. The cells were pelleted and plated onto LB agar plates with appropriate antibiotics and incubated at 37 °C overnight.

Commonly used antibiotics

Antibiotics	Stock concentration (mg/ml)	Storage	Working dilution
Ampicillin	100	-20 °C	1:1000
kanamycin	50	-20 °C	1:1000
Tetracycline.HCl*	50	-20 °C	1:1000

* Tetracycline needs to be stored in the dark.

2.10 Protein Expression in E. coli Cells

BL21 cells transformed with plasmids were spread on a LB plate with appropriate antibiotics. One colony from the plate was diluted in 50 ml LB broth with antibiotics in a 2.5 L flask and incubated on a shaker (250 rpm) at 37 °C overnight. 1 L pre-warmed fresh LB with antibiotics was added and the cells cultured for additional 3-4 hr until the OD₆₀₀ reached 0.6, then protein expression was induced by adding IPTG (isopropyl-β-thiogalactopyranoside, final concentration: 0.3 mM) and incubation for 4 hr. The cells were harvested and the pellet was frozen at -70 °C. The frozen cells were resuspended in 25 ml cold PBS supplemented with protease inhibitor mixture Complete™ (Roche Diagnostics), and lysed by French Press at 500 psi, 4-6 times until the suspension became transparent. After centrifugation of the lysate with a Beckman Ultracentrifuge at 100,000 g for 45 min at 4 °C, the supernatant was aliquoted and frozen at -70 °C.

2.11 Transfection of DNA into HEK 293 Cells

HEK 293 cells were maintained in MEM medium supplemented with 10 % (v/v) FCS, 2mM glutamine and 50 units/ml penicillin/streptomycin. For transfection, 80% confluent HEK 293 cells were split by 1:3. One day later, the medium was exchanged with 10 ml fresh medium per 10-cm dish. Another 2 hr later, the transfection mixture was prepared by mixing 300 μl of 1 M CaCl₂ with 900 μl H₂O containing 5 μg of each DNA, then with 1.2 ml of 2× BBS (see below), mixing carefully, and incubating 3 min at RT. The mixture was slowly added to the culture

medium. 1 min later, the culture dish was swirled gently and put back into the 37°C, 5% CO₂ incubator for 18 to 24 hr, then the medium was exchanged again. The cells were incubated for another 18 to 24 hr before harvesting.

2×BBS (BES-buffered solution)

50 mM *N,N*-bis(2-hydroxyethyl)-2-aminoethanesulfonic acid (BES)

280 mM NaCl

1.5 mM Na₂HPO₄·7H₂O

pH was adjusted to 6.95 with 1 M NaOH

2.12 Sumo-1 Conjugation *in vivo*

The following DNAs were co-transfected in different combinations into HEK293 cells as described above:

pEGFP-mGluR8a-C

pEGFP-C2

pECFP-sumo-1

pcDNA3-His₆-aos1

pEYFP-ube2a

pEGFP-Pias1

Two days after the transfection, cells were washed with PBS and harvested with 2x sample buffer supplemented with 20 mM N-ethylmaleimide, followed by boiling for 15 min at 95 °C and analysis by Western blot.

2x Sample buffer (for SDS-PAGE) 0.125 M Tris-Cl (pH 6.8) supplemented with 0.1% (w/v) SDS, 20% (v/v) glycerol, 0.2% (w/v) bromophenol blue and 4% (v/v) β-mercaptoethanol

2.13 GST-Pulldown

Proteins expressed in *E. coli* were prepared as described in 2.10. For expression of proteins in mammalian cells, combinations of plasmid DNA were transfected into HEK 293 cells as described in 2.11. Two days after transfection, the cells were harvested after briefly washing with PBS, followed by 2 hr solubilizing with 1% (v/v) Triton X-100 in PBS supplemented with

protease inhibitor mixture. After centrifugation for 45 min at 45,000 g, the supernatant was aliquoted and frozen at -70°C .

For GST pulldown, GST-fusion proteins were immobilized on glutathione-Sepharose 4B beads (Amersham Biosciences) by incubating 300 μl of bacterial lysate with 25 μl beads in 700 μl incubation buffer for 1 hr with gentle rotation at 4°C , followed by three washings with wash buffer. 40-120 μl of bacterial extract of an MBP fusion protein or 40 μl HEK cell extract of a GFP fusion protein were added and incubated with the beads for 2 hr and followed by washing as explained above. The protein binding beads were resuspended in 30- μl 2x SDS-PAGE sample buffer and boiled for 5 min.

Wash buffer: PBS (0.01M phosphate buffered 0.15 M saline, pH 7.4) supplemented with 0.1% (v/v) Triton X-100, 2 mM EDTA, 2 mM EGTA and 2 mM dithiothreitol.

Incubation buffer: Wash buffer supplemented with protease inhibitor mixture.

2.14 Western Blot

A 1.2 mm thick SDS-PAGE mini gel (Bio-Rad) was run at 15 mA constant current for the stacking gel and at 20 mA for the separating gel until the bromophenol blue tracking dye reached the bottom of the separating gel. The gel was electro-blotted at 10 V overnight to transfer the proteins to a nitrocellulose membrane (Schleicher & Schuell). The proteins on the membrane were stained with Ponceau S solution for 5 min followed by washing with water until protein bands appeared. The protein standards (Sigma) were marked. The membrane was incubated in blocking buffer for 1 hr on a shaker. After washing briefly with PBST, the primary antibody diluted in blocking buffer was applied, and incubated at 4°C overnight, followed by 3 times washing with PBST. The secondary antibody diluted in blocking buffer was applied, and incubated at RT for 1 hr; followed by 3 times washing with PBST. The blot was incubated with a mixture from the SuperSignal West Pico Chemiluminescent Substrate Kit (PIERCE, Rockford, IL, USA), detected by X-ray films, which were developed with Kodak X-OMAT 2000 processor.

PBST 0,05% (v/v) Tween20 in 0.01M PB-0.15M saline.

Ponceau S 2% Ponceau S (w/v) and 3% (w/v) trichloroacetic acid dissolved in H_2O .

Blocking buffer PBS supplemented with 5% (w/v) milk powder (nonfat) and 5% (w/v) BSA

Primary antibodies

Antibody	Company	Dilution used
GFP (rabbit)	Clontech	1:200
MBP (rabbit)	New England Biolab	1:10,000
mGluR8a (Guinea Pig)	Gift from Dr. Shigemoto	1:5000
Pias1 (rabbit)	Santa Cruz	1:50
Sentrin 1 (/SUMO-1, mouse)	Zytomed	1:200

Secondary antibodies

Antibody	Company	Dilution used
HRP-goat-anti-rabbit	Dianova	1:10,000
HRP-goat-anti-mouse	Dianova	1:10,000
HRP-goat-anti Guinea Pig	Biomol	1:10,000

3 RESULTS

3.1 Yeast Two-Hybrid Screens with the Tail Regions of mGluR8a and mGluR8b

To identify proteins interacting with the cytoplasmic C-terminal tail regions of mGluR8a and mGluR8b, two-hybrid screens were performed using the DupLexA yeast two-hybrid system. The yeast two-hybrid system has been proven to be a powerful method for identifying protein-protein interactions. The general principle of the LexA yeast two-hybrid system is shown in Figure 2A. Two proteins (X and Y) under test are fused separately with either a bacterial DNA-binding domain LexA, and the fusion construct is thus called the bait, or a yeast activation domain B42, and the fusion construct is called the prey. If X interacts with Y, the two fusion proteins will form a chimeric regulatory factor to activate reporter gene expression. In case of the mGluR8a/b screens (Figure 2B), the C-terminal tails of the receptor were fused with LexA separately and used as baits. A rat brain cDNA library fused with B42 was used as the pool of preys for screening. The DupLexA yeast two-hybrid system has two reporter genes: LacZ & LEU2. Both reporter genes are under the control of multiple LexA operators, but with different promoters: LacZ is under the control of minimal TATA region of the yeast GAL1 promoter, and LEU2 is under the control of the yeast LEU2 promoter. The multiple LexA operators contribute to the sensitivity and discrimination power of the two-hybrid assay. The different promoters help to eliminate some false positives and to confirm positive two-hybrid interactions. As expression of both B42 and LexA fusion proteins is under the control of GAL1 promoter, the whole test system is under the control of the carbon source in the medium. Hence expression is induced in Gal/Raf medium, but inhibited in medium containing glucose.

3.1.1 Test of the Baits' Ability to Enter the Nucleus and Bind LexA Operator

Before applying the baits to yeast two-hybrid screening, they had to be tested for nuclear localization and autoactivation of both reporter genes. Firstly, I examined whether they entered the nucleus and bound to the LexA operators. Both baits underwent separate cotransformation with pJK101 into EGY48. Single transformation of pJK101 was also performed as control. The plasmid pJK101 contains a LacZ reporter gene, whose expression is driven by the yeast GAL1 promoter. Two LexA operators have been placed between the GAL1 promoter and the LacZ

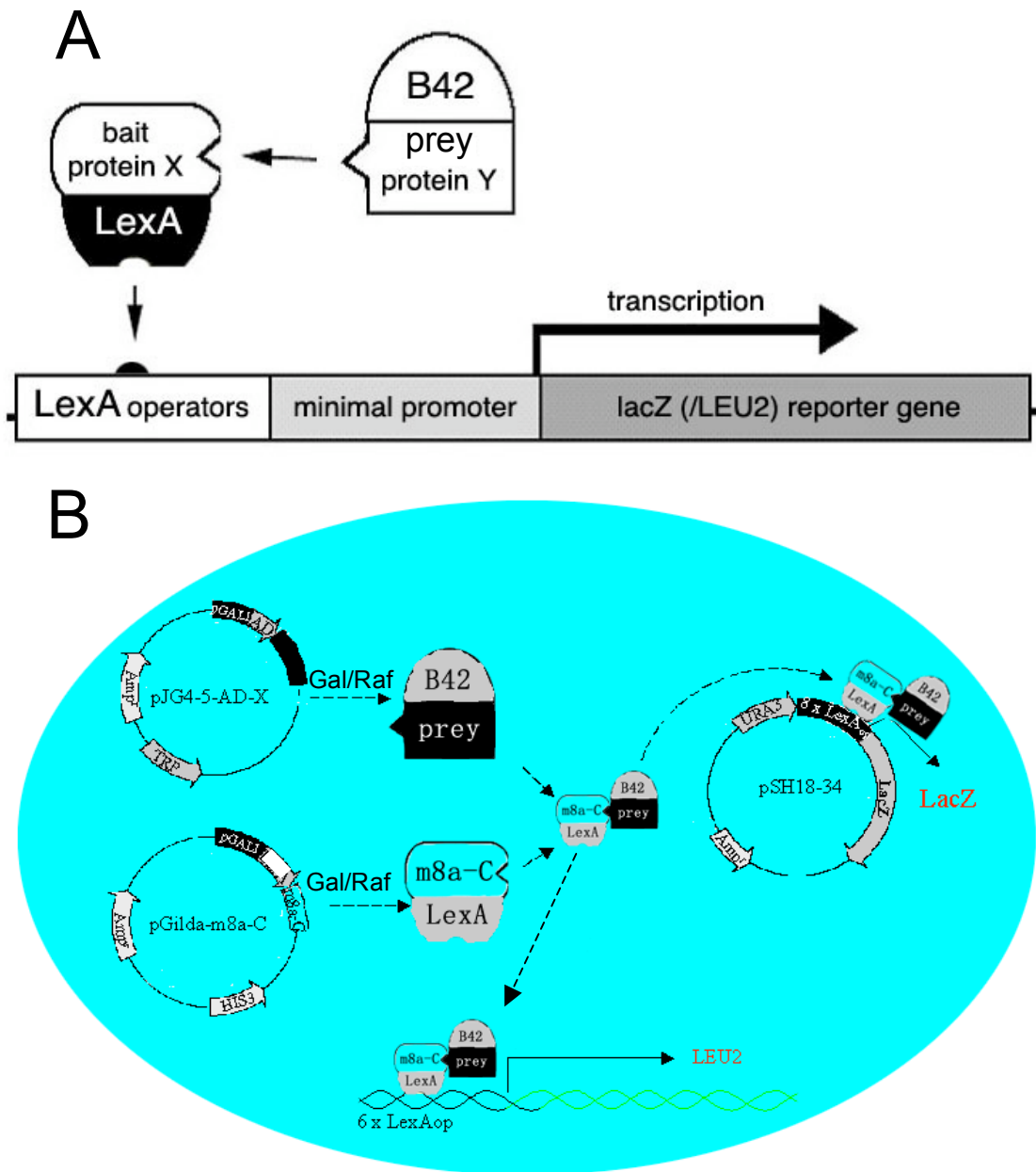


Figure 2. A. The principle of the LexA yeast two-hybrid system. Modified from CLONTECH MATCHMAKER LexA Two-Hybrid System-User Manual. The interaction between two proteins (X and Y) is tested in this system. X is fused with an E. coli DNA binding domain LexA and called the bait. Y is fused with a yeast activation domain B42 and called the prey. If X interacts with Y, a LexA-X-Y-B24 chimeric complex will form, which binds to the LexA operator and activates the reporter gene expression. B. The components of DupLexA yeast two-hybrid system used for mGluR8a-C screen. Bait, prey and LacZ reporter plasmids with different selection markers are cotransformed into EGY48 cells that contain another reporter gene, LEU2. The bait plasmid expresses LexA- mGluR8a-C. The prey plasmids express B42 fused with proteins encoded by a cDNA library. Expression of both B42 and LexA fusion proteins is under the control of yeast GAL1 promoters, therefore is controlled by glucose/galactose in the medium. LEU2 and LacZ genes have multiple LexA operators and will be activated if any library protein interacts with mGluR8a-C in the same yeast cell, thus the yeast cell can grow into a blue clone on a Gall/Raf/-HUTW/X-Gal plate.

gene. LexA fusion proteins will bind to these operators and delay the GAL1- driven LacZ expression.

The yeast clones were transferred onto a filter and lysed by freezing-thawing, X-Gal solution was then applied onto the filter to measure the LacZ activity in these yeast cells. 10 min later, all clones started to turn blue, but the group transformed with only pJK101 was stronger than those cotransformed with pJK101 and the baits. 30 min later, the difference was more pronounced, and lasted at least for 3 hours. This result proved that the LexA-mGluR8a-C and LexA-mGluR8b-C fusion proteins were able to enter the nucleus and to bind to the LexA operators.

3.1.2 Test for Autoactivation of the Bait Constructs

In the LexA yeast two-hybrid system, the integrated LEU2 nutritional reporter gene allows the otherwise Leu- auxotrophic host cell EGY48 to grow on SD induction medium lacking leucine when transformed with plasmids encoding interacting hybrid proteins. When lacZ transcription is activated in EGY48[pSH18-34], the cells produce β -galactosidase, whose activity can be visually monitored. It is therefore important that the bait constructs do not show any autoactivation of the reporter genes. Both bait constructs pGilda-mGluR8a-C and pGilda-mGluR8b-C had already been tested in our laboratory for lack of transactivation of the LacZ gene in the presence of galactose. A small-scale transformation was performed here to examine whether these baits were able to activate the other reporter gene, LEU2.

The bait and reporter plasmids were cotransformed into EGY48, and the cells were plated onto Glc/-UH plates to allow all cotransformed cells to grow. Four days after transformation, one clone from each group was picked up, diluted with water and plated on both SD/Gal/Raf/-UHL and SD/Gal/Raf/-UH 10-cm plates. Five days later, clone numbers were counted as listed in Table 4.

All yeast cells with the bait and reporter plasmids grew on SD/Gal/Raf/-UH plates, thus the number of clones growing on these plates was used to calculate the concentration of yeast suspension plated. As no prey plasmid was introduced, the growth of yeast cells on SD/Gal/Raf/-UHL was considered to be the result of autoactivation of the reporter gene LEU2 by the baits. According to Table 4, we obtained 76 yeast clones out of 7.85×10^6 for mGluR8a-C, and 100 yeast clones out of 2.4×10^7 for mGluR8a-C growing due to autoactivation (Table 4). This suggests there would be about 2,000-5000 clones with autoactivation in a screen under such

selective conditions, in case approx. 5×10^8 yeast cells would be screened as usual. This high value of autoactivation found with both baits is not acceptable for standard screening procedures. One possibility to suppress autoactivation is to decrease the concentration of galactose in the medium. After testing the growth of transformed yeast cells on SD/Gal/Raf/-UHL plates with different concentrations of galactose, a concentration of 1.5% was found to be the optimum.

Table 4. Clone numbers of cotransformants obtained with bait and reporter plasmids grown under permissive (*) and testing (**) conditions

Baits	Plates	Primary suspension	1:100	1:10,000	1:1,000,000
mGluR8a-C	SD/Gal/Raf/-UH*			785	
	SD/Gal/Raf/-UHL**	76			
mGluR8b-C	SD/Gal/Raf/-UH*				24
	SD/Gal/Raf/-UHL**	100			

EGY48 cells were cotransfected with reporter plasmids (*URA3*) and bait plasmids (*HIS3*) including either mGluR 8a-C or mGluR8b-C, and plated on Glc/-UH selective plates. One clone from each group was picked and plated on Gal/Raf plates as shown, with or without leucine in the medium. Only the plates with 20 and 1000 clones were counted and listed.

* Permissive growth condition for the cotransformed cells.

**Selective conditions for autoactivation of bait protein on reporter gene LEU2.

3.1.3 General Description of the Screening Procedure

The procedure of the two-hybrid screens is shown in Figure 3. 6.3×10^8 yeast cells were screened for mGluR8a and 8.4×10^8 for mGluR8b. 1,385 and 934 clones, respectively, were found to be positive by Leu- auxotrophy and expression of LacZ. PCR reactions were performed to amplify the insert cDNAs in the prey plasmids. Products with only single bands on agarose gels were selected and grouped by size, followed by Hae III digestion. The digestion patterns were compared on 1% agarose gels. Samples of identical size and restriction pattern were assigned to the same group. One to five purified PCR products of each group were selected for sequencing. In total, about 100 PCR products of each screen were sequenced.

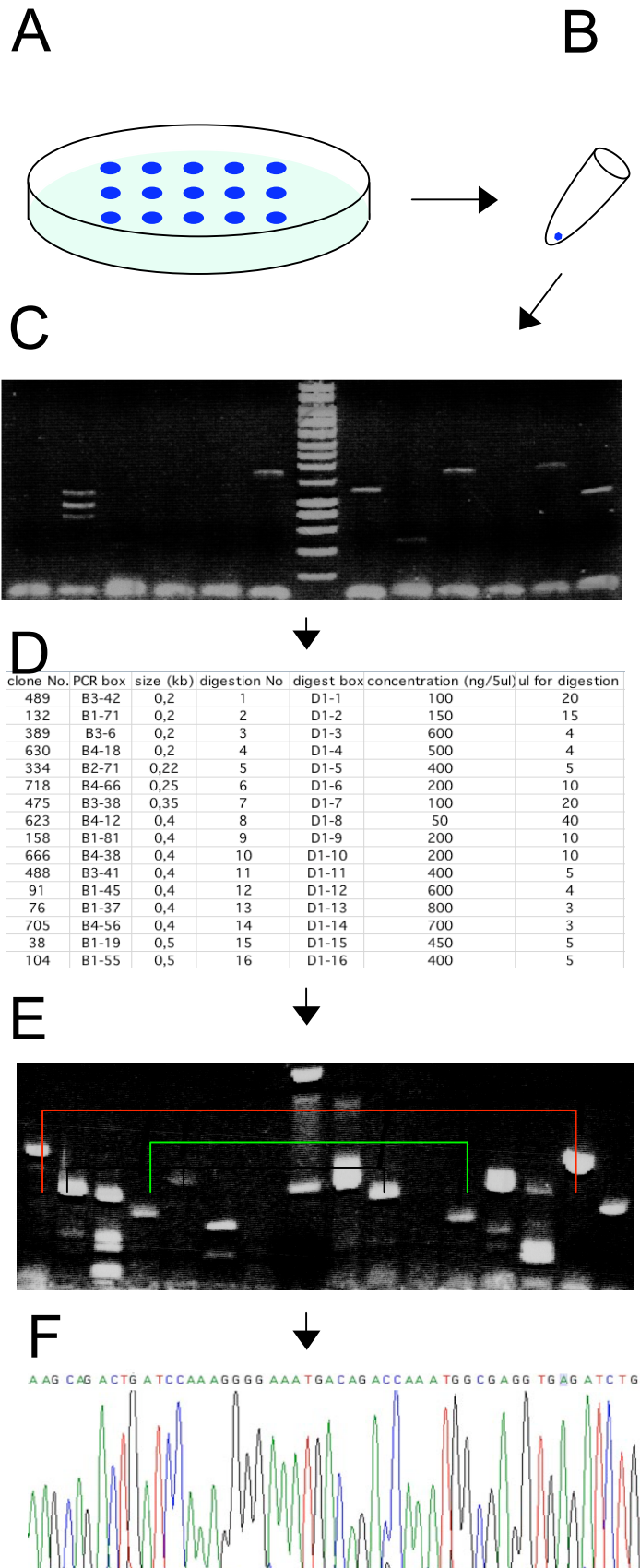


Figure 3. The yeast two-hybrid screening procedure.

- A. Positive clones obtained after screening.
- B. Freezing-thawing treatment of yeast cells with liquid nitrogen and water.
- C. Amplification of insertions by PCR. Only samples yielding single bands as revealed by agarose gel electrophoresis are selected for subsequent analysis.
- D. List of the PCR products according to size.
- E. Hae III digestion patterns of the PCR products. Samples with the same frequent pattern were grouped together.
- F. DNA sequencing of representative PCR products.

3.1.4 Results of the Yeast Two-Hybrid Screens

After DNA sequencing, about 30 proteins were identified as interacting candidates (Table 5). All clones were in-frame with the B42 activation domain. Some of them, especially those identified most frequently, were fished in both the mGluR8a-C and mGluR8b-C screens. There were also many candidates interacting with only one of the baits; however, most of these interactions were found only once.

Table 5. List of candidate interacting proteins of mGluR8a/b-C
Found in yeast two-hybrid screens

Baits	Candidate interacting protein cDNA homologues	Genebank No.	Clones
8a/b	Protein inhibitor of activated STAT 1 /Pias1	62653796	12/13
8a/b	Msx-interacting-zinc finger (Miz1)/Piasx β	16758049	12/9
8a/b	Ubiquitin conjugating enzyme E2I (Ube2i)/ube2a	4079642	9/3
8a/b	Polymyositis/scleroderma autoantigen 1/Pmscl1*	8132102	3/6
8a/b	Homeodomain-interacting protein kinase 3/Hipk3	13929113	2/2
8a	Neurofilament protein, middle polypeptide	8393822	6
8a	CDK103 mRNA	5931735	3
8b	Anaphase-promoting complex 2 (LOC227617)	62644719	2
8b	Ubiquitin-like 1 (Ubl1)/sumo1	57528278	2
8a/b	ADP-ribosylation factor-like 2 (Arl2) *	66911464	1/1
8a	cAMP-dependent protein kinase inhibitor protein mRNA /PKAi	6981393	1
8a	Creatine kinase-B (CKB) mRNA, 3' end	56388798	1
8b	Fas-associated factor 1/Faf1	15284035	1
8a	Guanine nucleotide binding protein, beta 2/G β 2	41351300	1
8a	Mitochondrial nd1 gene for NADH dehydrogenase subunit 1	13472	1
8a	NADH dehydrogenase (ubiquinone) 1 alpha subcomplex	33563265	1
8b	Ornithine aminotransferase (Oat)	40254768	1
8b	Protein inhibitor of activated STAT γ /Pias γ	62651709	1
8a	RIKEN cDNA 1810009N24 gene (1810009N24Rik)	62654507	1
8a	RIKEN cDNA 2810028A01 gene (2810028A01Rik)	62078862	1
8a	Chemokine ligand	62648835	1
8a	TATA element modulatory factor 1	63545828	1
8b	Thymosin beta-4 (Tmsb4x)	13592118	1
8a	Zinc finger protein of the cerebellum 1 (Zic1)	70778755	1

Yeast two-hybrid screens were performed with C-terminal tails of mGluR8a and mGluR8b as the baits. The insertions of prey cDNA from positive clones were amplified by PCR and sequenced. The cDNA sequences were compared with sequence database of NCBI BLAST.

*Not confirmed by yeast mating assay.

All of the predicted interacting proteins could be divided into 3 classes. The first comprises sumoylation proteins, including the first three most frequently found candidates: Pias1, Piasx β

and ube2a, together with two proteins found only for mGluR8b: sumo-1 and Pias γ . These proteins play different roles in the sumoylation pathway as detailed in Figure 1 of the Appendix II. Sumo-1 is the modifier, ube2a is the conjugating enzyme (E2), and Pias1, Piasx β and Pias γ are ligating enzymes (E3). The second class of identified proteins are related to apoptosis: Hipk3 and Fas-related protein. They will be discussed later. The third class includes all remaining gene products.

3.2 Yeast Mating Confirms that Sumoylation Proteins Interact with mGluR8a/b

After the two-hybrid screen, a yeast mating assay was performed to confirm the interactions between the candidate proteins and the mGluR8 bait sequences. The general idea of yeast mating is that two complementary yeast cells, carrying different plasmids introduced in the yeast two-hybrid screen, mate together to form a diploid yeast cell. The interactions between the bait and the prey proteins then again can be tested in the diploid cell. Taking advantage of the positive EGY48 clones identified so far, yeast mating has been proven to be an efficient procedure to quickly eliminate false positive candidates. It is also an effective method to test whether a prey protein fished with one bait also interacts with another one. The procedure is schematically depicted in Figure 4.

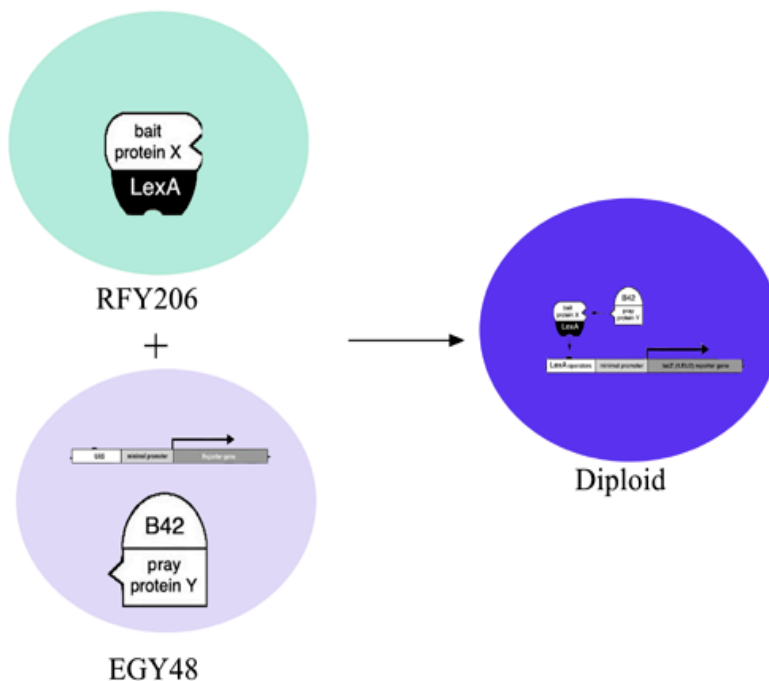


Figure 4. Principle of yeast mating. Two complementary yeast strains were used: EGY48 carried prey plasmids and both LEU2 and LacZ reporter genes. RFY206 contained only bait plasmids. After mating, two complementary yeasts were fused and formed a diploid cell, onto which the same test system as shown in Figure 3 was employed.

3.2.1 Segregation of Bait Plasmids from Yeast and Test for Autoactivation of the Prey Proteins

To prepare cells for mating, bait plasmids were segregated from the cotransformant EGY48, leaving the reporter and the prey plasmids in the cells according to the principle shown in Figure 5. Eleven clones of cotransformants of nine candidate cDNAs were treated in this way (Table 7). In addition, essential tests to check whether the prey proteins alone were able to activate the reporter gene(s) were performed. These clones were plated onto Gal/Raf/-UW/X-Gal. None of the nine candidate plasmids examined activated the LacZ reporter gene. Therefore the yeast cells containing these plasmids were used for the yeast mating assay.

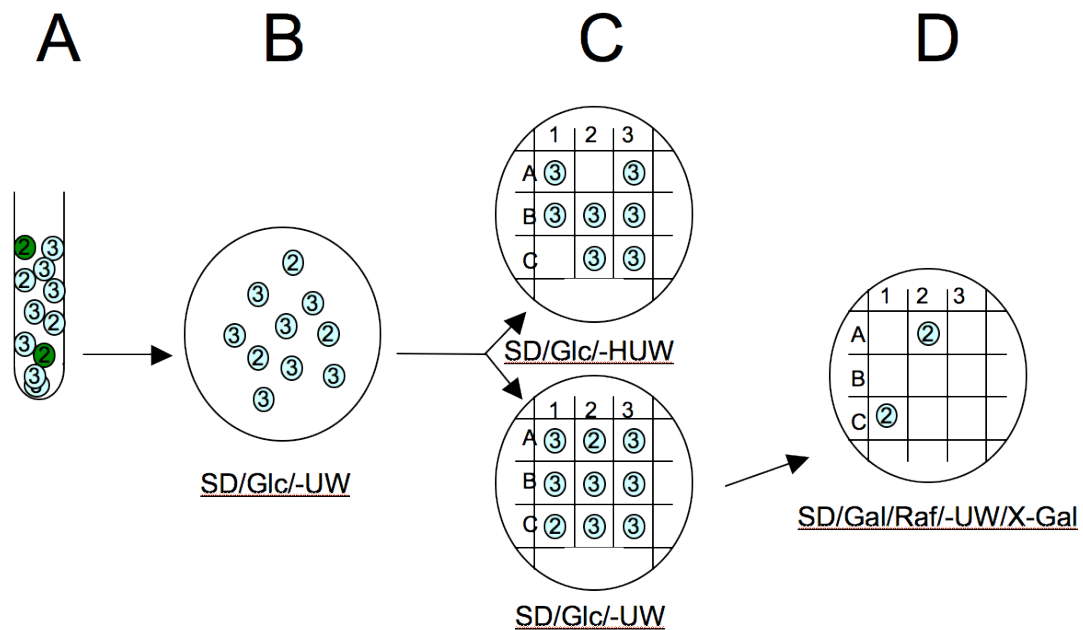


Figure 5. Segregation of bait plasmids from the yeast cells and test of the autoactivation potential of the prey proteins. A. Cells from a single clone were cultured in YPD+Glc medium. Some of the growing cells lost one or more of the three plasmids. The numbers of plasmids left in the cells are indicated. B. The yeast cells were spread onto a SD/Glc/-UW plate, only cells still containing both p18-34 and pJG4-5-X grew. C. The same clones were spread on two different plates with or without His. Two (e.g. A2 and C1) clones did not grow without His because they had lost pGilda-8a. D. Clones A2 and C1 were plated onto SD/Gal/Raf/-UW/X-Gal. None of them were blue, means the LacZ gene was not activated by the prey protein, hence they were verified further.

3.2.2 Yeast Mating Results

RFY206 cells (MAT α) carrying either empty bait plasmid pGilda, or bait plasmid inserted with either mGluR8a-C or mGluR8b-C, were incubated together with EGY48 cells (MAT α) that carried only one of the prey plasmids and the reporter plasmid. Both RFY206 and EGY48 are haploid, and they are of complementary mating type. RFY206 cells carry all selective markers for auxotrophy EGY48 cells have. Between these two complementary haploid cells yeast mating occurred: they fused and incorporated into a single diploid cell. The diploid cells share all common auxotrophy selective markers with both haploid cells, and thus can be tested in the same way as in the yeast two-hybrid screen.

When testing the diploid cells for Leu⁻ auxotrophy and LacZ expression, all of the cells expressing the five sumoylation proteins and some of the other candidates were found to be positive, and hence considered to be interaction partners of both mGluR8a and mGluR8b (table 7). Notably, Pias γ and sumo-1 that were found only with mGluR8b-C in the two-hybrid screen also gave positive signals with mGluR8a-C. Two other fusion proteins (Pmscl and arf1) failed to interact with mGluR8a-C and/or mGluR8b-C in the yeast mating assay; therefore they were deleted from the candidate list. As all sumoylation proteins were confirmed by yeast mating, I focussed on these proteins.

Table 7. Pias1 interacts with all group III, but not group II mGluRs in the yeast two-hybrid.

Bait Target	pGilda fused with tail of						
	mGluR2	mGluR3	mGluR4	mGluR6	mGluR7a	mGluR8a	(empty)
pJG4-5 (Neg control)	-	-	-	-	-	-	-
pJG4-5-Pias 1 (C-terminal)	-	-	+	+	++	+++	-

Yeast cells with reporter genes and prey plasmids containing a C-terminal domain of Pias1 were transformed with pGilda bait plasmids fused with C-terminal tails of the different group II and III mGluRs. The cotransformants were selected on Gal/Raf/-UHWL plates.

-, no clones observed on the plates.

Positive clones were estimated qualitatively as:

+, faint blue; ++, medium blue; +++, strong blue.

3.3 *Pias1* is the Primary Interaction Partner for mGluR8

For further confirmation of the results of the yeast two-hybrid screen, GST-pulldown experiments were performed. For this purpose, target plasmids were isolated from the yeast cells in order to subclone the insert into expression vectors and to generate fusion proteins.

3.3.1 Isolation of Prey Plasmids from Yeast Cells

The prey plasmids containing the cDNAs of the candidate interacting proteins were isolated from yeast according to the procedure illustrated in Figure 6. This is actually a new protocol taking advantage of the *LacZ* gene present in the reporter plasmids. Briefly, plasmid DNA was isolated

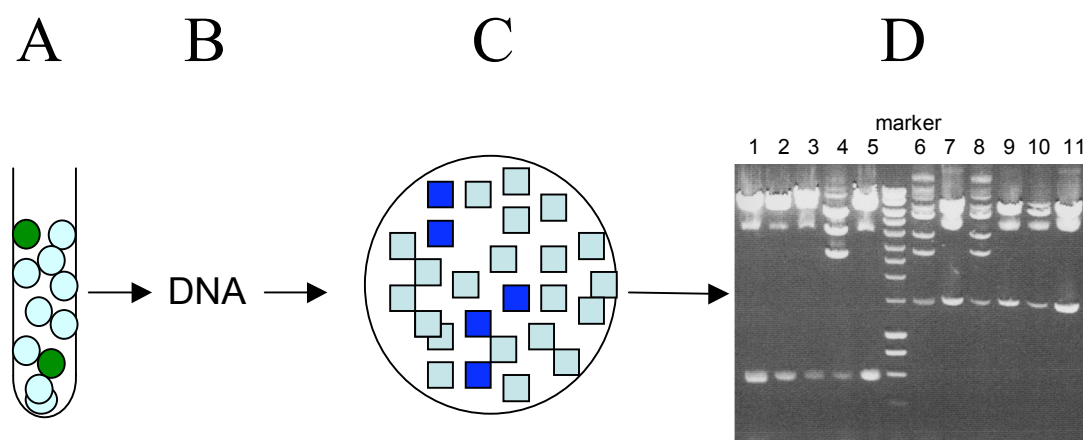


Figure 6. Isolation of target plasmids from yeast cells. A. A single clone was cultured in SD/Glc/-W medium. Some of the growing yeast cells lost some of their plasmids, but pJG4-5-X got enriched. B. Plasmid DNA was isolated from yeast cells and transformed into XL-1, which were plated onto LB-Amp/X-Gal plates. C. Some bacterial clones were blue, which suggested that they contained p18-34 with the *LacZ* reporter gene. Small scale cultures of WHITE clones were made, followed by preparation of plasmid DNA, then digestion with *ECorI/XhoI*. D. Gel electrophoresis of the digested samples. Clones 1, 2, 3, 5, 7, 9, 11, 12 contained only the target plasmid; clone 4, 6, 8 contained both the bait and the target plasmids.

from yeast and transformed into XL-1 bacterial cells. The bacteria were plated onto LB-Amp-X-Gal plates. Some bacterial clones were blue because they contained the reporter plasmid pSH18-34. pSH18-34 contains a *LacZ* gene that can be activated by the bacterial LexA full transcription

regulator protein. After isolating plasmid DNAs from the bacterial clones that were not blue and checking them by restriction analysis, all sumoylation related target plasmids were isolated, and their identity was confirmed by DNA sequencing.

3.3.2 Construction and Expression of MBP Fusion Proteins

Constructs for generating the MBP fusion proteins MBP-ube2a and MBP-PIAS γ were made by subcloning inserts from the corresponding target plasmids into pMAL-c2 (Figure 7). Successful expression of the recombinant proteins was checked by Western blotting with anti-MBP antibody (Figure 8, input lanes). Fusion constructs of all other clones are listed in Appendix I.

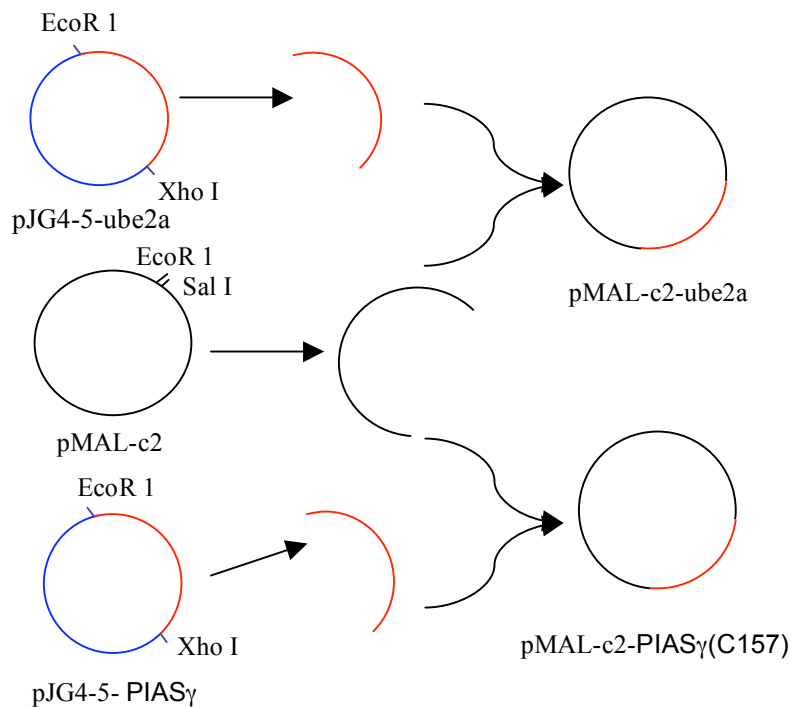


Figure 7. Strategy used for generating pMAL-c2-ube2a (A) and pMAL-c2-PIAS γ (B). The full-length fragment of ube2a and the C-terminal fragment of PIAS γ were cut from pJG4-5-ube2a and pJG4-5-PIAS γ , respectively, using EcoRI and XhoI sites, and inserted into pMAL-c2 between EcoRI and SalI sites.

3.3.3 GST Pulldown Assay

E. coli expressed GST-mGluR8a-C and mGluR8b-C fusion proteins were immobilized on glutathione beads. Candidate interacting proteins, ube2a, Pias1 and Piasy, were also expressed in bacteria as MBP-fusion proteins and incubated with the beads, followed by washing, elution with SDS sample buffer and analysis by SDS-PAGE and Western blotting with an antibody against MBP. Figure 8 shows that MBP-Pias1 could be affinity-purified with GST-mGluR8b-C bound to glutathione-Sepharose beads and, to a lesser extent, with immobilized GST-mGluR8a-C, but not GST alone. A comparatively weak interaction was also detected for the MBP fusion of the C-terminal region of Piasy, which similarly bound to both mGluR8-C isoforms. GST alone failed to bind MBP and all MBP-fusion proteins tested. MBP-ube2a did not exhibit detectable binding to any of the GST-mGluR8-C-termini under the conditions used (Figure 8).



Figure 8. GST-mGluR8-C fusion proteins interact with MBP-Pias1. GST, GST-mGluR8a-C and GST-mGluR8b-C were immobilized on Glutathione-Sepharose beads and incubated with 50 μ l of extracts from bacteria expressing MBP-fusion proteins of fulllength ube2a Pias1 and a C-terminal 157 AA fragment of Piasy (input lanes show protein expression in 20 μ l of bacterial extracts). After washing the beads repeatedly by incubation buffer, bound proteins were eluted with SDS-sample buffer, and analyzed by SDS-PAGE followed by Western blotting with an anti-MBP antibody. Note that MBP-Pias1 was retained on GST-mGluR8b-C and, to a lesser extent, on GST-mGluR8a-C, while GST failed to bind MBP-fusion proteins. Weak binding was also seen with MBP-Piasy on both mGluR-Cs.

GST pulldown experiments were also performed using mammalian expressed proteins. cDNA constructs encoding full-length Pias1, ube2a and sumo-1 were generated according to the strategies listed in Appendix I. CFP-sumo-1, YFP-ube2a and GFP-Pias1 were all efficiently

expressed in HEK 293 cells, and Triton-X 100 extracts of the transfected cells were used in binding assays (Figure 9). An interaction could be confirmed for mGluR8a-C and GFP-Pias1, while only very little or no YFP-ube2a was recovered in the bound protein fraction. GFP alone did not bind to GST-mGluR8a-C. In contrast to the results obtained in the original yeast-mating assay, GST-mGluR8a failed to bind CFP-sumo-1 (approx. molecular weight 40 kDa) under these assay conditions but enriched two high molecular weight (≥ 90 kDa) sumo-conjugated proteins from the HEK cell lysate. The identities of these proteins are unknown, but an unbiased mass-spectrometry based analysis of sumo-conjugated HEK cell proteins has identified several candidates in the respective molecular weight range (Zhao et al., 2004).

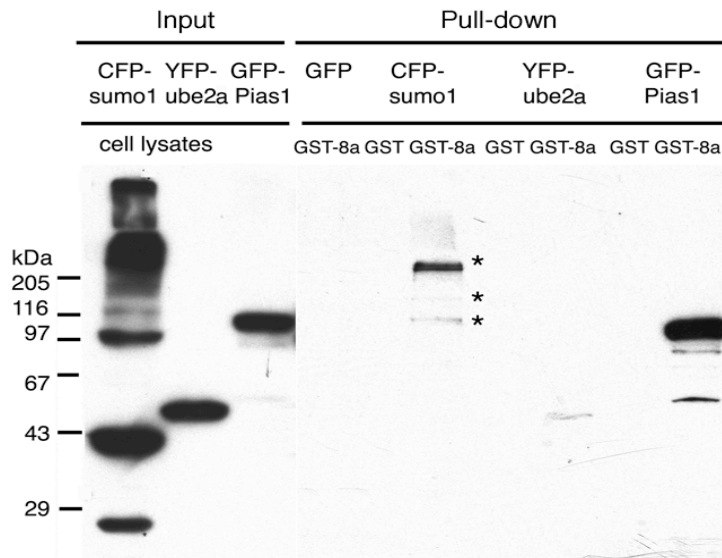


Figure 9: GST-mGluR8a-C interacts with GFP-Pias1, but not YFP-ube2a and CFP-sumo-1. Ube2a, Pias1 and sumo-1 tagged with different GFP variants were expressed in HEK 293 cells (input: 10 μ l of HEK cell extracts; left panel). 50 μ l Triton-X100 extracts of the transfected cells were incubated with GST or GST-mGluR8a-C, respectively (right panel). After the GST pull-down procedure, bound proteins were eluted by SDS sample buffer, separated by SDS-PAGE electrophoresis, and immunoreactive bands were detected by Western blotting with an anti-GFP antibody. Note that GFP-Pias1 binds to GST-mGluR8a-C but not to GST. Only a very weak interaction is detected with YFP-ube2a. Asterisks mark high molecular weight bands of unknown identity that were bound from extracts expressing CFP-sumo-1. Note that free sumo-1 was not recovered.

Taken together, these GST pulldown results prove that, of the sumoylation proteins found, Pias1 is the most robust binding partner of mGluR8.

3.4 Pias1 Interacts with All Group III mGluRs

A

	<u>G-protein $\beta\gamma$/Ca²⁺/CaM binding domain</u>	<u>putative sumoylation site ΦKXE</u>	yeast 2-hybrid
mGluR8A	HPEQNVQKRKRFSKAVVTAATMQSKLIQKGNDRPNGEV KSEL CESLETNTSSTKTTYISYSDHSI		+++
mGluR7A	HPE LNVQKRKRFSKAVVTAATMSSRLSHKPSDRPNGE AKTEL CENVDPNSPAAKKYVSYNNLVI		+(+)
mGluR4	HPEQNVPKRKRSLKAVVTAATMSNKFTQKGNFRPNGE AKSEL CENLETPALATKQTYVYTNHAI		+
mGluR6	HPEQNVQKRKRSLKKTSTMAAP-----PQN-----ENAEDAK		+
mGluR2	QPQKNVSHRAPTSRFGSAAPRASANLGQGGSGQFVTVCNGREVVDSTTSSL		-
mGluR3	QPQKNVVTHRLHLNRFVSGT-----ATTYSQSSASTYVPTVCNGREVLDSTTSSL		-

B

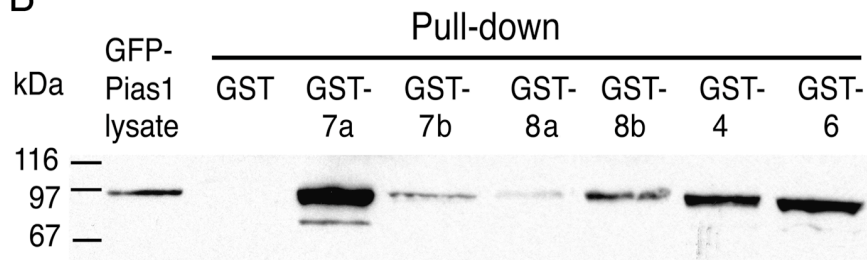


Figure 10. Pias1 interacts with all group III, but not group II, mGluRs.

A: Alignment of rat group II and group III mGluR-C-termini starting from the predicted end of transmembrane domain VII. The first three lysines of all group III mGluR (mGluR4, 6, 7 and 8) C-terminal tails are located in the highly conserved 5' coding region which binds both G-protein $\beta\gamma$ and calmodulin. In the more variable C-terminal region, additional lysines are found, some of which are conserved among isoforms. Bold letters: Sites homologous to the consensus sumoylation motif YKXE. Note that group II mGluRs (mGluR2 and 3, bottom) only contain a single conserved lysine in position +4 after the predicted end of the last transmembrane domain.

B. Mammalian expressed GFP-Pias1 interacts with GST fusion proteins of all group III mGluR C termini. GFP-Pias1 was expressed in HEK293 cells, and an aliquot (10 μ l) of the cell lysate separated in the *left lane*. Pull-down assays with 100 μ l of HEK lysate on GST, or GST-mGluR-Cs as indicated, were performed as described under "Experimental Procedures." Bound protein was detected after SDS-PAGE by Western blotting with an anti-GFP antibody. Note that GFP-Pias1 binds to all GST-mGluR-C termini but not to GST. Amounts of immobilized GST fusion protein were similar for all fusion proteins, as indicated by Western blotting with anti-GST (data not shown), except for GST-mGluR8a for which only 25% of the average protein level was bound.

To examine whether binding of Pias1 is shared by all presynaptic members of the mGluR family (including group II and group III receptors), binary yeast two-hybrid assays were performed with Pias1 and all group II/III mGluRs. Cells of a positive clone from the two-hybrid screen, which

encoded the C-terminal domain of Pias1 and had been segregated from the bait plasmids, were transformed with bait plasmids containing the C-terminal tails of different mGluRs and tested for reporter gene activation. In these assays, mGluR8a-C showed the strongest interaction, followed by mGluR7a-C and then mGluR6-C / mGluR4-C (Figure 10 A). In contrast, neither mGluR2-C nor mGluR3-C interacted with Pias1. I also subcloned the full-length mouse Pias1 cDNA into the target plasmid and tested two-hybrid interactions in yeast cells using the same protocol. All cotransformants grew under the permissive (SD/Glc/-UHW), but none of them under selective (SD/Gal/Raf/-UHWL/X-Gal) conditions. As Pias1 contains a SAP domain in the N-terminal region that binds to A/T rich DNA sequences, it is possible that full-length Pias1 binds to exposed regions of yeast nuclear DNA, thereby losing its ability to bind to the bait that is located at the LexA operator. Indeed, no interaction was observed in our experiments between the full-length Pias1 and C-terminus of any mGluR tested.

Next, the interactions between Pias1 and all group III mGluRs were examined in GST pulldown experiments, using mammalian cell generated GFP-Pias1 and the respective GST-fused C-terminal tail of the mGluRs (Figure 10 B). While GST failed to bind GFP-Pias1 and conversely GFP did not interact with GST-mGluR7a-C, all group III mGluR C-termini showed some interaction. The strongest binding was detected with mGluR7a-C, mGluR4-C and mGluR6-C. The weak band recovered with GST-mGluR8a could be attributed to substantially less GST-fusion protein being retained on the agarose beads (shown in Figure 11). In conclusion, all group III mGluR-C-terminal tails were able to bind GFP-Pias1.

3.5 Mapping of the Pias1 Binding Domain of mGluR7a-C and mGluR8a-C

To determine which domains of mGluR7a-C and mGluR8a-C interact with Pias1, the binding of mammalian expressed CFP-Pias1 to respective truncated GST-fusion proteins was tested. A schematic drawing of the truncation mutants used is shown in Figure 11A. The mGluR7a-C truncation constructs did not overlap while those for mGluR8a-C overlapped by three amino acids. Also, the positions of the truncations were different in the respective C-terminal tails: for mGluR7a-C, GST-mGluR7a-N38 ends, and GST-mGluR7a-C27 starts, just before the conserved Lys889. For mGluR8a-C, GST-mGluR8a-N24 only included the proximal signal transduction domain with the G-protein $\beta\gamma$ and Ca^{2+} /calmodulin binding sites (El Far et al., 2001), while GST-mGluR8a-C44 contained all conserved lysines outside of this signalling domain including the

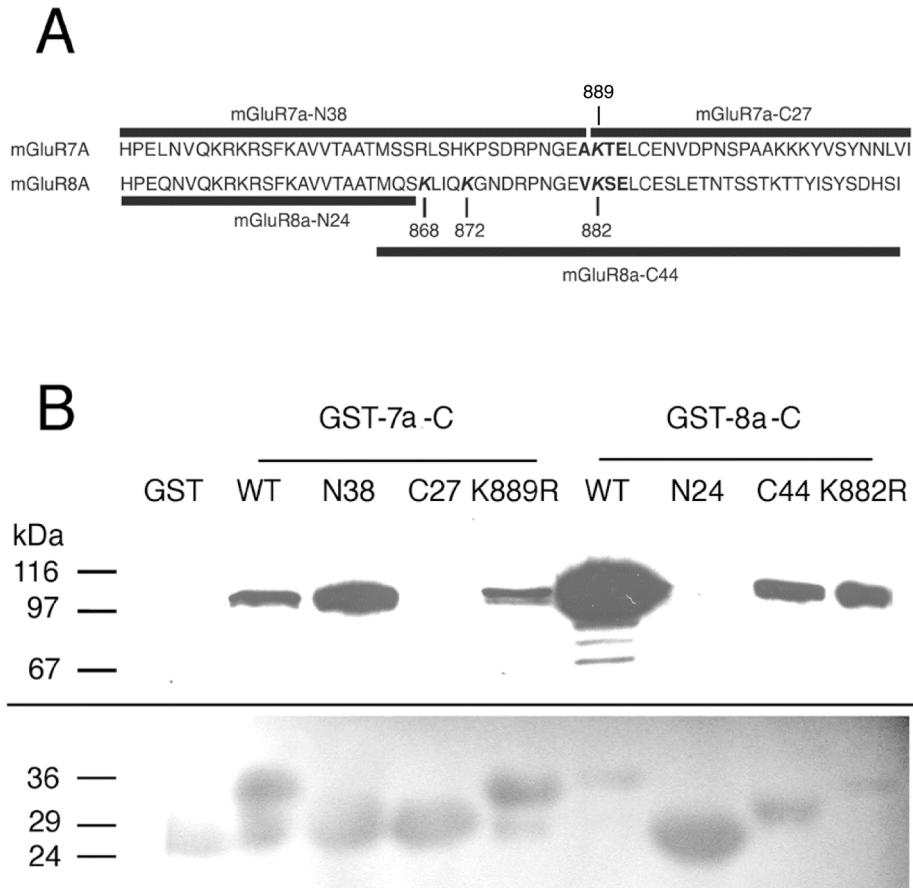


Figure 11. Mapping of the Pias1 binding region of mGluR7a-C and mGluR8a-C.

A: mGluR7a-C and mGluR8a-C truncations and position of the consensus sumoylation motif. Schematic representation of mGluR7a and mGluR8a truncated fragments. The position of the consensus sumoylation motif is indicated in bold. Note that mGluR7a-N38, which binds GFP-Pias1, does not contain the consensus sumoylation site but overlaps with mGluR8a-C44 in the region proximal to the consensus motif. Single or multiple point mutations were introduced into the mGluR8a-C cDNA at all lysine codons that are conserved between mGluR8a and mGluR8b (K868R, K872R, K882R).

B: Mapping of the Pias1 interaction site with mGluR8a-C. Upper panel: GST-fusion proteins of mGluR7a-C and mGluR8a-C immobilized on glutathione-agarose beads were used in pull-down assays with 60 μ l CFP-Pias1 expressed in HEK 293 cells. Western blots were stained with an anti-GFP-antibody. Pias1 failed to bind to GST-mGluR7a-C27 and GST-mGluR8a-N24, whereas the K882R (mGluR8a) and K889R (mGluR7a) substitutions within the consensus sumoylation motif had no effect. Lower panel: Relative amounts of GST or GST-fusion protein bound onto the beads were revealed by Ponceau protein staining. Note that low levels of immobilized GST-mGluR8a-C strongly bound large amounts of CFP-Pias1, while high levels of immobilized GST-mGluR8a-N24 failed to bind under identical conditions.

putative sumoylation site K882. GST-fusion protein levels were normalized and tested semiquantitatively for amount retained on beads (Ponceau S stain on nitrocellulose membrane, Figure 11B, lower panel). Lower protein levels were seen particularly for GST-mGluR7a-N38, GST-mGluR7a-K889R, GST-mGluR8a-C and mGluR8a-K882R. Binding of CFP-Pias1 was found with GST-mGluR7a-N38 and mGluR8a-C44, while the complementary truncations GST-mGluR7a-C27 and GST-mGluR8a-N24 failed to interact. In sequence alignments (Figures 10A and 11A), mGluR7a-N38 and mGluR8a-C44 overlap by 17 amino acids but are only identical in the last 6 residues preceding the consensus sumoylation motif (sequence DRPNGE; see amino acids 875-880 of mGluR8a). We therefore deduce that these residues are important for Pias1 recruitment to group III mGluRs.

3.6 *In vivo* Sumoylation of mGluR8a-C

There are two ways to examine whether a protein can be sumoylated. The first option is to perform *in vitro* sumoylation assays. Here, the substrate protein is incubated with all components of the sumoylation machinery: sumo-1 Δ C4 (matured sumo-1, with a deletion of the last four residues at C-terminus, exposing the Gly-Gly motif to be activated), aos1/uba2 (E1), ube2a (E2) and ATP, Mg²⁺, with or without E3 (e.g. Pias1), at 37 °C for 1-2 h. The resulting sumoylation products can then be detected on Western blots by their increased molecular weight, which is that of the substrate plus the molecular weight of sumo-1, in case of mono-sumoylation. This method is fast, but it needs complicated procedures for purifying all recombinant proteins, some of which are not well expressed in bacteria. In addition, according to the literature, *in vitro* assays do not faithfully reproduce physiological substrate selection mechanisms (Johnson, 2004). A better possibility is therefore to perform *in vivo* sumoylation assays. Here, the substrate protein is cotransfected with sumo-1, with or without the different sumoylation enzymes, into mammalian cells, which then are analysed for sumoylation products. This method needs highly specific antibodies to visualize the sumoylated products. This approach was selected here because it allows visualization mGluR8a-C sumoylation in mammalian cells.

3.6.1 *in vivo* Sumoylation of mGluR8a

To demonstrate whether mGluR8a-C can be sumoylated, I performed *in vivo* sumoylation assays. GFP-mGluR8a-C and the following tagged components of the sumoylation pathway were co-

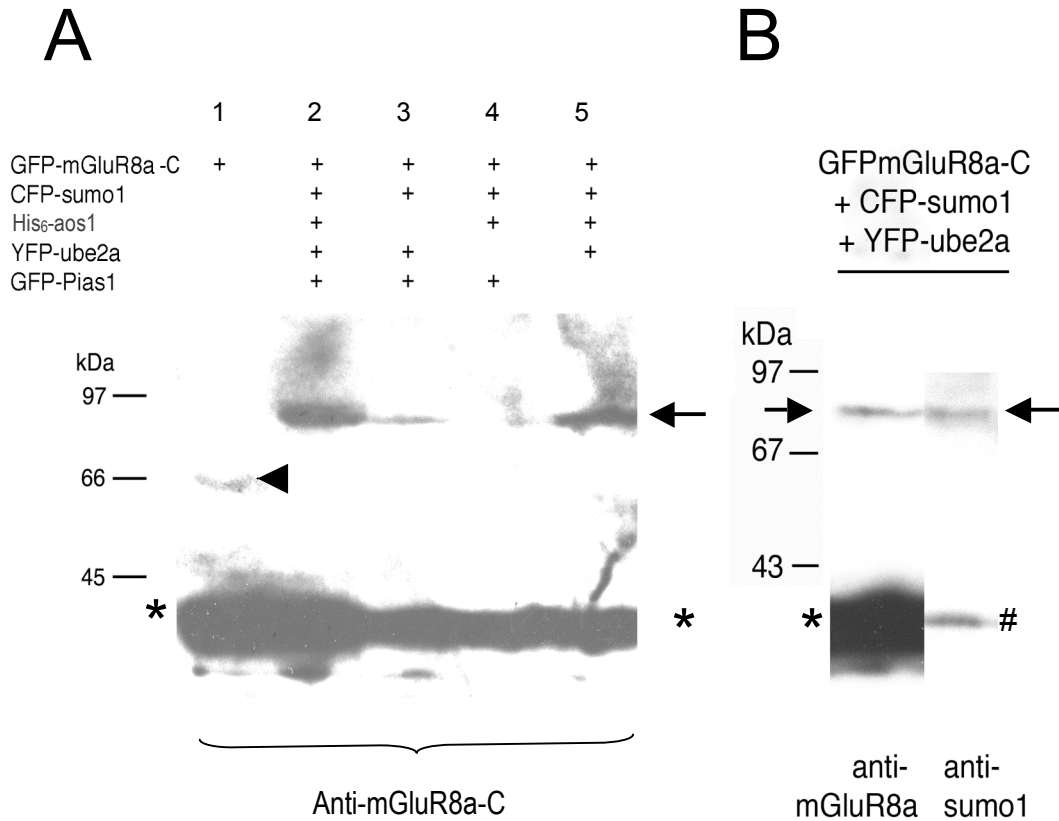


Figure 12. Preliminary analysis of GFP-mGluR8a-C sumoylation *in vivo*. Different combinations of GFP-mGluR8a-C, CFP-sumo-1, His₆-aos1, YFP-ube2a and GFP-Pias1 were transfected into HEK293 cells as indicated. Two days after transfection, the cells were washed and harvested with sample buffer containing SDS and NEM and processed to SDS-PAGE followed by Western blot using either anti-mGluR8a or anti-sumo-1 antibodies.

A. All samples were blotted with anti-mGluR8a antibody. A major GFP-mGluR8a-C (38 kD) band (*) was detected in all lanes.

Lane 1, single transfection of GFP-mGluR8a-C. A very weak extra band (arrow head) was detected corresponding to the molecular weight (≈ 55 kD) of the GFP-mGluR8a-C (38 kD) + 1x sumo-1 (15 kD).

Lane 2-5, cotransfection of GFP-mGluR8a-C, CFP-sumo-1 and the indicated sumoylation enzymes. Except for lane 4 from a transfection without YFP-ube2a, an additional band (arrow) was detected corresponded to the molecular weight (≈ 80 kD) of GFP-mGluR8a-C (38 kD) + 1x CFP-sumo-1 (50 kD).

B. Samples were from triple cotransfected HEK393 cells. The additional 80 kD band (arrow) can be detected by both anti-mGluR8a and anti-sumo-1 antibodies.

Left lane, the 80 kD band was detected by anti-mGluR8a antibody.

Right lane, the same 80 kD band was also detected with anti-sumo-1 antibody on a parallel section of the same nitrocellulose strip as used for left lane. #, free CFP-sumo-1 detected by anti-sumo-1 antibody.

expressed in HEK 293 cells in different combinations: CFP-sumo-1, one of E1-component His₆-aos1, YFP-ube2a (E2) and GFP-Pias1 (E3). After detergent extraction of the transfected cells in the presence of protease inhibitors, the extracts were separated by SDS-PAGE and Western blotted with an antibody against the C-terminal tail of mGluR8. Under these conditions, a significant fraction (about 1-5%) of the mGluR8a-C immunoreactivity present displayed a size shift to approx. 80 kDa, consistent with the addition of a single CFP-sumo-1 molecule (Figure 12A). Parallel Western blotting showed that the 80-kDa band was also recognized by anti-sumo-1 antibody (Figure 12B), thus confirming that this band indeed represented sumoylated GFP-mGluR8a-C. It also suggested that mGluR8a-C was conjugated to a single sumo-1 molecule. Notably, in cells singly transfected with GFP-mGluR8a-C, a much weaker band at about 55 kD was also revealed by anti-mGluR8a antibody. This approximate molecular weight corresponds to the size of GFP-mGluR8a-C conjugated to endogenous sumo-1 (Figure 12A). The 80 kD sumo-1 conjugation product disappeared when YFP-ube2a was omitted from the transfection mixture (lane 4 of Figure 12A). Apparently, ube2a is essential for conjugation. The addition of the aos1,

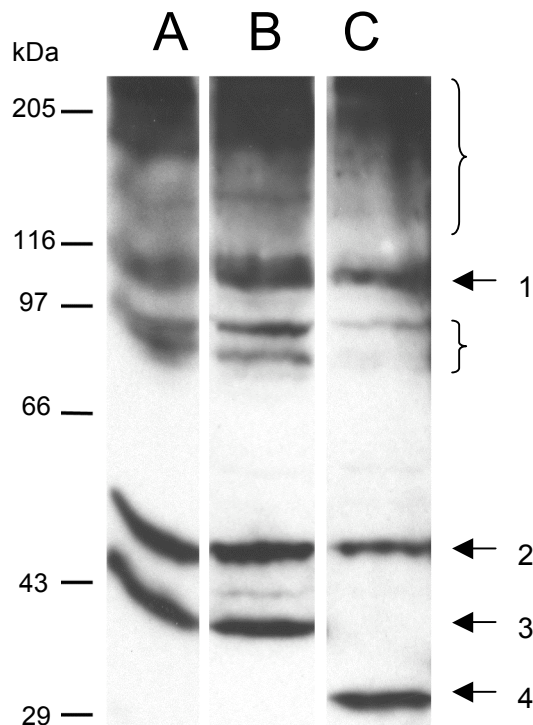


Figure 13. GFP fusion protein expression upon cotransfection. GFP-mGluR8a-C (lane A), GFP-mGluR8b-C (lane B) or GFP (lane C) were cotransfected with CFP-sumo-1, E1-components His₆-aos1, YFP-ube2a (E2) and GFP-Pias1 (E3). The cell extracts were analysed by Western blotting with anti-GFP antibody. 1# indicates GFP-Pias1, 2# YFP-ube2a and 3# GFP-mGluR8a-C (lane A) or GFP-mGluR8b (lane B). 4# corresponds to free GFP (lane C). The remaining bands (in brackets) probably represent other proteins conjugated to CFP-sumo-1.

a component of E1 enzyme, also enhanced the amount of sumoylation product as judged by semiquantitative Western blotting, whereas the addition of E3 had no effect. Analyzing the same

Western blot with anti-GFP antibody showed that all GFP-fused proteins, including GFP-Pias1, were well expressed (Figure 13); this excludes potential expression problems. Alternatively, Pias1 may be endogenously expressed in HEK293 cells. Western blot analysis of HEK293 cell extracts with anti-Pias1 antibody confirmed this idea (Figure 14). Clearly, there was endogenous Pias1 detectable in these cells, which may have been accounted for sumoylation of mGluR8a-C. Although the cotransfection of multiple DNAs mentioned above resulted in sumoylation, it was obvious that the expression level of each protein was low. After successive optimization, the triple cotransfection of sumo-1, mGluR8a-C and ube2a was found to yield the most reproducible results.

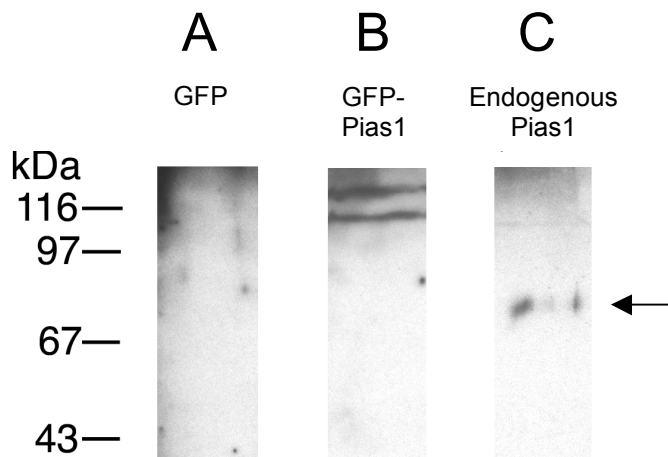


Figure 14. Endogenous expression of Pias1. A and B, an anti-Pias1 antibody was tested for specificity by Western blot of 10 μ l Triton X-100 extracted recombinant proteins expressed in HEK 293 cells. GFP-Pias1 (lane B), but not GFP (lane A), was detected. In the sample of nucleus fraction (P1) of untransfected HEK 293 cells, this antibody stained a band of about 70 kD (arrow), corresponding to the size of endogenous Pias1.

In the various experiments performed in parallel, the results of the sumoylation assay showed considerable variability. This may have been caused by variability in the activity of isopeptidases. There are several proteins in mammalian cells that act as isopeptidase and cut sumo conjugations from its substrates. The isopeptidases are very active. I therefore examined whether the addition of N-ethylmaleimide (NEM), an isopeptidase inhibitor, might improve the results (Suzuki et al., 1999). Fresh aliquots of cells cotransfected with GFP-mGluR8a-C, CFP-sumo-1 and YFP-ube2a were solubilized by 1% Triton X-100, with or without NEM. After centrifugation, SDS-PAGE electrophoresis and Western blot with anti-mGluR8a antibody; only

the pellet treated with NEM displayed a size shift of the mGluR8a-C band indicating sumoylation (Figure 15). This suggests that addition of NEM can inhibit desumoylation to some degree, but not completely, as the supernatant of NEM treated aliquot did not show a band of appropriate molecular weight.

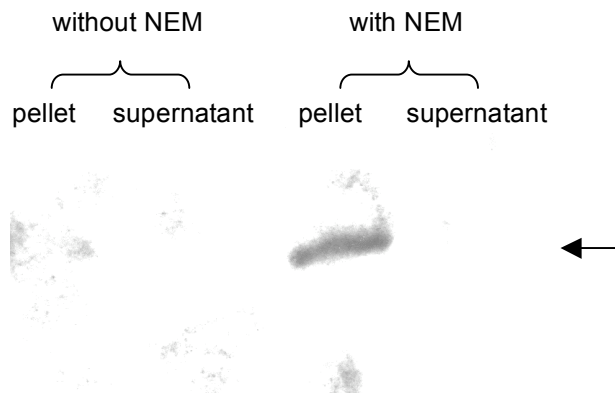


Figure 15. NEM inhibits desumoylation. Fresh aliquots of cells cotransfected with GFP-mGluR8a-C, CFP-sumo-1 and YFP-ube2a were solubilized with 1% (v/v) Triton X-100 and protease inhibitors, with or without NEM for 2 hr. After centrifugation, samples were analysed by SDS-PAGE and Western blotting with anti-mGluR8a-C antibody. Note: arrow refers to the sumoylated GFP-mGluR8a band. GFP-mGluR8a ran out of the gel.

3.6.2 mGluR8a-C Is Sumoylated on Lysine 882

Sumoylation involves the covalent conjugation of the C-terminal of sumo to the ϵ -NH₂ group of a Lys side chain acceptor site. Many but not all of the acceptor Lys residue lie within a consensus sequence Φ KXE/D, where Φ is a large hydrophobic amino acid; K, the Lys residue; X, any amino acid; E/D, glutamate or aspartate. Here, Lys substitutions were introduced to identify the sumoylation site. This method is commonly used to confirm sumoylation of a substrate (Johnson, 2004). Site selection was based on two criteria obtained from the GST pulldown assay: the acceptor Lys should be located within C44 of mGluR8a and conserved in both mGluR8a and mGluR8b. Accordingly, three Lys residues (K868, K872, K882) were selected as candidate sumoylation sites. Substitution of target lysines by equally charged arginines can be used to identify sumoylation motifs while corresponding alanine substitutions have been shown to result in reduced binding of E2 to substrate proteins, like the Ran GTPase-activating protein (RanGAP1) (Sampson et al., 2001). Several KR mutations were made here

including single, double and triple substitutions of the three Lys residues with Arg. All mutations were checked by DNA sequencing (Appendix I).

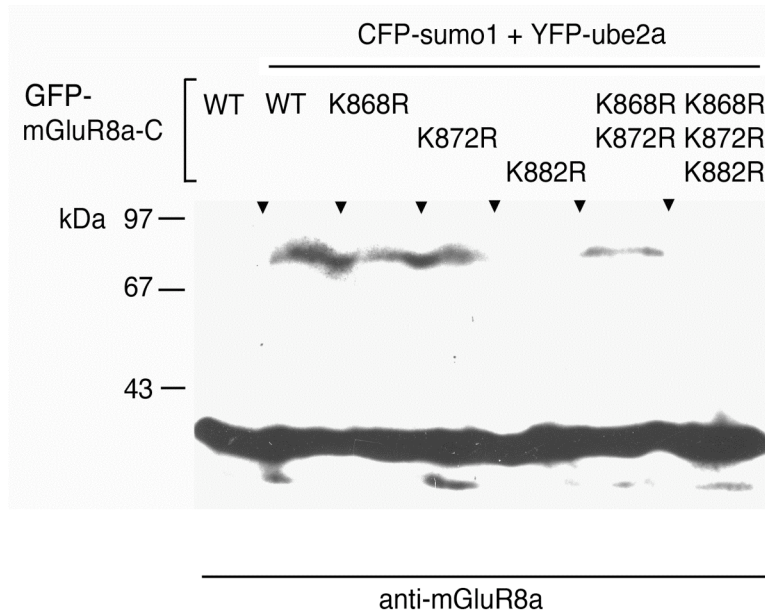


Figure 16. mGluR8a-C is sumoylated on lysine 882. GFP-mGluR8a-C and the indicated CFP- and GFP-tagged enzymes of the sumoylation pathway were co-expressed in HEK 293 cells. 48 h after transfection, cells were harvested with SDS sample buffer supplemented with protease inhibitors and 20 mM N-ethylmaleimide. The extracts were subjected to SDS-PAGE followed by Western blotting with an antibody directed against the mGluR8-CTD. In the presence but not absence of enzymes of the sumoylation cascade, a size shift of mGluR8a-C to ca. 80 kDa, i.e. the approximate size of the mGluR8a-C-CFP-sumo-1 conjugate, was observed. Single or combined arginine substitutions of K882 abolished sumo-conjugation, while substitution of K868 and K872 had no effect.

The results of the sumoylation assays are shown in Figure 16. Modification of mGluR8a-C was abolished upon replacing Lys882 by arginine within the C-terminal tail (for positions of lysine substitutions, see Figure 11A). Triple arginine substitution including K882 also abolished sumo-conjugation, while single or combined substitution of K868 and K872 did not interfere with this modification. Notably, sumo-conjugation did not occur on the neighbouring lysines K868 or K872 when the consensus sumoylation residue K882 had been substituted. Also, K882R substitution or the triple mutation K868R/K872R/K882R did not lead to sumoylation of one of the remaining four lysines in the C-terminal tail of mGluR8a (Figure 16). Thus, in transfected

cells sumoylation of mGluR8a-C occurs specifically at lysine 882 located within the conserved consensus sumoylation motif. Notably, arginine substitution of K882 in mGluR8a-C and of the homologous lysine K889 in mGluR7a-C did not affect binding of CFP-Pias1 in the GST pull-down assay (Figure 11B). This further suggests that the interaction of Pias1 with mGluRs does not depend on an intact sumoylation consensus motif in the C-terminal tail.

3.7 Yeast Two-Hybrid Screen with the C-terminal tail of mGluR4b

During my PhD project, I also performed yeast two-hybrid screens with the C-terminal tail of mGluR4b. The yeast transformation had been performed by Dr. José Airas (see J. Airas, PhD thesis, 2001). Basically, the intracellular C-terminus of mGluR4b had been subcloned into pGilda and used as a bait to screen a rat brain cDNA library in the same way as for mGluR8a-C. The cotransformants were amplified, and aliquots were stored at -70°C . José had analysed a small number of the transformants, and found cDNA encoding SGT (Small Glutamine-rich Tetratricopeptide-repeat-containing protein) and PxF (Peroxisomal Farnesylated protein) as candidate interacting proteins. I joined the project for a more extensive screen.

Table 7: Results of the yeast two-hybrid screen with mGluR4b-C

Candidate interacting proteins	Number of clones	Frequency (%)	Confirmed by Yeast mating?
SGT	70	59,8	+
Proteasome, subunit K	11	9,4	+
PLZF	8	6,8	+
26 S proteasome, subunit S5a	7	6,0	+
PxF	4	3,4	+
14-3-3	3	2,6	-
Transthyretin	2	1,7	+
Zeta crystalin	2	1,7	+
Calmodulin	1	0,9	+
DNA J-like	1	0,9	+
Regulator of sterodogenic factor-1	1	0,9	+
NapI-4	1	0,9	-
Chromosome II, clone mCIT-268-p-2	1	0,9	-
Testis cDNA	1	0,9	+
Pancreas cDNA	1	0,9	-

mGluR4b-C was used as the bait to screen a rat brain cDNA library in the yeast two-hybrid system. The candidate interacting proteins in this list were identified after DNA sequencing of insertions in prey constructs of positive clones .

1.5x10⁸ yeast cells were screened, about 260 clones proven to be positive by Leu- auxotrophy and expression of LacZ. DNA sequencing revealed 15 cDNAs that might correspond to proteins that are candidate interactors for mGluR4b. 60% of the clones represented SGT. 15% of them belonged to proteasomal proteins, either subunit K or subunit S5a. 7% encoded a transcriptional repressor, promyelocytic leukemia zinc-finger protein (PLZF). 3.4% corresponded to PxF. The results are summarized in Table 7.

To confirm the results of the yeast two-hybrid screen, yeast mating was performed with all candidates found. For most of the candidates, again, positive results were obtained (see Table 7). Of these candidate clones, the SGT cDNA was most frequently isolated. SGT has originally been discovered because of its putative interaction with envelope proteins of two viruses (Callahan et al., 1998). It forms complexes with the synaptic proteins CSP (cysteine string protein) and Hsc70 (heat-shock protein 70 cognate), which functions as an ATP-dependent chaperone. Overexpression of SGT in cultured neurons inhibits neurotransmitter release (Tobaben et al., 2001). Furthermore, SGT specifically coimmunoprecipitates with β -amyloid peptide (A $_{\beta}$); and inhibition of SGT expression results in suppression of toxicity associated with A $_{\beta}$ expression (Fonte et al., 2002).

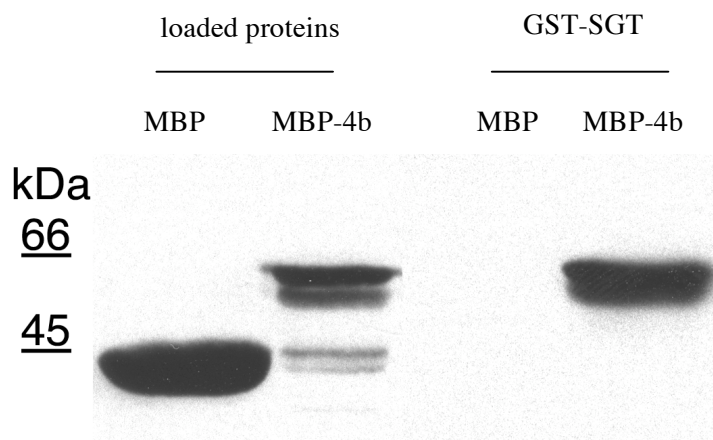


Figure 17: A GST pull-down verified the interaction between mGluR4b and SGT. GST-SGT was immobilized on glutathione-agarose beads and incubated with bacterial extracts with MBP or MBP-fusion of mGluR4b-C. After washing with incubation buffer, bound proteins were eluted with SDS-sample buffer, and aliquots analyzed by SDS-PAGE followed by Western blotting with an anti-MBP antibody. The amount of samples loaded onto the left slots as control was about 20% of that used in the pull-down assay.

Thus, a GST pulldown was performed to examine whether overexpressed recombinant SGT protein would bind to mGluR4b-C. GST-SGT was immobilized on Glutathione beads, and incubated with MBP-mGluR4b-C or MBP. After washing, MBP-mGluR4b-C was retained on the beads as indicated by Western blotting using anti-MBP antibody, while MBP alone failed to bind the fusion protein (Figure 17). This is considered to be a specific interaction between SGT and mGluR4b-C.

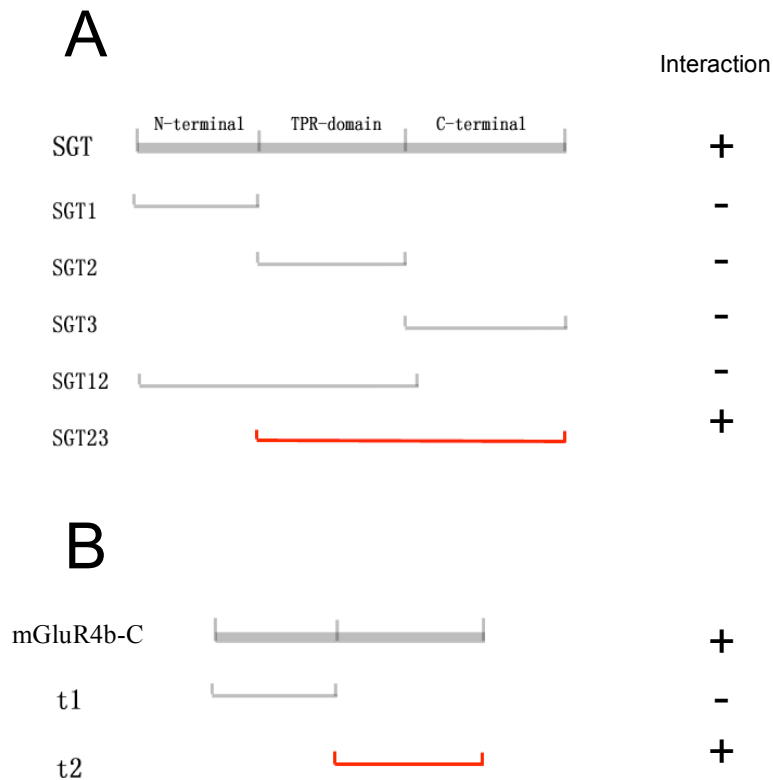


Figure 18: Interaction of SGT and mGluR4b-C fragments in the yeast two-hybrid assay. Different fragments were generated by PCR and inserted into the plasmids used for yeast-two-hybrid screening. A, SGT fragments were tested for interaction with full-length mGluR4b-C. B, mGluR4b tail fragments were tested with full-length SGT, respectively.

+, interaction was detected in binary two-hybrid assay.

-, no interaction was detected in binary two-hybrid assay.

I also mapped the interaction domains of SGT and mGluR4b-C by yeast two-hybrid assays. As shown in Figure 18, SGT contains a TPR (Tetratricopeptide-repeat) domain between its N- and

C- domains. Five cDNA fragments of SGT were generated by PCR, including three domains and two large fragments including the TPR domain and the N- and C-terminal regions, respectively (Figure 18). The mGluR4b tail sequence was divided into 2 fragments according to second structure prediction. The SGT fragments were cloned into the prey vector pJG4-5, and the mGluR4b-C fragments into the bait vector pGilda. Yeast two-hybrid assays were performed using full-length SGT and the mGluR4b-C fragments, or full-length mGluR4b-C and SGT fragments. The results are summarized in Figure 18 and show that the C-terminal half of mGluR4b-C interacted with SGT, and that both the TPR domain and the carboxyterminal region of SGT were required for this interaction.

3.8 Database Search for Genomic mGluR4b Sequences

When the experiments described above had been performed, a paper from Dr. Ferraguti's lab was published that shed serious doubts on the existence of the splice variant mGluR4b (Corti et al., 2002). These authors had made numerous unsuccessful attempts to amplify by RT-PCR the sequence corresponding to the published C-terminus of mGluR4b from several rat brain areas (cerebellar cortex, olfactory bulb, neocortex and hippocampus). In contrast, amplification of the mGluR4a sequence was always achieved. Apparently other laboratories had also failed to amplify mGluR4b. Hence, I performed a profound search of the human genome database but no evidence for the existence of the mGluR4b splice form was found.

mGluR4b had been originally cloned from a rat cDNA library and published in 1997 (Thomsen et al., 1997). According to that report, the mGluR4b cDNA was identical to that of mGluR4a, but contained a 620-nucleotide deletion, which started just after the seventh transmembrane domain. So mGluR4b had a completely different predicted C-terminal tail compared to mGluR4a. The corresponding DNA and amino acid sequences are shown in Figure 19. We hence examined the rat genome database for mGluR4 gene. The last several exons and introns are shown in Figure 20; the 620 nucleotide deletion extends over the last two exons of the mGluR4 gene, but neither of the termini of the deletion fragment contains a typical exon/intron boundary signal (GT---AG); hence mGluR4b cannot be an alternative splice variant of mGluR4a. Also, a stringent BLAST search of EST sequences did not reveal any other homologues, except for mGluR4a and the published mGluR4b variant. We therefore have to conclude that the mGluR4b variant does not exist, but represents a cloning artifact. Hence, only one form of mGluR4 exists, mGluR4a.

7th transmembrane domain

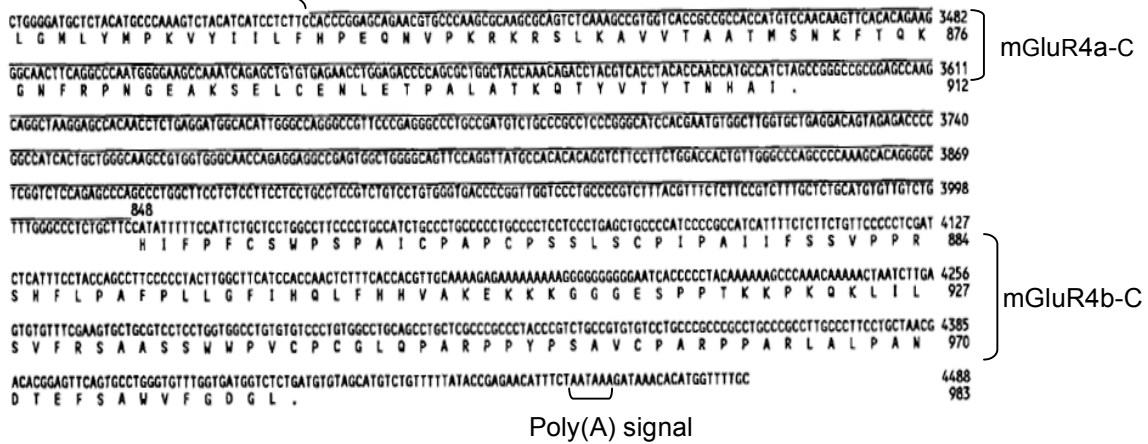


Figure 19. The C-terminal tail sequences of mGluR4a and mGluR4b. The upper brace shows the position of the predicted seventh transmembrane domain. The overline shows the 620 nucleotide deletion described to yield mGluR4b-C. The bottom bracket shows the poly(A) signal. The predicted C-terminal domain sequences of mGluR4a and b are indicated. Modified from Thomsen et al. (1997).

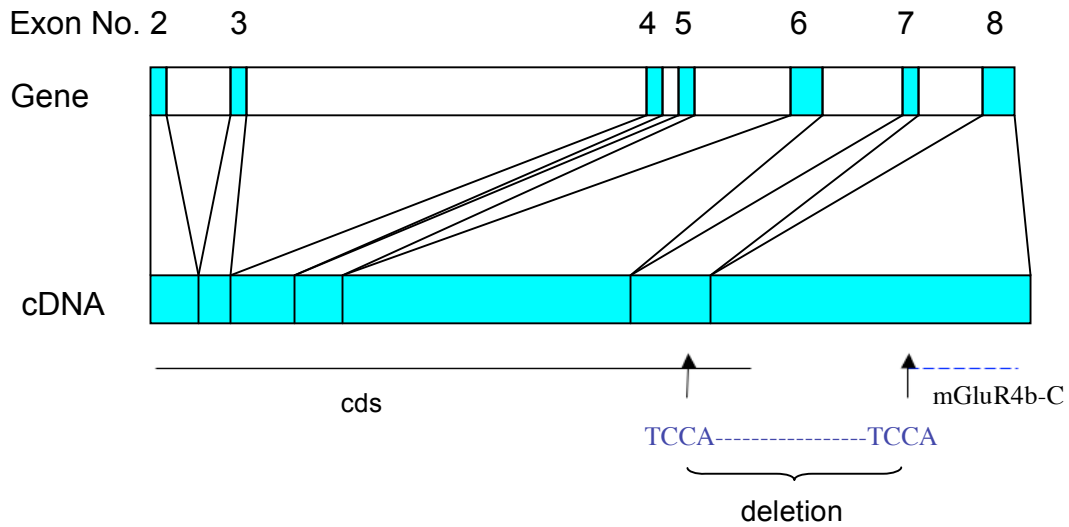


Figure 20. Structures of the last seven exons of the mGluR4 gene and the corresponding cDNA. The deletion thought to create mGluR4b lies inside the last 2 exons and does not contain typical intron boundary signals (5' GT---AG 3').

4 DISCUSSION AND PROSPECTS

To identify proteins that may interact with mGluR8, yeast two-hybrid screens were performed with the C-terminal tails of both mGluR8a and mGluR8b as baits. About thirty candidate interacting proteins were found, five of them related to sumoylation: Pias1, Piasx β , Pias γ , ube2a and sumo-1. Yeast mating verified that all these proteins interact with the C-termini of both mGluR8a and mGluR8b. GST pulldown and binary yeast two-hybrid assays revealed that Pias1 was the most prominent interaction partner not only for mGluR8, but all group III mGluRs. Binary yeast two-hybrid assays argue against the possibility of group II mGluRs also serving as interacting partners for Pias1. *In vivo* sumoylation assays, combined with site-directed mutagenesis, confirmed that the C-terminal tail of mGluR8a could be sumoylated at K882. Of four components (one modifier + three enzymes) in the sumo-conjugation pathway, only E1 was not found in the yeast two-hybrid screens. This is reasonable because E1 does not interact with substrates directly. E1 acts in the sumoylation pathway by activating sumo, then passing it to the conjugating enzyme E2 (See Appendix II, Figure 1).

Table 8. Prediction of possible sumoylation sites of full-length mGluR8a

No.	Position*	Group	Score
1	K576	QLIPI IKLE WHSPW	0.94
2	K882	RPNGE VKSE LCESL	0.93
3	K68	VPCGE LKKE KGIHR	0.91
4	K741	KARGV LKCD ISDLS	0.91
5	K498	TNQLH LKVE DMQWA	0.91
6	K57	LFPVH AKGE RGVPC	0.79
7	K170	NILRL FKIP QISYA	0.74
8	K252	CIAQS QKIP REPRP	0.39

*AA1-584 are predicted to be extracellular N-terminal region.

4.1 Prediction of Full-length mGluR8 Sumoylation

In vivo sumoylation assays revealed that GFP-mGluR8a-C was conjugated to sumo-1 upon overexpression of sumo-1 and the sumoylation machinery in mammalian cells. An intriguing question would be whether the full-length mGluR8 is also sumoylated in the same way. A prediction of sumoylation sites of full-length rat mGluR8a (AAB09537) revealed eight possible sumoylation sites (<http://www.abgent.com/doc/sumoplot>, Table 8). Six of them are located in

the extracellular N-terminal region, and one in the second extracellular loop; thus all these sites are not available for conjugation by sumo-1 (Figure 21). K882 is the only predicted sumoylation site that lies intracellularly and has been identified as a sumoylation site in the current study. Therefore it is likely that K882 is the only sumoylation site of full-length mGluR8.

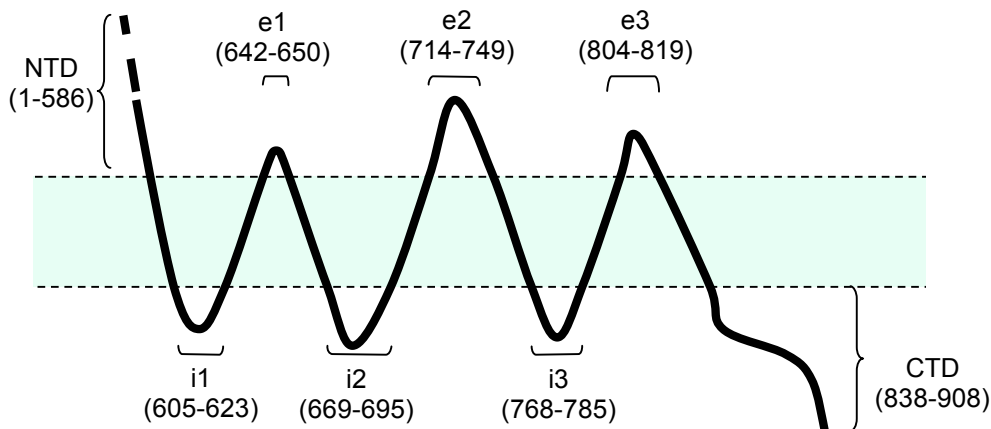


Figure 21. Prediction of transmembrane domain of rat mGluR8a (AAB09537). Protein sequence of full-length mGluR8a was submitted to the following PredictProtein Server:

<http://www.embl-heidelberg.de/predictprotein/predictprotein.html>

The prediction results are schematized in the figure. N- and C-terminal regions are indicated as NTD and CTD, respectively. Extracellular- (e1-3) and intracellular (i1-3) loops are indicated with brackets and numbers for AA sequence range.

4.2 Interacting Motifs of mGluRs and Pias1

The pull-down assays with truncations or point mutants of the mGluR7a- and mGluR8a-C-terminal tails showed that binding of Pias1 to the receptor C-termini can occur independently of the presence of the proposed sumoylation site (mGluR7a-N38) or the target lysine residue (mGluR8a-K882R, mGluR7a-K889R). Thus, it seems that a minimal binding sequence may exist outside of the consensus conjugation site. By using partial constructs of mGluR8a-C and mGluR7a-C, this minimal binding sequence was deduced to reside within six amino acids preceding the consensus conjugation site (mGluR8a 875-880, DRPNGE), a motif that is conserved among mGluR7 and mGluR8 isoforms and, to a lesser extent, in mGluR4. Notably,

Pias1 binding was also found with mGluR6 in both yeast two-hybrid and pull-down assays. Among group III mGluRs, mGluR6 is unusual for several reasons: it is localized postsynaptically, is exclusively expressed in retina and lacks the ability to interact with Ca^{2+} /calmodulin, which recognizes all other group III mGluRs (O'Connor et al., 1999; El Far et al., 2000; Airas et al., 2001). mGluR6 also lacks the consensus sumo-conjugation motif and harbours only two (PxxE) of the six amino acids within the DRPNGE motif common to all other group III mGluRs. If mGluR6 shares the motif for binding Pias1 with mGluR4, 7 and 8, these two amino acids may be sufficient to mediate Pias1-binding. Alternatively, other more homologous motifs, including three-dimensional determinants, of the receptor C-terminal tails that are also present in mGluR6 may contribute to the binding of Pias1. It is also possible that these receptors bind Pias1 at different regions. Group II mGluRs, which lack both the consensus sumoylation site and the proposed Pias1-interaction domain, did not show any interaction with Pias1 in the yeast two-hybrid system.

The domains of Pias1 that mediate the interaction with group III mGluRs are not defined yet. The fact that our two-hybrid screen isolated a Pias1 fragment encoding only the C-terminal amino acids 514-721 suggests that binding to the target sequence occurs downstream of the SP-RING domain (residues 401-453) of Pias1 that is supposed to bind E2 (Kahyo et al., 2001).

4.3 Possible Functions of mGluR Sumoylation

An important question is what the physiological consequences of sumo-modification of mGluR8 are. As no results from the current research can answer this question directly, some possibilities are raised here for consideration in the future.

4.3.1 Alternative 1: Sumoylation Antagonizes other Modifications

Lysine residues act as acceptors not only for sumo modification but also for ubiquitination and other ubiquitin-like modification reactions; moreover they are also sites of methylation and acetylation (Johnson, 2004; Hay, 2005). Unlike sumoylation that happens mostly at highly conserved motifs, ubiquitination, acetylation or methylation sites are not so restricted (DiAntonio and Hicke 2004; Roth et al. 2001; Cheng et al. 2005). Acetylation and methylation are common histone protein modifications (Cheng et al., 2005; Martin-Ruiz et al., 2001). They have not been reported to modify mGluR8. Sumoylation has been shown to antagonize ubiquitination of the

same Lys residues of transcription factor NF- κ B (Desterro et al., 1998), NF- κ B essential modulator (NEMO) (Hay, 2004, 2005) and proliferating cell nuclear antigen (PCNA) (Stelter and Ulrich, 2003). If antagonism between ubiquitination and sumoylation exists at mGluR8a, there should be ubiquitination at this receptor, or at least at some other mGluRs. An ubiquitin E3 ligase, the mammalian homologue of *Drosophila* seven in absentia (Siah-1A), has been shown to interact with group I mGluRs within the region that also interacts with calmodulin (Hu et al., 1999; Ishikawa et al., 1999). The binding of Siah-1A blocks calmodulin binding and mediates ubiquitination and subsequent degradation of group I mGluRs (Ishikawa et al., 1999; Moriyoshi et al., 2004). Thus, Siah1A is considered to be a selective ubiquitin ligase that mediates ubiquitination-dependent degradation of group I mGluRs and thus contributes to their posttranslational down-regulation (Moriyoshi et al., 2004). As binding of calmodulin is also common to Group III mGluRs and plays an important role in mGluR signalling (El Far and Betz, 2002), it is possible that the ubiquitination mediated blockade of calmodulin signalling and degradation of the receptors also happens to group III mGluRs. As the interaction between mGluR7a and Siah-1A was not proven by yeast two-hybrid (Ishikawa et al., 1999), it is possible that some other ubiquitin E3 ligase may bind and trigger ubiquitination of the receptor. In this case, the binding of Pias proteins and subsequent sumoylation may interfere with ubiquitination. Besides, it has been shown that PKA directly phosphorylates mGluR4a, mGluR7a and mGluR8a at single conserved serine residues within the N-terminal region of their tail domains (Cai et al., 2001). It is not known, but possible, that the binding of Pias1 to the center of mGluR8a-C is related to binding of phosphorylation and dephosphorylation enzymes to somewhere of mGluR8a-C.

4.3.2 Alternative 2: Sumoylation Interferes with Other Binding Proteins

The C-termini of mGluRs are the binding sites for many proteins related to different functions of the receptors: targeting, functional recycling, interaction with the cytoskeleton, membrane assembly, allosteric activation and signaling modulation of the receptors (Figure 22) (Fagni et al. 2004). Not many binding partners of mGluR8a have been identified yet. It is known that N-terminal to the sumoylation site there are binding sites for G-proteins and CaM, which are supposed to be important for mGluR signalling (El Far et al., 2001), as discussed above. Interestingly, the binding site of Pias1 is near to that of filamin A, a protein related to the

cytoskeleton (Enz, R. 2002. Figure 22). Thus it appears possible that sumo conjugation may cause detachment of mGluRs from the cytoskeleton, thereby allowing for internalization or redistribution of the receptors.

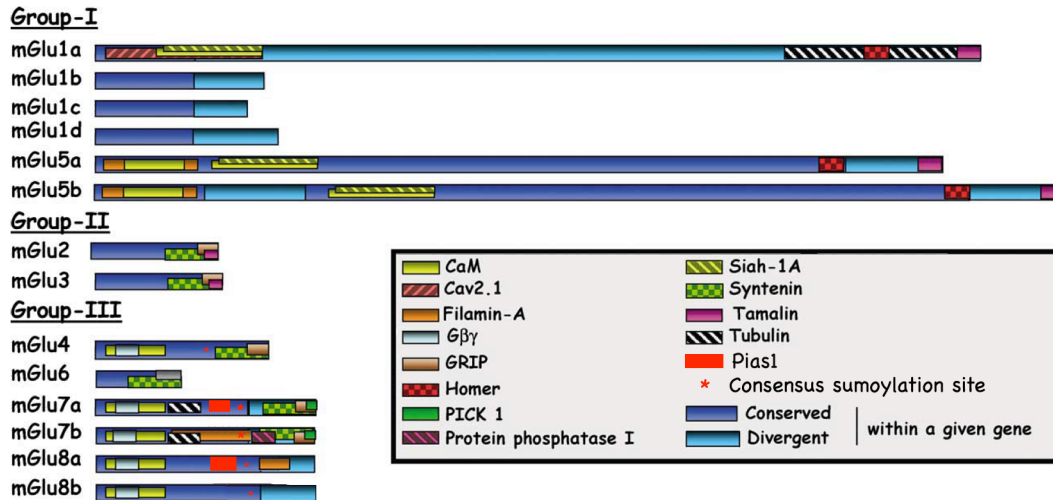


Figure 22. Binding domains of mGluRs. Modified from Fagni et al. (2004). The figure represents the C-terminus of the three groups of mGluRs. The dark and light blue bands indicate the homologous and divergent amino acid sequences within a given *mGlu* gene. Colored boxes represent the interaction domains of the indicated proteins. Calmodulin competes with Siah-1A on mGlu1a, mGlu5a and mGlu5b receptors, and with Gβγ subunits on mGlu4, mGlu7a, mGlu7b, mGlu8a and mGlu8b receptors. Other overlapping protein binding domains exist on mGlu1a (homer, tamalin and tubulin), mGlu5a and mGlu5b (calmodulin with filamin-A), mGlu2, mGlu3 and mGlu4 (syntenin, GRIP, PICK1 and tamalin), but whether or not these protein bindings are competitive has not been established. GST pull-down assays showed interaction between tamalin and group-II mGluRs, but co-immunoprecipitation experiments obtained from rat brain extracts did not confirm these interactions. Surprisingly, interactions of syntenin and GRIP with mGlu4 and mGlu7b were found in GST pull-down, but not in yeast two-hybrid screen experiments. *Abbreviations:* CaM, Calmodulin; Siah-1A, seven in absentia homolog-1A; GRIP, glutamate receptor interacting protein; PICK1, protein interacting with C kinase 1. Tamalin, syntenin, GRIP and PICK1 are PDZ domain-containing proteins.

4.4 Pias 1 may function as an Adaptor in the Sumoylation of mGluR8

Sumo-1, ube2a and Pias proteins were all found in the yeast two-hybrid screens, but only Pias proteins were confirmed by GST pulldown to interact with C-termini of mGluR8a mGluR8b, whereas recombinant ube2a and sumo-1 failed to bind mGluR8a-C in these assays. This is

consistent with the role each protein plays in the sumoylation pathway. Sumo-1 is the modifier; three enzymes catalyze its conjugation to a substrate, so no direct interaction between sumo and the substrate is needed for sumoylation. Nevertheless, an interaction is required between the sumo molecule and the substrate on the areas around the isopeptide bond, which is at least permissive for bond formation. This interaction can be detected by the highly sensitive NMR chemical shift perturbation assay (Song et al., 2004). However, such an interaction may be too weak to be detected in GST-pulldown, especially under the stringent washing conditions used in the current experiments. The identification of sumo-1 as an interacting protein of mGluR8b in the yeast two-hybrid screen and of both mGluR8a and mGluR8b in the yeast mating assays might have resulted from sumo conjugation of the baits in yeast. The mammalian sumo-1 protein has been shown to function in yeast cells because it can rescue the lethality of the *smt3* deletion yeast mutant (Takahashi et al., 1999).

The sumoylation conjugating E2 enzyme ube2a functions as an intermediate in the sumoylation pathway: it accepts sumo from E1 and transfers it to the substrate with the help of E3. Ube2a may be able to bind the substrates via their sumoylation consensus sequences Φ KXE/D, but the interaction is considered to be weak and insufficient for efficient modification (Pichler et al., 2004). Most proteins are sumoylated efficiently only in the presence of E3 ligases (Pichler et al., 2004). The interaction between ube2a and the mGluR8 C-terminal tails detected in the yeast two-hybrid screens could be mediated by some other proteins in yeast cells, e.g. siz1 and siz2 that are abundant and mediate nearly all SMT3¹ conjugation in yeast.

Pias1 and Piasy showed strong interaction with the C-terminal tails of mGluR8a/b in both the yeast two-hybrid screens and GST-pulldown assays. The interacting fragments of all Pias proteins found here are their C-terminal regions. This is consistent with many other observations which established the C-terminal domains of Pias proteins as important interaction regions for sumoylation substrates (Johnson, 2004). Hence, Pias proteins are thought to act as adaptors in the sumoylation pathway. They recruit the substrates through their C-terminal, or in fewer cases, N-terminal domains, and take them to the conjugating enzyme E2 by their RING domains interacting with E2.

¹ SMT3: yeast homologue of sumo-1. For more information, see the appendix II review.

4.5 Other Candidates

There are some other proteins that were found in the yeast two-hybrid screens, but here have not been studied further in this thesis.

4.5.1 Faf1 and Hipk3

Faf1 (Fas-associated factor 1) was found as a candidate interacting protein of mGluR8b-C, and Hipk3 (homeodomain-interacting protein kinase 3) of both mGluR8a-C and mGluR8b-C, in yeast two-hybrid screens. Both Hipk3 and Faf1 interact with the cell surface death receptor Fas that leads to apoptosis (Rochat-Steiner et al., 2000; Ryu et al., 2003). Thus, Faf1 and HIKP3 may link mGluR8 to a function in cell fate determination. This seems to be consistent with the report that mGluR8-deficient mice are about 8% heavier than their wild-type age-matched controls after reaching 4 weeks of age (Duvoisin et al., 2005). Notably, Pias1 KO mice also show a size change: they are smaller than their wild type littermates (Liu et al., 2004). Although Pias1 is an E3 ligase for many proteins, it will be interesting to see whether the weight changes after knockout of these two genes might be related; and especially, whether Faf1 and HIKP3 trigger the molecular machinery which controls animal weight.

4.5.2 PKAi

It is known that cAMP-dependent protein kinase (PKA) signalling is important for mGluR8 regulation. mGluR8 has been shown to be phosphorylated by PKA, and activation of PKA by forskolin inhibits group III mGluR-mediated responses at glutamatergic synapses in the hippocampus (Cai et al., 2001). *In vivo* microdialysis showed that intra-periaqueductal gray (PAG) perfusion of (S)-3,4-DCPG, a selective agonist of mGlu8 receptor, increased glutamate and decreased GABA extracellular concentrations (Marabese et al., 2005). The effect was abolished by intra-PAG perfusion with N-[2-(p-bromocinnamyl-amino) ethyl]-5-isoquinoline-sulfonamide dihydrochloride (H-89), a PKA inhibitor (Marabese et al., 2005). The finding of PKAi (cAMP-dependent protein kinase inhibitor) as an interaction partner of mGluR8a in the yeast two-hybrid screen performed here suggests that there are endogenous proteins that may antagonize the effect of PKA by directly interacting with the receptor. Further investigations unravel how mGluR is coupled to the dual but diverging pathways of PKA signalling.

5 REFERENCES

- Aiba A, Chen C, Herrup K, Rosenmund C, Stevens CF, Tonegawa S (1994a) Reduced hippocampal long-term potentiation and context-specific deficit in associative learning in mGluR1 mutant mice. *Cell* 79:365-375.
- Aiba A, Kano M, Chen C, Stanton ME, Fox GD, Herrup K, Zwingman TA, Tonegawa S (1994b) Deficient cerebellar long-term depression and impaired motor learning in mGluR1 mutant mice. *Cell* 79:377-388.
- Airas JM, Betz H, El Far O (2001) PKC phosphorylation of a conserved serine residue in the C-terminus of group III metabotropic glutamate receptors inhibits calmodulin binding. *FEBS Lett* 494:60-63.
- Bradbury MJ, Campbell U, Giracello D, Chapman D, King C, Tehrani L, Cosford ND, Anderson J, Varney MA, Strack AM (2005) Metabotropic glutamate receptor mGlu5 is a mediator of appetite and energy balance in rats and mice. *J Pharmacol Exp Ther* 313:395-402.
- Cai Z, Saugstad JA, Sorensen SD, Ciombor KJ, Zhang C, Schaffhauser H, Hubalek F, Pohl J, Duvoisin RM, Conn PJ (2001) Cyclic AMP-dependent protein kinase phosphorylates group III metabotropic glutamate receptors and inhibits their function as presynaptic receptors. *J Neurochem* 78:756-766.
- Callahan MA, Handley MA, Lee YH, Talbot KJ, Harper JW, Panganiban AT (1998) Functional interaction of human immunodeficiency virus type 1 Vpu and Gag with a novel member of the tetratricopeptide repeat protein family. *J Virol* 72:5189-5197.
- Cheng X, Collins RE, Zhang X (2005) Structural and sequence motifs of protein (histone) methylation enzymes. *Annu. Rev. Biophys. Biomol. Struct.* 34:267-94
- Ciccarelli R, Di Iorio P, Bruno V, Battaglia G, D'Alimonte I, D'Onofrio M, Nicoletti F, Caciagli F (1999) Activation of A(1) adenosine or mGlu3 metabotropic glutamate receptors enhances the release of nerve growth factor and S-100beta protein from cultured astrocytes. *Glia* 27:275-81.
- Conn PJ, Pin JP (1997) Pharmacology and functions of metabotropic glutamate receptors. *Annu Rev Pharmacol Toxicol* 37:205-237.
- Corti C, Aldegheri L, Somogyi P, Ferraguti F (2002) Distribution and synaptic localisation of the metabotropic glutamate receptor 4 (mGluR4) in the rodent CNS. *Neuroscience* 110:403-420.
- Corti C, Restituito S, Rimland JM, Brabet I, Corsi M, Pin JP, Ferraguti F (1998) Cloning and characterization of alternative mRNA forms for the rat metabotropic glutamate receptors mGluR7 and mGluR8. *Eur J Neurosci* 10:3629-3641.
- Desterro JM, Rodriguez MS, Hay RT (1998) SUMO-1 modification of IkappaBalpha inhibits NF-kappaB activation. *Mol Cell* 2:233-239.
- DiAntonio A, Hicke L (2004) Ubiquitin-dependent regulation of the synapse. *Annu Rev Neurosci* 27:223-246.
- Duvoisin RM, Zhang C, Ramonell K (1995) A novel metabotropic glutamate receptor expressed in the retina and olfactory bulb. *J Neurosci* 15:3075-3083.
- Duvoisin RM, Zhang C, Pfankuch TF, O'Connor H, Gayet-Primo J, Quraishi S, Raber J (2005) Increased measures of anxiety and weight gain in mice lacking the group III metabotropic glutamate receptor mGluR8. *Eur J Neurosci* 22:425-436.
- El Far O, Airas J, Wischmeyer E, Nehring RB, Karschin A, Betz H (2000) Interaction of the C-terminal tail region of the metabotropic glutamate receptor 7 with the protein kinase C substrate PICK1. *Eur J Neurosci* 12:4215-4221.

- El Far O, Betz H (2002) G-protein-coupled receptors for neurotransmitter amino acids : C-terminal tails, crowded signalosomes. *Biochem. J.* 365:329-336
- El Far O, Bofill-Cardona E, Airas JM, O'Connor V, Boehm S, Freissmuth M, Nanoff C, Betz H (2001) Mapping of calmodulin and Gbetagamma binding domains within the C-terminal region of the metabotropic glutamate receptor 7A. *J Biol Chem* 276:30662-30669.
- Enz R (2002) The actin-binding protein Filamin-A interacts with the metabotropic glutamate receptor type 7. *FEBS Lett* 514:184-188.
- Fagni L, Ango F, Perroy J, Bockaert J (2004) Identification and functional roles of metabotropic glutamate receptor-interacting proteins. *Seminars in Cell & Developmental Biology* 15:289-298
- Fonte V, Kapulkin V, Taft A, Fluet A, Friedman D, Link CD (2002) Interaction of intracellular beta amyloid peptide with chaperone proteins. *Proc Natl Acad Sci U S A* 99:9439-9444.
- Gill G (2004) SUMO and ubiquitin in the nucleus: different functions, similar mechanisms? *Genes Dev* 18:2046-2059.
- Hay RT (2004) Modifying NEMO. *Nat Cell Biol* 6:89-91.
- Hay RT (2005) SUMO: a history of modification. *Mol Cell* 18:1-12.
- Iacovelli L, Capobianco L, Iula M, Di Giorgi Gerevini V, Picascia A, Blahos J, Melchiorri D, Nicoletti F, De Blasi A (2004) Regulation of mGlu4 metabotropic glutamate receptor signaling by type-2 G-protein coupled receptor kinase (GRK2). *Mol Pharmacol* 65:1103-1110.
- Ishikawa K, Nash SR, Nishimune A, Neki A, Kaneko S, Nakanishi S (1999) Competitive interaction of seven in absentia homolog-1A and Ca²⁺/calmodulin with the cytoplasmic tail of group 1 metabotropic glutamate receptors. *Genes Cells* 4:381-390.
- Johnson ES (2004) Protein modification by SUMO. *Annu Rev Biochem* 73:355-382.
- Kahyo T, Nishida T, Yasuda H (2001) Involvement of PIAS1 in the sumoylation of tumor suppressor p53. *Mol Cell* 8:713-718.
- Koulen P, Brandstatter JH (2002) Pre- and Postsynaptic Sites of Action of mGluR8a in the mammalian retina. *Invest Ophthalmol Vis Sci* 43:1933-1940.
- Linden AM, Bergeron M, Baez M, Schoepp DD (2003a) Systemic administration of the potent mGlu8 receptor agonist (S)-3,4-DCEPG induces c-Fos in stress-related brain regions in wild-type, but not mGlu8 receptor knockout mice. *Neuropharmacology* 45:473-483.
- Linden AM, Baez M, Bergeron M, Schoepp DD (2003b) Increased c-Fos expression in the centromedial nucleus of the thalamus in metabotropic glutamate 8 receptor knockout mice following the elevated plus maze test. *Neuroscience* 121:167-178.
- Linden AM, Johnson BG, Peters SC, Shannon HE, Tian M, Wang Y, Yu JL, Koster A, Baez M, Schoepp DD (2002) Increased anxiety-related behaviour in mice deficient for metabotropic glutamate 8 (mGlu8) receptor. *Neuropharmacology* 43:251-259.
- Liu B, Mink S, Wong KA, Stein N, Getman C, Dempsey PW, Wu H, Shuai K (2004) PIAS1 selectively inhibits interferon-inducible genes and is important in innate immunity. *Nat Immunol* 5:891-898.
- Liu MT, Rothstein JD, Gershon MD, Kirchgessner AL (1997) Glutamatergic enteric neurons. *J Neurosci* 17:4764-4784.
- Lu YM, Jia Z, Janus C, Henderson JT, Gerlai R, Wojtowicz JM, Roder JC (1997) Mice lacking metabotropic glutamate receptor 5 show impaired learning and reduced CA1 long-term potentiation (LTP) but normal CA3 LTP. *J Neurosci* 17:5196-5205.

- Malherbe P, Kratzeisen C, Lundstrom K, Richards JG, Faull RL, Mutel V (1999) Cloning and functional expression of alternative spliced variants of the human metabotropic glutamate receptor 8. *Brain Res Mol Brain Res* 67:201-210.
- Marabese I, de Novellis V, Palazzo E, Mariani L, Siniscalco D, Rodella L, Rossi F, Maione S (2005) Differential roles of mGlu8 receptors in the regulation of glutamate and gamma-aminobutyric acid release at periaqueductal grey level. *Neuropharmacology* 49 Suppl:157-166.
- Marchese A, Benovic JL (2004) Ubiquitination of G-protein-coupled receptors. *Methods Mol Biol* 259:299-305.
- Martin-Ruiz R, Puig MV, Celada P, Shapiro DA, Roth BL, Mengod G, Artigas F (2001) Control of serotonergic function in medial prefrontal cortex by serotonin-2A receptors through a glutamate-dependent mechanism. *J Neurosci* 21:9856-9866.
- Masu M, Iwakabe H, Tagawa Y, Miyoshi T, Yamashita M, Fukuda Y, Sasaki H, Hiroi K, Nakamura Y, Shigemoto R, et al. (1995) Specific deficit of the ON response in visual transmission by targeted disruption of the mGluR6 gene. *Cell* 80:757-765.
- Masugi M, Yokoi M, Shigemoto R, Muguruma K, Watanabe Y, Sansig G, van der Putten H, Nakanishi S (1999) Metabotropic glutamate receptor subtype 7 ablation causes deficit in fear response and conditioned taste aversion. *J Neurosci* 19:955-963.
- Mishra RK, Jatiani SS, Kumar A, Simhadri VR, Hosur RV, Mittal R (2004) Dynamins interact with members of the sumoylation machinery. *J Biol Chem* 279:31445-31454.
- Moriyama Y, Hayashi M, Yamada H, Yatsushiro S, Ishio S, Yamamoto A (2000) Synaptic-like microvesicles, synaptic vesicle counterparts in endocrine cells, are involved in a novel regulatory mechanism for the synthesis and secretion of hormones. *J Exp Biol* 203:117-125.
- Moriyoshi K, Iijima K, Fujii H, Ito H, Cho Y, Nakanishi S (2004) Seven in absentia homolog 1A mediates ubiquitination and degradation of group 1 metabotropic glutamate receptors. *Proc Natl Acad Sci U S A* 101:8614-8619.
- Nakanishi S (1994) Metabotropic glutamate receptors: synaptic transmission, modulation, and plasticity. *Neuron* 13:1031-1037.
- Nakanishi S, Masu M, Bessho Y, Nakajima Y, Hayashi Y, Shigemoto R (1994) Molecular diversity of glutamate receptors and their physiological functions. *Exs* 71:71-80.
- Nakanishi S, Nakajima Y, Masu M, Ueda Y, Nakahara K, Watanabe D, Yamaguchi S, Kawabata S, Okada M (1998) Glutamate receptors: brain function and signal transduction. *Brain Res Brain Res Rev* 26:230-235.
- O'Connor V, El Far O, Bofill-Cardona E, Nanoff C, Freissmuth M, Karschin A, Airas JM, Betz H, Boehm S (1999) Calmodulin dependence of presynaptic metabotropic glutamate receptor signaling. *Science* 286:1180-1184.
- Pekhletski R, Gerlai R, Overstreet LS, Huang XP, Agopyan N, Slater NT, Abramow-Newerly W, Roder JC, Hampson DR (1996) Impaired cerebellar synaptic plasticity and motor performance in mice lacking the mGluR4 subtype of metabotropic glutamate receptor. *J Neurosci* 16:6364-6373.
- Pelkey KA, Lavezzari G, Racca C, Roche KW, McBain CJ (2005) mGluR7 is a metaplastic switch controlling bidirectional plasticity of feedforward inhibition. *Neuron* 46:89-102.
- Pichler A, Knipscheer P, Saitoh H, Sixma TK, Melchior F (2004) The RanBP2 SUMO E3 ligase is neither HECT- nor RING-type. *Nat Struct Mol Biol* 11:984-991.

- Pin JP, Duvoisin R (1995) The metabotropic glutamate receptors: structure and functions. *Neuropharmacology* 34:1-26.
- Pothecary CA, Jane DE, Salt TE (2002) Reduction of excitatory transmission in the retino-collicular pathway via selective activation of mGlu8 receptors by DCPG. *Neuropharmacology* 43:231-234.
- Rajan S, Plant LD, Rabin ML, Butler MH, Goldstein SA (2005) Sumoylation silences the plasma membrane leak K⁺ channel K2P1. *Cell* 121:37-47.
- Rochat-Steiner V, Becker K, Micheau O, Schneider P, Burns K, Tschopp J (2000) FIST/HIPK3: a Fas/FADD-interacting serine/threonine kinase that induces FADD phosphorylation and inhibits fas-mediated Jun NH(2)-terminal kinase activation. *J Exp Med* 192:1165-1174.
- Roth SY, Denu JM, Allis CD (2001) Histone acetyltransferases. *Annu. Rev. Biochem.* 70:81-120
- Ryu SW, Lee SJ, Park MY, Jun JI, Jung YK, Kim E (2003) Fas-associated factor 1, FAF1, is a member of Fas death-inducing signaling complex. *J Biol Chem* 278:24003-24010.
- Sachdev S, Bruhn L, Sieber H, Pichler A, Melchior F, Grosschedl R (2001) PIASy, a nuclear matrix-associated SUMO E3 ligase, represses LEF1 activity by sequestration into nuclear bodies. *Genes Dev* 15:3088-3103.
- Sampson DA, Wang M, Matunis MJ (2001) The small ubiquitin-like modifier-1 (SUMO-1) consensus sequence mediates Ubc9 binding and is essential for SUMO-1 modification. *J Biol Chem* 276:21664-21669.
- Sansig G, Bushell TJ, Clarke VR, Rozov A, Burnashev N, Portet C, Gasparini F, Schmutz M, Klebs K, Shigemoto R, Flor PJ, Kuhn R, Knoepfel T, Schroeder M, Hampson DR, Collett VJ, Zhang C, Duvoisin RM, Collingridge GL, van Der Putten H (2001) Increased seizure susceptibility in mice lacking metabotropic glutamate receptor 7. *J Neurosci* 21:8734-8745.
- Saugstad JA, Kinzie JM, Shinohara MM, Segerson TP, Westbrook GL (1997) Cloning and expression of rat metabotropic glutamate receptor 8 reveals a distinct pharmacological profile. *Mol Pharmacol* 51:119-125.
- Schmid S, Fendt M (2005) Effects of the mGluR8 agonist (S)-3,4-DCPG in the lateral amygdala on acquisition/expression of fear-potentiated startle, synaptic transmission, and plasticity. *Neuropharmacology*.
- Shigemoto R, Kinoshita A, Wada E, Nomura S, Ohishi H, Takada M, Flor PJ, Neki A, Abe T, Nakanishi S, Mizuno N (1997) Differential presynaptic localization of metabotropic glutamate receptor subtypes in the rat hippocampus. *J Neurosci* 17:7503-7522.
- Snead OC, 3rd, Banerjee PK, Burnham M, Hampson D (2000) Modulation of absence seizures by the GABA(A) receptor: a critical role for metabotropic glutamate receptor 4 (mGluR4). *J Neurosci* 20:6218-6224.
- Song J, Durrin LK, Wilkinson TA, Krontiris TG, Chen Y (2004) Identification of a SUMO-binding motif that recognizes SUMO-modified proteins. *Proc Natl Acad Sci U S A* 101:14373-14378.
- Stelter P, Ulrich HD (2003) Control of spontaneous and damage-induced mutagenesis by SUMO and ubiquitin conjugation. *Nature* 425:188-191.
- Suzuki T, Ichiyama A, Saitoh H, Kawakami T, Omata M, Chung CH, Kimura M, Shimbara N, Tanaka K (1999) A new 30-kDa ubiquitin-related SUMO-1 hydrolase from bovine brain. *J Biol Chem* 274:31131-31134.

- Swanson CJ, Bures M, Johnson MP, Linden AM, Monn JA, Schoepp DD (2005) Metabotropic glutamate receptors as novel targets for anxiety and stress disorders. *Nat Rev Drug Discov* 4:131-144.
- Takahashi Y, Iwase M, Konishi M, Tanaka M, Toh-e A, Kikuchi Y (1999) Smt3, a SUMO-1 homolog, is conjugated to Cdc3, a component of septin rings at the mother-bud neck in budding yeast. *Biochem Biophys Res Commun* 259:582-587.
- Taylor DL, Diemel LT, Pocock JM (2003) Activation of microglial group III metabotropic glutamate receptors protects neurons against microglial neurotoxicity. *J Neurosci* 23:2150-2160.
- Thomas NK, Wright RA, Howson PA, Kingston AE, Schoepp DD, Jane DE (2001) (S)-3,4-DCPG, a potent and selective mGlu8a receptor agonist, activates metabotropic glutamate receptors on primary afferent terminals in the neonatal rat spinal cord. *Neuropharmacology* 40:311-318.
- Thomsen C, Pekhletski R, Haldeman B, Gilbert TA, O'Hara P, Hampson DR (1997) Cloning and characterization of a metabotropic glutamate receptor, mGluR4b. *Neuropharmacology* 36:21-30.
- Tobaben S, Thakur P, Fernandez-Chacon R, Sudhof TC, Rettig J, Stahl B (2001) A trimeric protein complex functions as a synaptic chaperone machine. *Neuron* 31:987-999.
- Tong Q, Ouedraogo R, Kirchgessner AL (2002) Localization and function of group III metabotropic glutamate receptors in rat pancreatic islets. *Am J Physiol Endocrinol Metab* 282:E1324-1333.
- Yokoi M, Kobayashi K, Manabe T, Takahashi T, Sakaguchi I, Katsuura G, Shigemoto R, Ohishi H, Nomura S, Nakamura K, Nakao K, Katsuki M, Nakanishi S (1996) Impairment of hippocampal mossy fiber LTD in mice lacking mGluR2. *Science* 273:645-647.
- Zhao Y, Kwon SW, Anselmo A, Kaur K, White MA (2004) Broad spectrum identification of cellular small ubiquitin-related modifier (SUMO) substrate proteins. *J Biol Chem* 279:20999-21002.

ACKNOWLEDGEMENTS

First of all, I would like to thank Prof. Heinrich Betz, especially for giving me the opportunity to continue my PhD study. Four years ago, I joined his lab with little experience in neurochemistry. Now I have got much practice in Biochemistry and Molecular Biology; and more important, much knowledge in this field. At the same time, I would also like to thank Prof. Ernst Bamberg for accepting me as an external student. His agreement is as important as Heinrich's invitation letter for my PhD study.

Then I will thank Dr. Astrid Scheschonka, my group leader, special thanks for her support for the work, contribution to the writing and patience with my slow writing capacity. Then I wish to thank Dr. Oussama El Far, my former group-leader, a patient scholar especially experienced in two-hybrid screening. I am lucky to do the two-hybrid screens under his direction, using the optimized, effective protocol. Dr. Jose Airas, with whom I had no chance to work together, also contributed to the initial experience of the mGluR4b project, although it ended with nothing for unexpected reason.

Four-year life in Frankfurt is unforgettable. I am grateful to many persons who have given a lot of help to my family and me. Dr. Bertram Schmitt, who picked me up from the airport on the first day, then my wife two months later. My colleagues, Anja Arends, Greta Ann Herin, Chuansheng Zhang, Anina Moritz and Liane Bauer for their kind help in correcting my manuscript and translating so many bills in my life. And so many friends in and out of the institute, including those who have left, we share the nice wine and beer, and pleasure.

In addition, special thanks to Dr. Ryuichi Shigemoto for his generous supply of an anti-mGluR8 antibody; Dr. Frauke Melchior for kindly providing the E1, E2 and sumo-1 cDNAs; Dr. Thamas Segerson and Dr. Jaroslav Blahos for the mGluR8 cDNAs; and Dr. Mijin Sohn from Shuai lab for the Pias1 cDNA.

I also want to share the pleasure with my family. My wife worked hard to make a warm family for me. She takes up nearly all of the housework. Our two lovely babies, Kai and Guny, bring much pleasure to my life.

CURRICULUM VITAE

Biographical

Name	TANG, Zhongshu
Date of birth	May, 03, 1969
Place of birth	Anhui, China
Nationality	Chinese
Family state	Married

Education

Doctor of Philosophy 2001-	Department of Neurochemistry Max-Planck-Institute for Brain Research Frankfurt am Main, Germany Dissertation Advisor: Heinrich Betz, MD, Prof.
Master of Sciences 1995-1998	Shanghai Institute of Physiology, Chinese Academy of Sciences Shanghai, China Dissertation Advisor: Changfu Zhou, Prof.
Bachelor of Sciences 1989-1993	Department of Biology Anhui Normal University Wuhu, China

Employment experience

Research Assistant 1998-2001	Shanghai Institute of Physiology, Chinese Academy of Sciences Shanghai, China
Teacher for Biochemistry 1993-1995	Huainan Normal University Huainan, China

Publications

1. Tang Z, El Far O, Betz H, Scheschonka A. (2005) PIAS1 interaction and sumoylation of metabotropic glutamate receptor 8. J Biol Chem 280: 38153-38159.

2. Xu L, Sheng J, Tang Z, Wu X, Yu Y, Guo H, Shen Y, Zhou C, Paraoan L, Zhou J (2005) Cystatin C prevents degeneration of rat nigral dopaminergic neurons: in vitro and in vivo studies. *Neurobiol Dis* 18:152-165.
3. Guo H, Tang Z, Yu Y, Xu L, Jin G, Zhou J (2002) Apomorphine induces trophic factors that support fetal rat mesencephalic dopaminergic neurons in cultures. *Eur J Neurosci* 16:1861-1870.
4. Tang Z, Yu Y, Guo H, Zhou J (2002) Induction of tyrosine hydroxylase expression in rat fetal striatal precursor cells following transplantation. *Neurosci Lett* 324:13-16.
5. Shen Y, Yu Y, Guo H, Tang Z, Yu FS, Zhou J (2002) Identification and comparative analysis of differentially expressed proteins in rat striatum following 6-hydroxydopamine lesions of the nigrostriatal pathway: up-regulation of amyloid precursor-like protein 2 expression. *Eur J Neurosci* 16:896-906.
6. Xu H, Tang Z, Zhou C (2001) Schwann cells promote the survival and growth of cholinergic neurons both in co-culture and co-graft. *Chin J Neuroanat* 17:1-5.
7. Tang Z, Xu H, Zhou C (2000) Neurotrophic Effects of Primarily Cultured Schwann Cells Is Regulated By Their Interactions with Neural Cells. *Chin J Neurosci* 16: 228-231.
8. Zhou J, Shen Y, Tang Z, Xu L, Bradford HF, Yu Y (2000) Striatal extracts promote the survival and phenotypic expression of rat fetal dopaminergic neurons in vitro. *Neurosci Lett* 292:5-8.
9. Zhou J, Yu Y, Tang Z, Shen Y, Xu L (2000) Differential expression of mRNAs of GDNF family in the striatum following 6-OHDA-induced lesion. *Neuroreport* 11:3289-3293.

APPENDIX I: GENERATION AND VERIFICATION OF CONSTRUCTS

Figure 23. Generation and verification of KR mutants of GFP-mGluR8a-C	
-----	65
Figure 24. Generation and verification of full-length mGluR8a constructs	
-----	66
Figure 25. Generation and verification of constructs with His-tagged proteins	
-----	69
Figure 26. Generation and verification of pBK-CMV- Δ Lac-m8a-GFP construct	
-----	71
Figure 27. Schematic of generating fluorescence tagged sumo-1, ube2a an Pias1 constructs	
-----	72
Figure 28. Generation and conformation of GFP-mGluR8a-C-N24/-C44 constructs	
-----	73

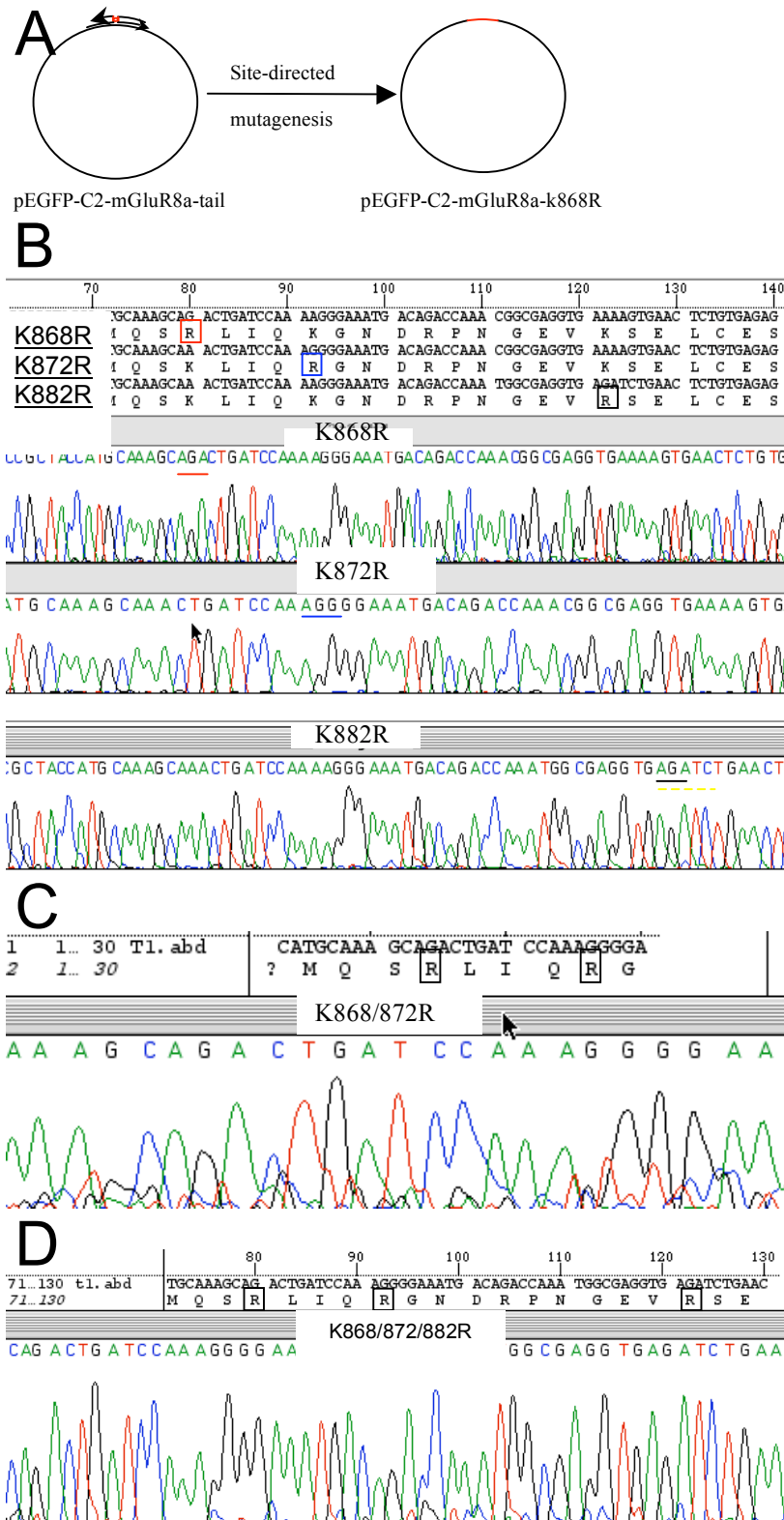
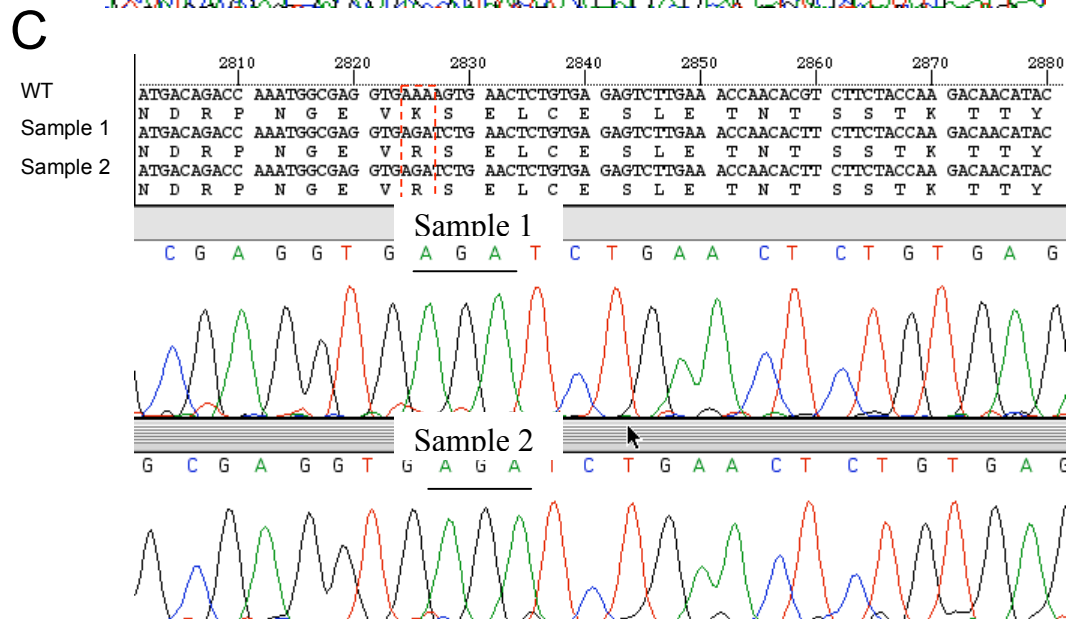
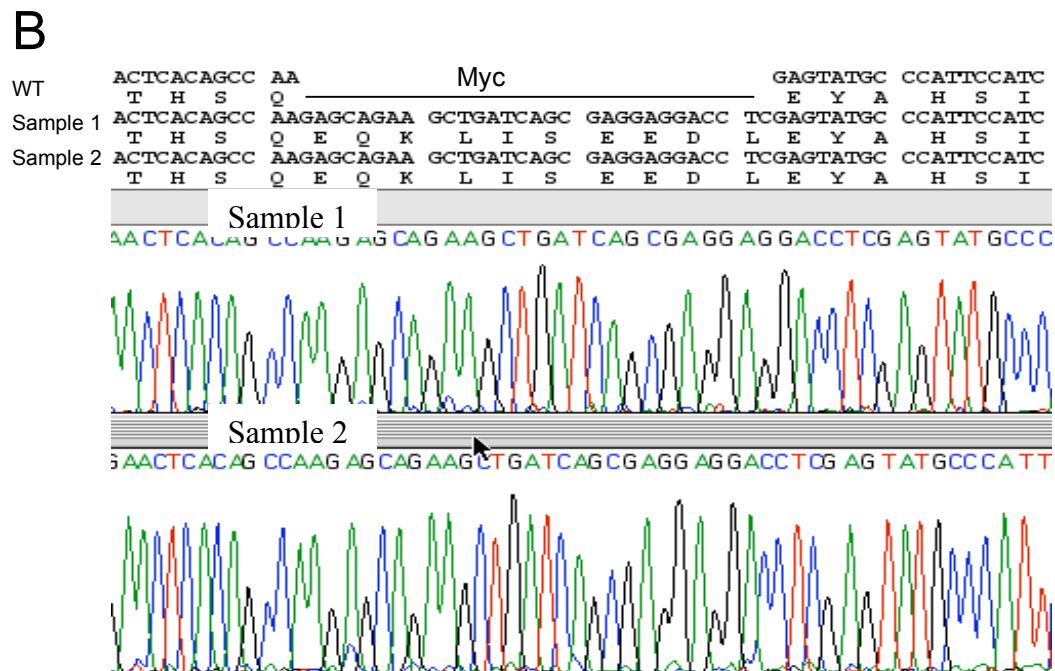
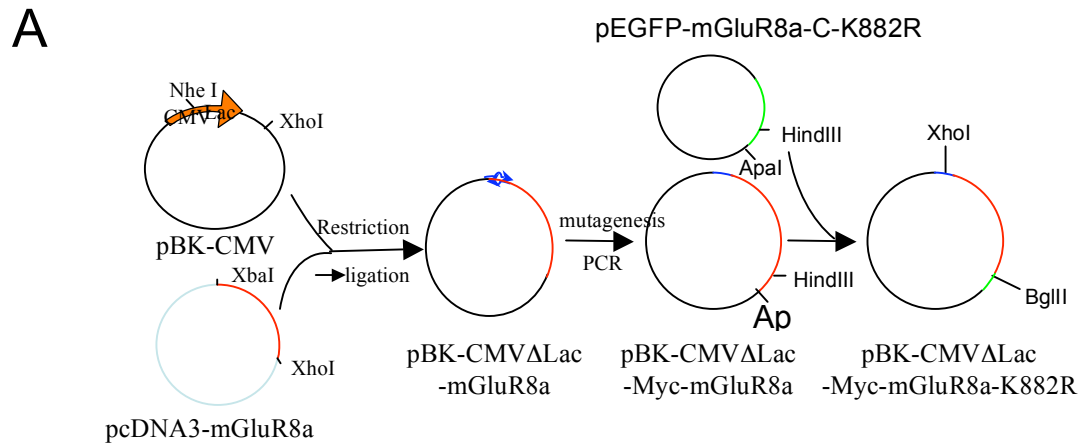
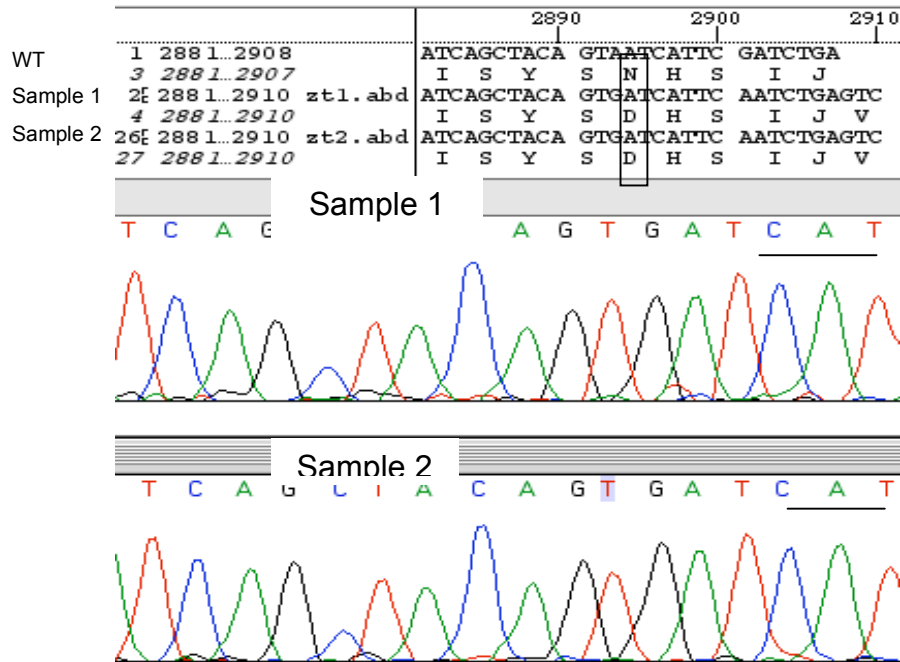


Figure 23. Generation and verification of KR mutants of GFP-mGluR8a-C.

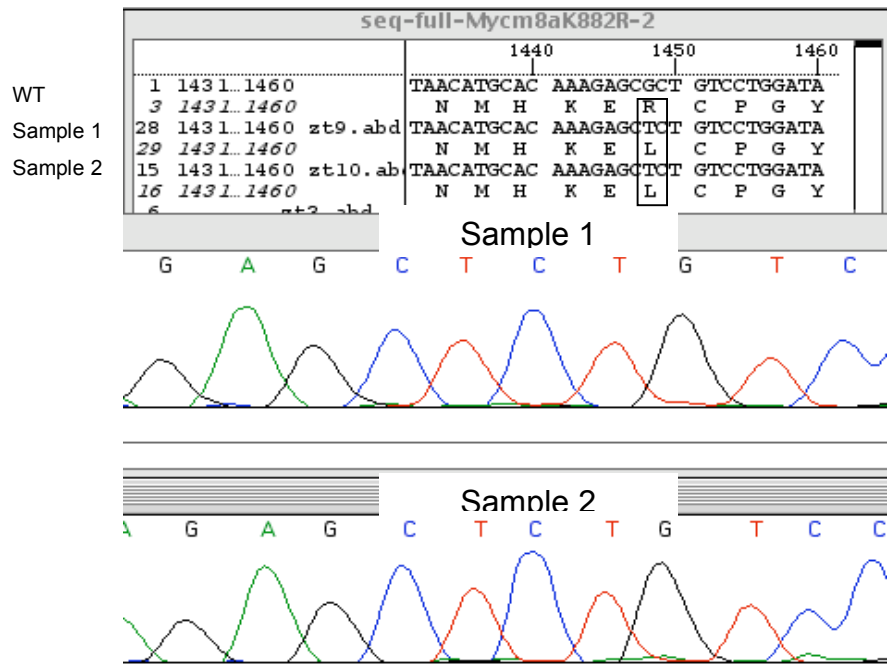
- A. KR mutants were generated by site-directed mutagenesis. Note that a Bgl II site is induced around R882 (yellow dashed underline in B).
- B. All single mutant sites were proven to be correct by DNA sequencing.
- C. K868/872R double mutant sites were verified to be correct by DNA sequencing.
- D. K868/872/882R triple mutant sites were controlled to be correct by DNA sequencing.



D



E



F

↓

O00222-human	401	KVQFVIDAVYSMAVALHNMHKDLC	PGYIGLCPRM	STIDGK	440
NP_032200-mouse	401	KVQFVIDAVYSMAVALHNMHKE	LCPGYIGLCPRM	V	IDGK 440
AAB09537-rat	401	KVQFVIDAVYSMAVALHNMHKE	R	LC	PGYIGLCPRMVTIDGK 440

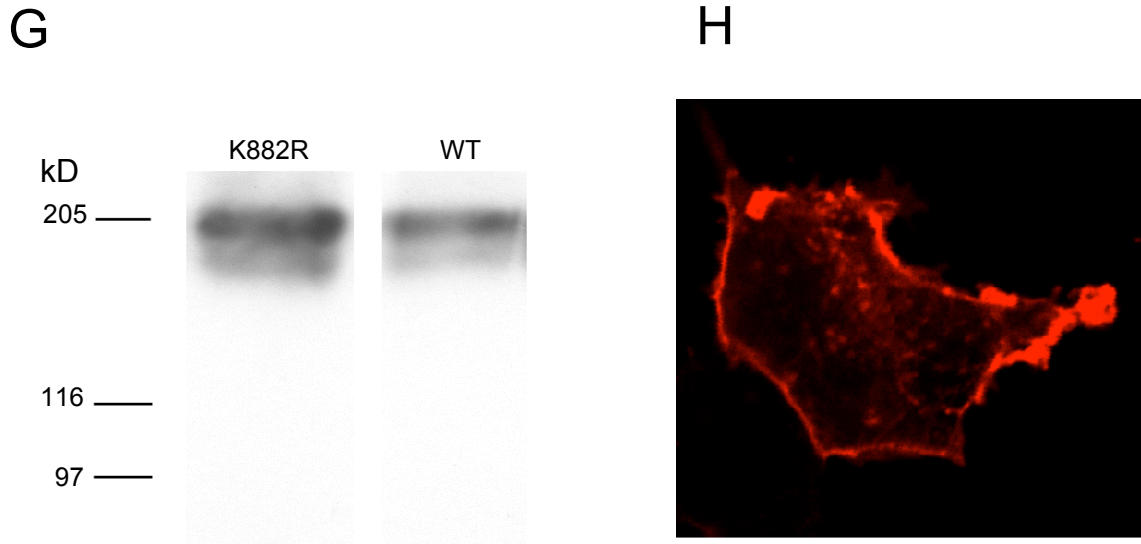
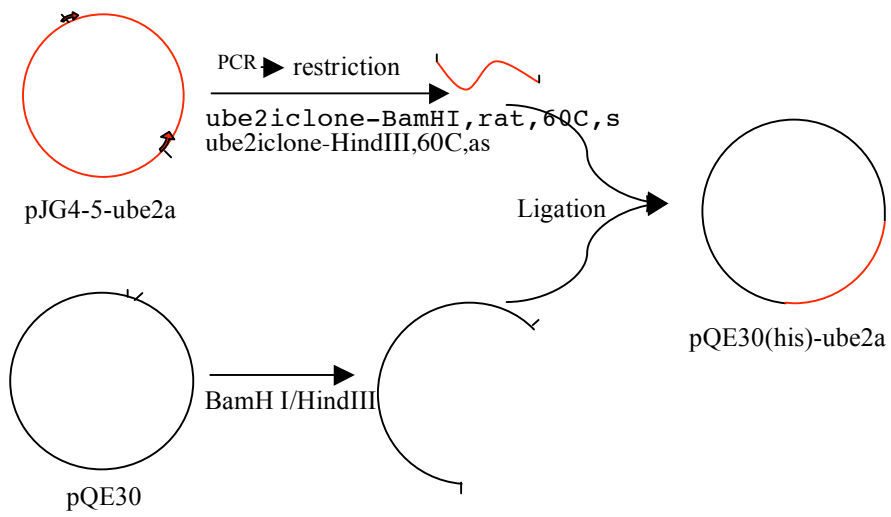
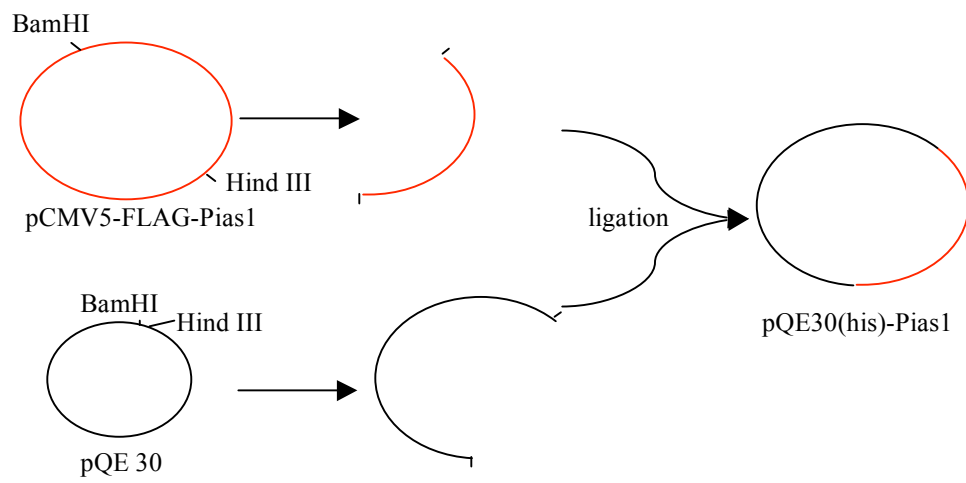
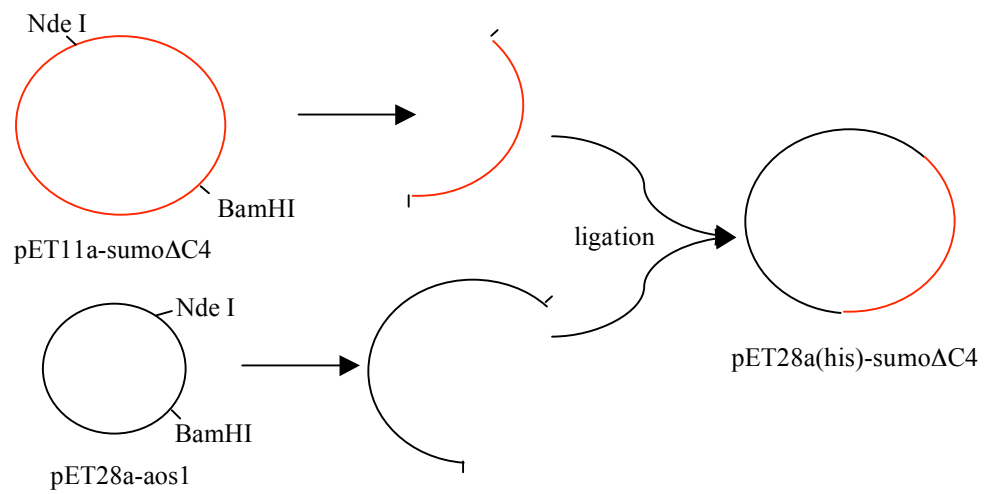


Figure 24. Generation and verification of full-length mGluR8a constructs.

- A. pBK-CMV Δ Lac-mGluR8a was generated by shifting a full-length rat mGluR8a cDNA from a pcDNA3 construct to pBK-CMV between NheI and XhoI sites, thus resulted deletion of the Lac-promotor in the vector; and was further mutated with primers encoding a Myc tag. A K882R substitution was introduced by shuffling the corresponding fragment from a GFP-mGluR8a-C-K882R (mouse) plasmid. Note that new XhoI and BglII sites were introduced into the Myc tag and R882 sequences, respectively.
- B. Myc tag was checked by DNA sequencing to have been inserted at the correct position.
- C. K882R substitution was also approved by DNA sequencing to be correct.
- D. Asp905 (black box) was induced spontaneously from the mouse mGluR8a-C cDNA construct to substitute the Asn905 in the rat full-length mGluR8a construct.
- E. The full-length Myc-mGluR8a-K882R was sequenced to be same as cDNA No. AAB09537 except for AA423 (black box), which is an Arg in AAB09537, but is a Lys in two DNA sequencing samples.
- F. L423 (indicated by a red arrow) is common between mouse and human mGluR8, consistent with DNA sequencing results. Thus it is likely that AA423 in rat mGluR8 is also a Lys.
- G. Expression of the full-length MycGluR8a was demonstrated by Western blotting using anti-Myc antibody, as a dimer about 200 kD.
- H. The full-length MycGluR8a is incorporated into membrane after being transfected into HEK 293 cells, demonstrated by anti-Myc staining.

A**B****C**

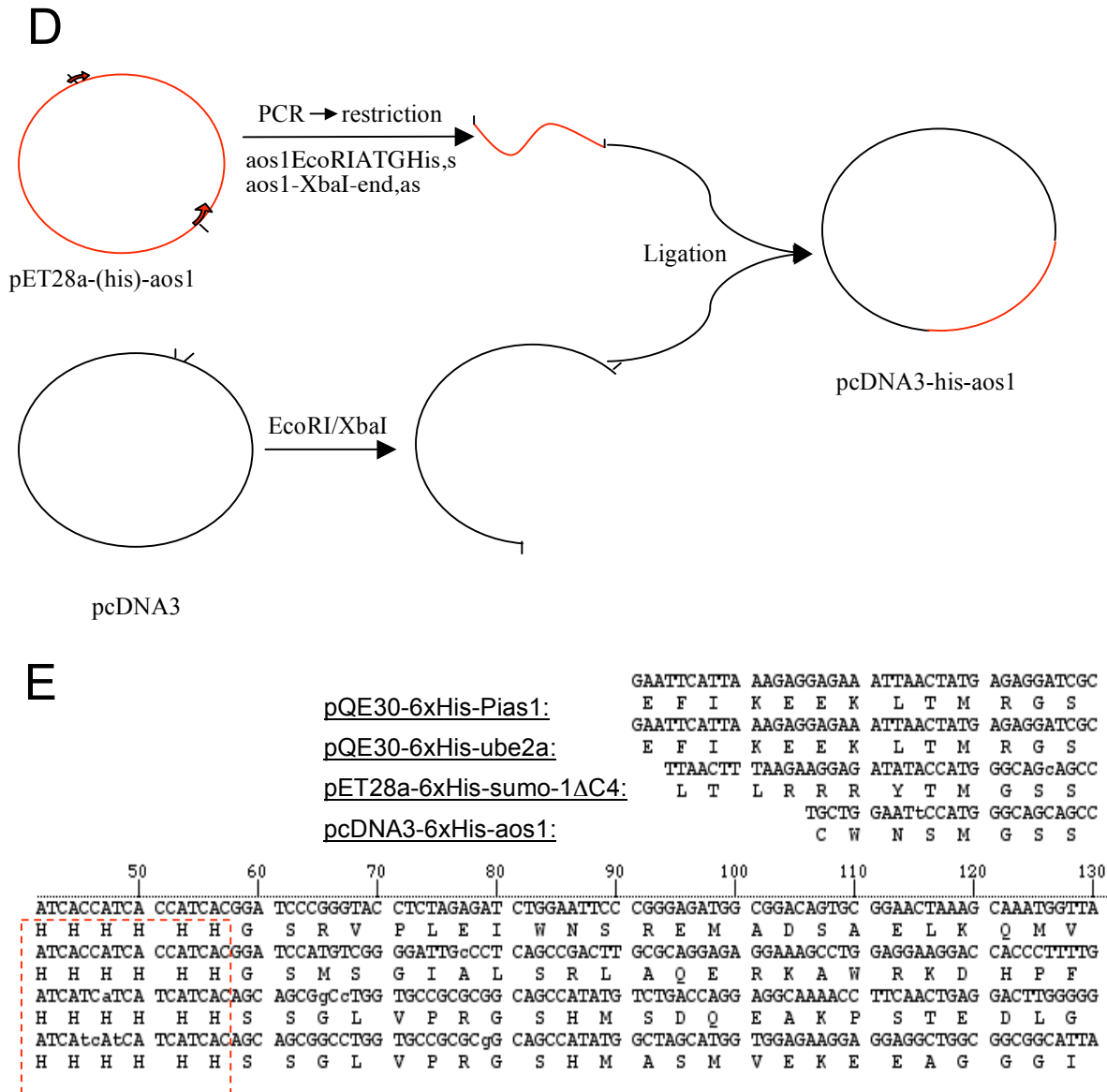


Figure 25. Generation and verification of constructs with His-tagged proteins.

- pQE30-6xHis-ube2a was generated by inserting the full-length ube2a cDNA amplified by PCR into pEQ30.
- pQE30-6xHis-Pias1 was made by inserting the Pias1 from pCMV5 construct into pQE30.
- pET28a-6xHis-sumo-1ΔC4 was created by inserting the sumo-1ΔC4 fragment from the pET11a vectort into pET28a.
- pcDNA3-6xHis-aos1 was constructed by inserting the 6xHis-aos1 fragment from pET28a-aos1 amplified by PCR into pcDNA3.
- Verification of constructs A-D by DNA sequencing. 6xHis tags are indicated in red box.

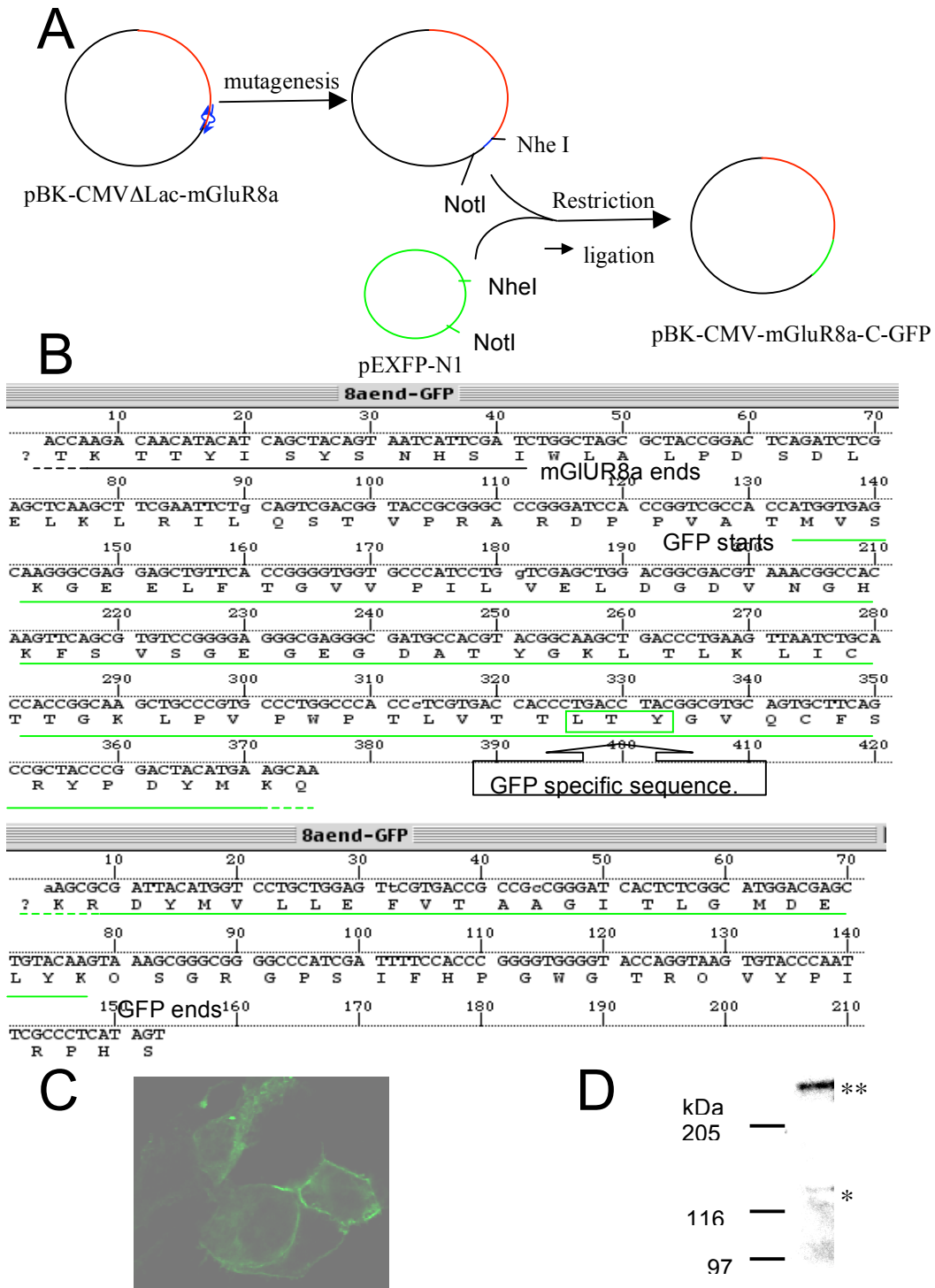


Figure 26. Generation and verification of pBK-CMV- Δ Lac-m8a-GFP construct.

- A NheI site was introduced before the stop codon of full-length mGluR8a. GFP sequence was inserted at the end of mGluR8a cDNA sequence.
- Verification of the sequence. GFP (green underline) follows the end of mGluR8a (black underline) without stop codon. A stop codon follows the end of GFP.
- mGluR8a-GFP incorporated into membrane after transfection into HEK293 cells.
- Western blot of mGluR8a-GFP expressed in HEK293 cells, using anti-mGluR8a-C antibody.
*, monomer (135 kDa); **, dimer (270 kDa) of mGluR8a-GFP .

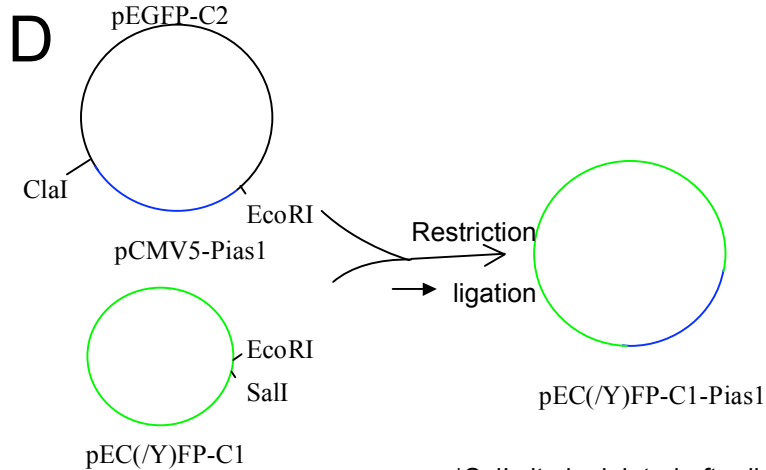
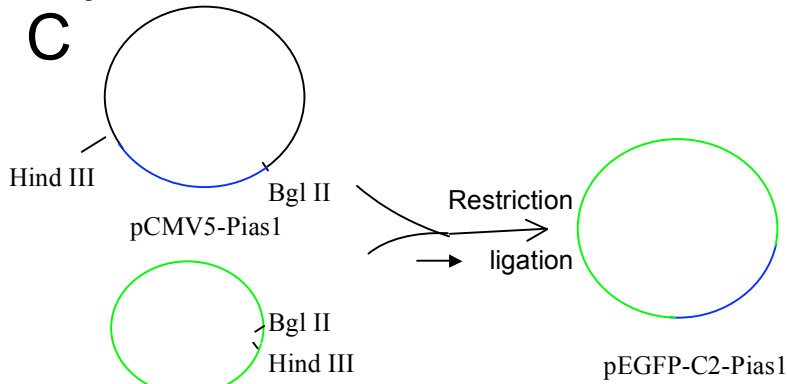
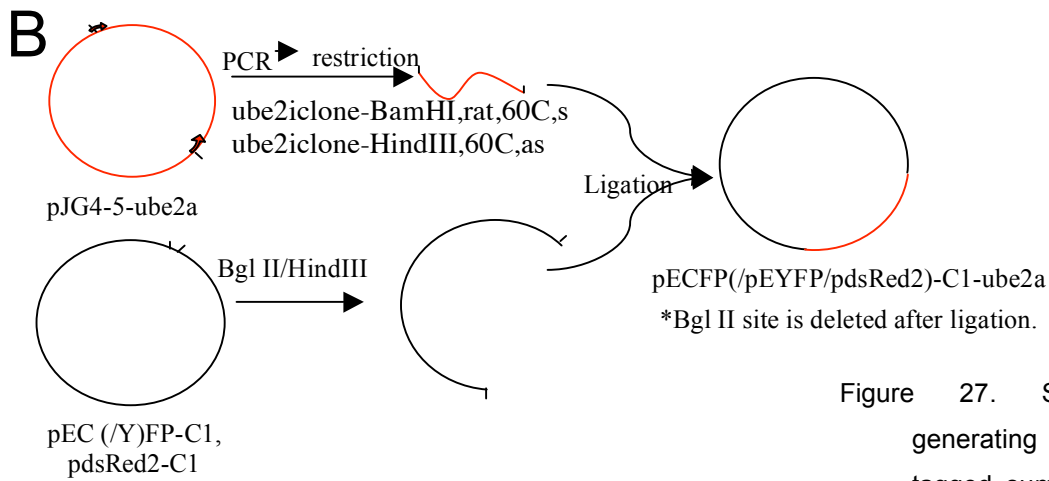
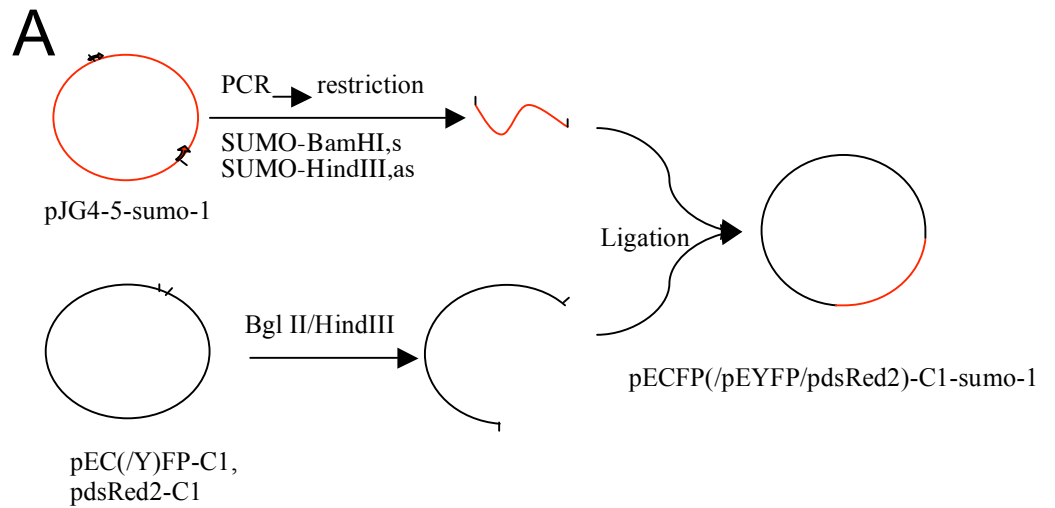


Figure 27. Schematic of generating fluorescence tagged sumo-1, ube2a and Pias1 constructs.

- A. Sumo-1 constructs were generated by inserting the sumo-1 amplified by PCR into corresponding vectors.
- B. Ube2a constructs were created by inserting the ube2a amplified by PCR into corresponding vectors.
- C. GFP-Pias1 construct was assembled by inserting the Pias1 from pCMV5 construct into pEGFP-C2.
- D. CFP- and ds-Red-Pias1 constructs were made by inserting the Pias1 from pCMV5 construct into corresponding vectors.

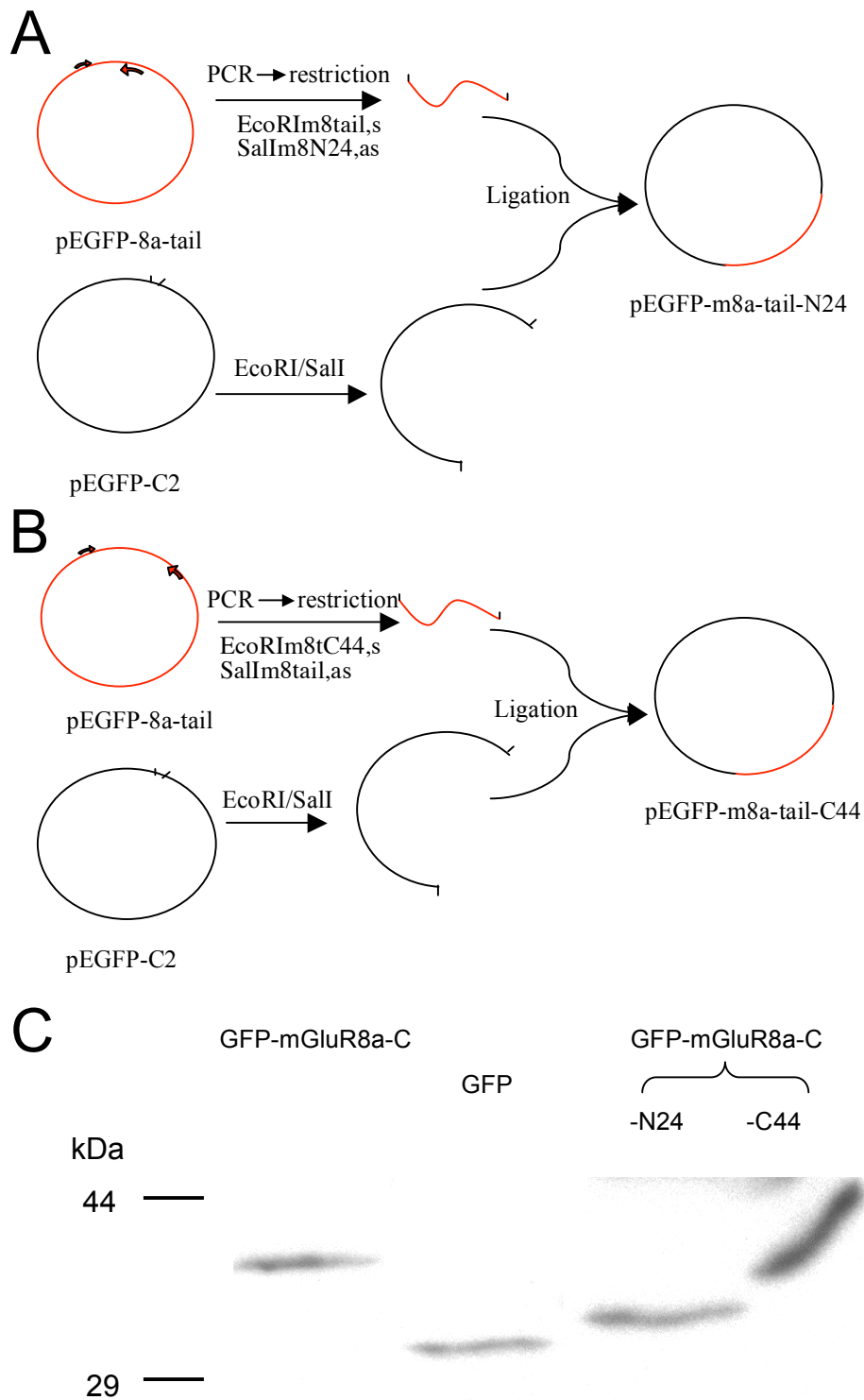


Figure 28. Generation and conformation of GFP-mGluR8a-C-N24/-C44 constructs.

- pEGFP-mGluR8a-C-N24 was constructed by inserting N24 fragment amplified by PCR into pEGFP-C2.
- pEGFP-mGluR8a-C-C44 was created by inserting C44 fragment amplified by PCR into pEGFP-C2.
- Proteins expressions were checked by transfection into HEK cells, followed by Western blotting using anti-GFP antibody. All protein bands were in the appropriate molecular weight range.

APPENDIX II: REVIEW

SUMOYLATION: STRUCTURES AND MECHANISMS

SUMOYLATION PATHWAY	75
SUMOYLATION MACHINERY: SUMO AND ENZYMES	75
Sumo	77
E1	79
E2.....	84
E3.....	87
Pias proteins.....	87
RanBP2.....	90
Pc2.....	91
SUMOYLATION COMPLEX	92
Sumoylation model.....	92
Prospective of the Model	95
REFERENCES:	96

Sumoylation is a posttranslational modification in which sumo¹ (small ubiquitin-like modifier) proteins are covalently bound to the ϵ -NH₂ group of Lys residues of substrates (Melchior, 2000; Johnson, 2004). Sumoylation has been shown to modify a large number of proteins with important roles in many cellular processes, including gene expression, chromatin structure, signal transduction and maintenance of the genome (Gill, 2004). Sumoylation is mechanistically related to ubiquitination, so many studies were performed using ubiquitination as a model system. The structures of most proteins and protein complexes involved in sumoylation and other related modifications have been analysed by X-ray crystallography or NMR chemical shift perturbation, thus provide insight into the mechanism of sumoylation. This review describes the structures and functions of modifiers and enzymes involved in the ubiquitin, sumo and Nedd8 modification pathways. Some of the descriptions of structures are cited from the corresponding original research papers.

SUMOYLATION PATHWAY

The enzymatic machinery that adds and removes sumo is related to the ubiquitination machinery (Gill, 2004). Like ubiquitin, sumo proteins are also expressed as precursors that need to be proteolytically processed by C-terminal hydrolases to make the C-terminal Gly-Gly motif available for conjugation. This step is called maturation (Figure 1A).

The sumoylation procedure requires sumo and three enzymes: sumo-activating enzyme (E1), sumo-conjugating enzyme (E2) and sumo ligase (E3) (Gill, 2004; Johnson, 2004), which catalyze three different steps (Figure 1A). The first one is called activation, which actually includes two sub-steps: adenylation and thioester transference within E1. As a result, a thioester bond is formed between the COOH group of the sumo C-terminal Gly residue and the activating residue Cys of E1. ATP and Mg²⁺ are required for sumo activation. In the second conjugation step, the sumo is transferred from E1 to the active Cys site of E2, forming an E2-sumo thiolester intermediate. Finally, sumo is transferred in a ligation reaction to the amino group of a substrate lysine with the assistance of a sumo-ligating enzyme (E3).

The isopeptide bond between sumo and the substrate can be cleaved by isopeptidases. This step is called de-sumoylation (Figure 1A). The isopeptidases are also C-terminal hydrolases that catalyze sumo maturation (Johnson, 2004).

SUMOYLATION MACHINERY: SUMO AND ENZYMES

¹ Abbreviations: sumo, small ubiquitin-like modifier; Ubl, ubiquitin-like modifier; UbL, ubiquitin-like domain; E1, activating enzyme; E2, conjugating enzyme; E3, ligase; uba, ubiquitin activating enzyme; ubc, ubiquitin conjugating enzyme.

Fewer components or isoforms are known for the early enzymatic steps in the sumoylation system than in the ubiquitination system. For ubiquitination, there is only one form of

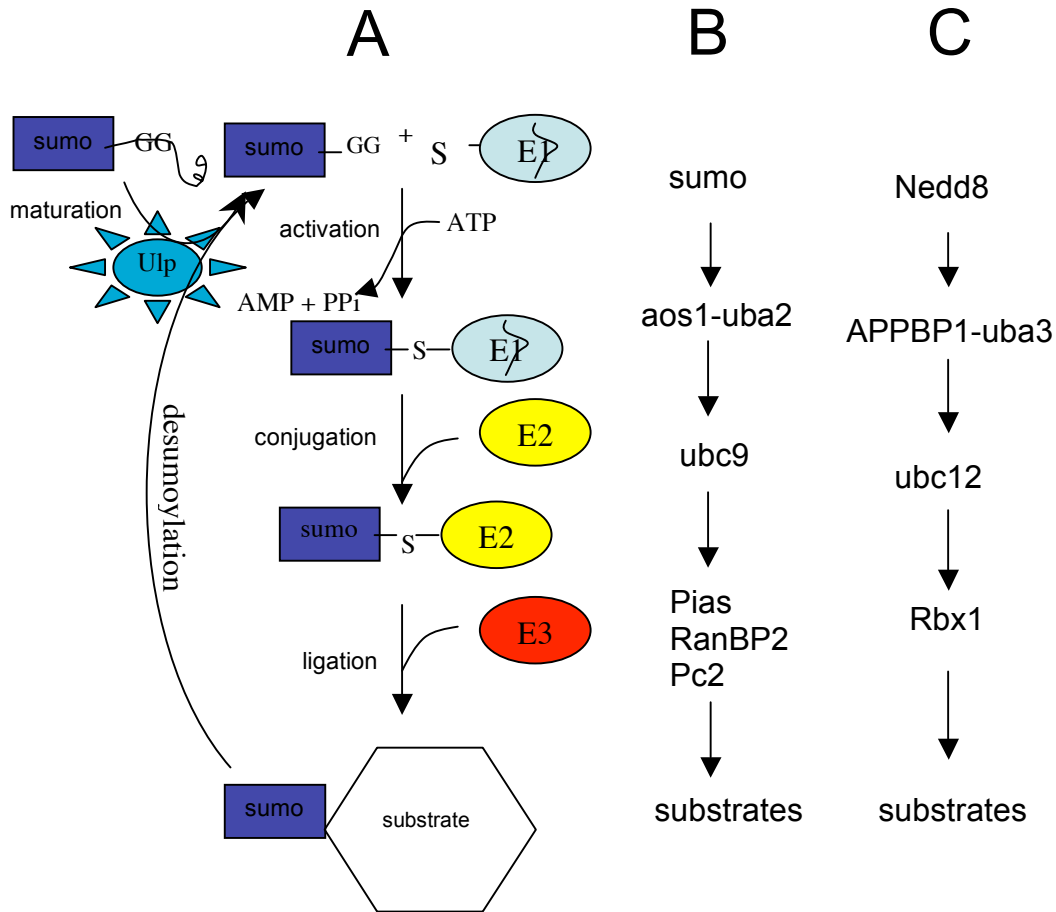


Figure 1. Sumoylation machinery. A. The sumo conjugation pathway. Free sumo is generated from either maturation of the sumo precursor or dissociation from a sumoylated substrate. For sumo conjugation, sumo is firstly activated by and forms a thioester bond with the activating enzyme E1, then transferred to the conjugating enzyme E2 and at last to the substrate, B. Schematic diagram of individual steps in the sumoylation cascade. C. Schematic of individual steps in the neddylation cascade. A and B are modified from Johnson (2004). C is modified from Huang et al. (2004a).

ubiquitin, one E1, a significant but limited number of E2 enzymes, and a large number of E3 enzymes. Several E3 proteins interact with the same E2, and several E2 enzymes may also interact with the same E3. Each E3 recognizes a set of substrates that shares one or more ubiquitination signals, and cooperates with one or a few E2 (Pickart, 2001). In the sumoylation system, four sumo proteins have been identified; substrates are coupled by one E1, one E2 and several E3 enzymes. A similar conjugation mode is found for Nedd8, another

ubiquitin-like modifier. The enzymes involved in sumoylation and neddylation² are shown in Figure 1B and 1C, respectively.



Figure 2. Alignment of ubiquitin, sumo-1 to 4, SMT3 and Nedd8. All sequences are of Homo sapiens, except for SMT3 from *Saccharomyces cerevisiae*. The red box indicates consensus sumoylation motifs. The blue box indicates residues compatible for binding of corresponding E1.

Sumo

It is interesting that sumo, E1 and E2 of sumoylation pathway were all cloned in 1995, but their function in sumoylation were all identified two years later (Melchior, 2000). Four mammalian sumo proteins have been identified so far. The alignment of sumo proteins with ubiquitin and Nedd8 is shown in Figure 2. Sumo-1 has only 18% amino acid sequence identity with ubiquitin, but their structures are quite identical. Sumo-1 shares about 43% sequence identity with sumo-2 and sumo-3, which have 96% sequence identity. Phylogenetic analyses indicate that the sumo-3 gene derives from the sumo-2 gene (Su and Li, 2002). Sumo-4 shares 87% sequence homology with sumo-2. Sumo-1 does not contain a consensus sumoylation motif Φ KXE³, whereas the other three do. Thus, sumo-2 and, to a less extent, sumo-3, have been shown to form polymer chains, while sumo-1 has not (Tatham et al., 2001; Johnson, 2004).

² Neddylation, the conjugation of Nedd8 (Neural cell expressed developmentally down-regulated protein 8) to the substrate.

³ Φ KXE, a consensus motif among many sumoylation sites, where Φ is a large hydrophobic amino acid; K, the Lys residue; X, any amino acid; E/D, glutamate or aspartate.

Sumo-1/-2/-3 are found in all eukaryotes and are required for viability of most eukaryotic cells, including budding yeast, nematodes, fruit flies, and vertebrate cells in culture. In multicellular organisms, sumo conjugation takes place in all tissues at all developmental stages (Johnson, 2004). Sumo-1 to 3 were shown to be localized at the nuclear membrane, nuclear bodies and cytoplasm, respectively (Su and Li, 2002). The distribution of sumo-4 has not yet been reported. Sumo-4 mRNA was detected mainly in the kidney (Bohren et al., 2004). E1 and E2 do not appear to have any substantial preference for either sumo-1 or sumo-2/3 (Tatham et al., 2005). Sumo-1 is the modifier of most substrates identified. Sumo-2 and -3 are assumed to be functionally identical, and only a few sumo-2/-3 modified substrates have been found so far (Johnson, 2004). It was shown that PML⁴ is covalently modified by all three sumo proteins (Kamitani et al., 1998). The sumo-2 chain has been observed on the histone deacetylase HDAC4 in cells; it forms a di-sumoylated conjugate that disappears when the sumo attachment site in sumo-2 is mutated (Tatham et al., 2001). A β production has been found to decrease with overexpression of sumo-3, and increase with dominant-negative sumo-3. It is interesting that K11R mutant of sumo-3, a mutant of the consensus sumoylation motif that abolishes poly(sumo-3) chain formation and hence can only be monomerically conjugated to target proteins, has an opposite effect on A β generation (Li et al., 2003). The crystal structures of ubiquitin, SMT3, sumo-1-3 and Nedd8 all resemble the $\beta\alpha\beta\beta\alpha\beta$ fold (Figure 3A-B) (Bayer et al., 1998; Whitby et al., 1998; Huang et al., 2004; Ding et al., 2005), and the polypeptide back bones match well when they are overlaid (Figure 3C). Hydrophobic residues are located at the helix-sheet interface, are highly conserved, and contribute to the maintenance of the globular and compact fold (Ding et al., 2005). Similarly, the consensus Lys sites of SMT3 and sumo-2/3 and the two glycine residues at the C-terminus of ubiquitin, SMT3 and all sumo proteins are highly conserved (Ding et al., 2005). A comparison of sumo-2 and sumo-1 surfaces shows a region near the C-terminus with significantly different charge distributions. This may explain the distinct intracellular locations of these sumo isoforms (Huang et al., 2004). Both ubiquitin and sumo-2/3 can form poly-chains. The Lys sites for poly-ubiquitin formation are located in the compact core of the ubiquitin molecule. Conversely, the consensus Lys sites of sumo-2, -3 and -4 for poly-sumo chain formation lie in the N-terminal free strand. So it can be imagined that there are much larger contact areas between ubiquitin molecules than between sumo molecules. The function of this difference remains to be understood.

⁴ PML, a RING finger protein with tumor suppressor activity, has been implicated in the pathogenesis of acute promyelocytic leukemia (PML) that arises following a reciprocal chromosomal translocation that fuses the PML gene with the retinoic acid receptor α (RAR α) gene.

Sumo-1 conjugation onto substrates or catalytic enzymes always occurs with its C-terminus. Eleven residues of sumo-1 have been shown to aid in direct contacting with uba2, a subunit of sumoylation E1 ligase; seven of those residues lie in the very C-terminal tail (Lois and Lima, 2005). The first two β -sheets and the first helix are also important for the contact with substrates such as DNA glycosylase, ube2-25k, and isopeptidase SENP2 (Reverter and Lima, 2004; Baba et al., 2005; Pichler et al., 2005). The functions of other regions of sumo proteins, especially the N-terminal free loops that make sumo proteins distinct from ubiquitin, are still unknown.

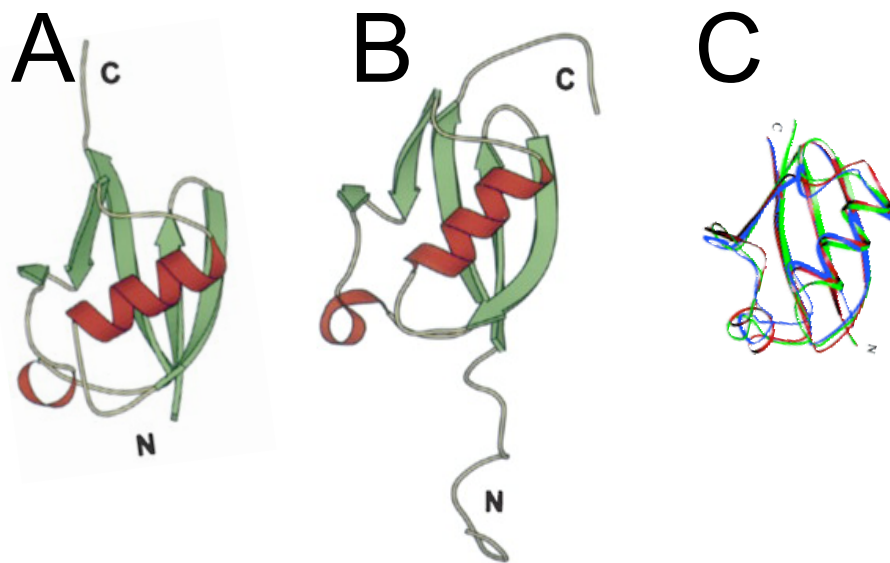


Figure 3. Structures of ubiquitin (A) and sumo-1 (B). C. Backbone superposition of the core structures of sumo-3 C47S (red), sumo-1 (green), and ubiquitin (blue). A and B are taken from Gill, (2004), C from Ding et al., (2005).

E1

The activating enzyme E1 facilitates the conjugation of ubiquitin and ubiquitin-like proteins through adenylation, thioester transfer within E1, and thioester transfer from E1 to the conjugating enzyme E2 (Lois and Lima, 2005). Ubiquitin, sumo and Nedd8 all are activated by one isoform of E1. But unlike the ubiquitin specific E1 enzyme that is a monomer uba1, the E1s involved in the sumo and Nedd8 modification pathways are all heterodimers of two subunits. Sumo specific E1 enzyme is a complex with two subunits: aos1 and uba2. Nedd8 specific E1 enzyme is also a complex with two subunits: APPBP1 and uba3. Aos1 and APPBP1 resemble the N-, uba2 and uba3 the C-termini of ubiquitin E1. The alignment of uba1, aos1/uba2 and APPBP1/uba3 is shown in Figure 4, 5A. Aos1 is composed of only one

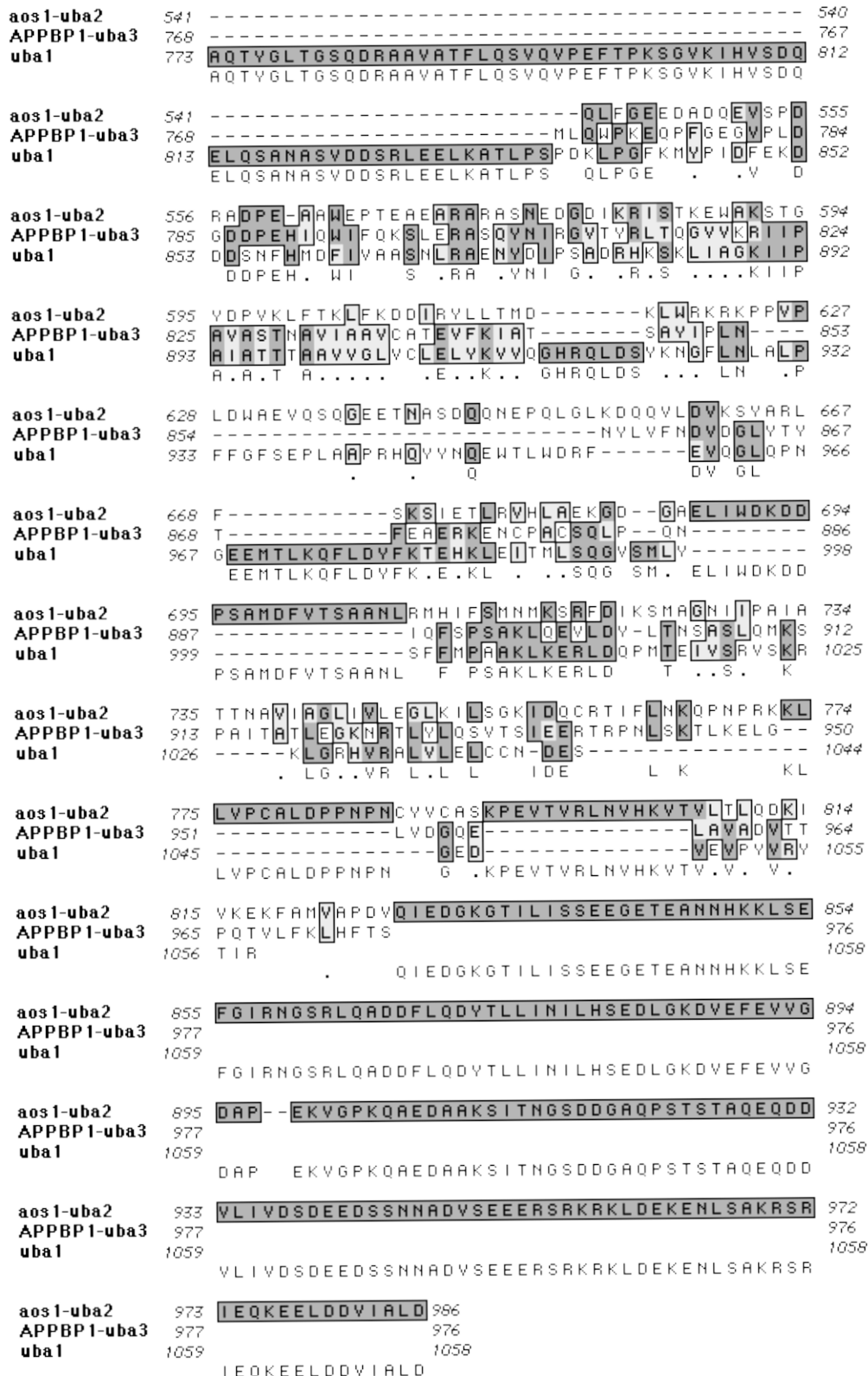


Figure 4. The alignment of aos1-uba2, APPBP1-uba3 complexes and uba1, the activating enzymes of sumo, Nedd8 and ubiquitin, respectively. The pink box (AA370-375 for aos1-uba2 complex) indicates locations of nucleotide binding center. The blue box (AA495 for aos1-uba2 complex) indicates residues permissive for corresponding modifiers. The red box (AA519 for aos1-uba2 complex) indicates catalytic residues. All protein sequences are of Homo sapiens.

domain that participates in adenylation of sumo. Uba2 includes three domains: the catalytic Cys domain, the adenylation domain and the ubiquitin-like (UbL) domain which is structurally similar to ubiquitin and other ubiquitin-like modifiers (Lois and Lima, 2005). The uba2 adenylation domain, which is separated by the catalytic Cys domain into two parts, forms a pseudosymmetric heterodimer with the aos1 subunit. Sumo-1 is recognized exclusively by residues emanating from uba2, as no direct interactions are observed between sumo-1 and the aos1 subunit (Lois and Lima, 2005). The UbL domain of E1 shows strong interaction with E2, which is considered to be essential for recruiting E2 to E1 (Lois and Lima, 2005). The C-terminal extension of uba2 is not conserved in all E1 enzymes. The yeast uba2 C-terminal extension contains a nuclear localization signal (NLS) (Dohmen et al., 1995). APPBP1 has two domains: the adenylation domain resembles aos1, and the Cys domain resembles part of uba2. Ubiquitin E1 protein uba1 contains all domains that sumo or Nedd8 E1 enzyme complexes share. The alignment of aos1/uba2 and APPBP1/uba3 with uba1 reveals that they may be derived from a common ancestor with different allocations of the functional domains to the subunits (Figure 4, 5A).

The structure of the mammalian Ubl activating enzyme Nedd8 E1 complex APPBP1/Uba3 was published in 2003 (Walden et al., 2003a). Expectedly, the sumo activating enzyme complex aos1/uba2 was found to resemble that of APPBP1/Uba3 (Lois and Lima, 2005). Part of the ubiquitin E1 protein was also successfully crystallized recently, including the ubiquitin-binding domain and parts of the cysteine and the adenylation domains (Szczepanowski et al., 2005). Its corresponding regions resemble those of the former two complexes. The E1 structure contains a big groove with the adenylation domain at the base, UbL and Cys domains on both sides (Figure 5B). The adenylation domain has a typical Gly-x-Gly-x-x-Gly nucleotide binding motif (Walden et al., 2003b), which is conserved among ubiquitin, sumo and Nedd8 activating enzymes (Figure 4). One molecule of ATP is located in a pocket close to this motif. The upper part of the groove is further divided into two clefts by a loop (L_{CA}) between the Cys domain and the adenylation domain. The catalytic site Cys173 lies in the Cys domain side of L_{CA} . Cleft 1 is the space between the ubiquitin-like domain and part of the catalytic cysteine domain. Cleft 2 has the left portion of the catalytic cysteine domain as its only wall and is open to one side of the complex (Lois and Lima, 2005).

Despite of the high similarities among the structures of all known Ubls and corresponding E1s, the modifiers bind to their enzymes very specifically. Prerequisite for this specificity are pairs of residues between the modifiers and the corresponding E1s (Walden et al., 2003b). The corresponding residues of all Ubls are at position -5, that is, a Glu in sumo-1, a Gln in

sumo-2/3/4, an Ala for Nedd8 and an Arg for ubiquitin (Figure 2). The corresponding residues are Thr495 in uba2, Arg190 of uba3, and Gln608 of ubiquitin E1 (Figure 4).

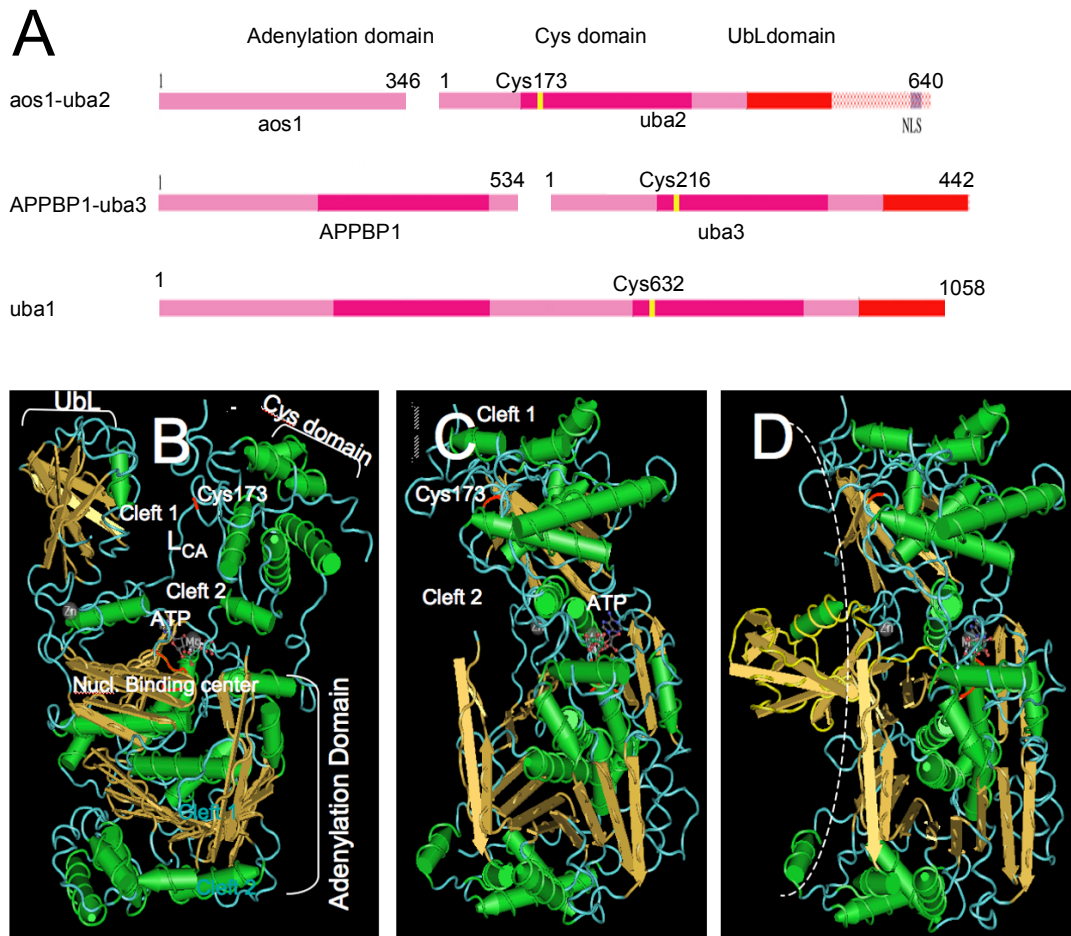


Figure 5, Structure of the sumo activating enzyme E1. A. Schematic representations of sumo E1 complex aos1/uba2, Nedd8 E1 complex APPBP1/uba3 and ubiquitin E1 uba1. Pink, light red and deep red columns represent adenylation, Cys and ubiquitin-like domains, respectively. Catalytic Cys sites are colored in yellow. B. Structure of human aos1/uba2 complex. The complex contains a big groove that is divided into 2 clefts by the free loop L10. Adenylation, ubiquitin-like (UbL) and Cys domains are marked by brackets. The catalytic residue Cys173 (red) lies at the Cys domain end of L10. An ATP molecule is bound to the nucleotide binding motif. C. Side view of B. One sumo-1 molecule bound at the nucleotide binding center. B-D are modified from the NCBI structure 1Y8R depicted by Lois and Lima (2005).

Actually these pairs of residues do not show strong interactions, they just function as permissive factors. Ubiquitin cannot bind to the APPBP1-Uba3 complex because its Arg72 is repelled by Arg190 of uba3. An ubiquitin carrying an R72A mutation can bind APPBP1-Uba3, whereas an A72R mutation of Nedd8 can not bind uba3 any more (Walden et al., 2003b). More interestingly, the -5 residue of Nedd8 is also specific for recognition by Nedd8

specific protease NEDP1 (Shen et al., 2005). Note that the sumo E1 enzyme catalyse all four sumo isoforms, but the corresponding -5 residues are different between sumo-1 and somo-2/3/4. It is unclear whether Glu in sumo-1 and Gln in sumo-2/3/4 at the aligned position make any difference in these sumo isoforms interacting with E1.

E2

All sumo proteins share a conjugating enzyme E2, which is called *ubc9* for yeast and human, and also called *ube2i* or *ube2a* in other species. While mouse and human *ubc9* proteins are identical, there is a ~56% identity between the mammalian and *S. cerevisiae* orthologues (Dohmen, 2004). Sumo E2 is also of high homology to the E2 enzymes of Nedd8 and ubiquitin. The alignment of sumo E2 *ubc9*, Nedd8 E2 *ubc12* and a ubiquitin E2 *ubcH7* is shown in Figure 6.

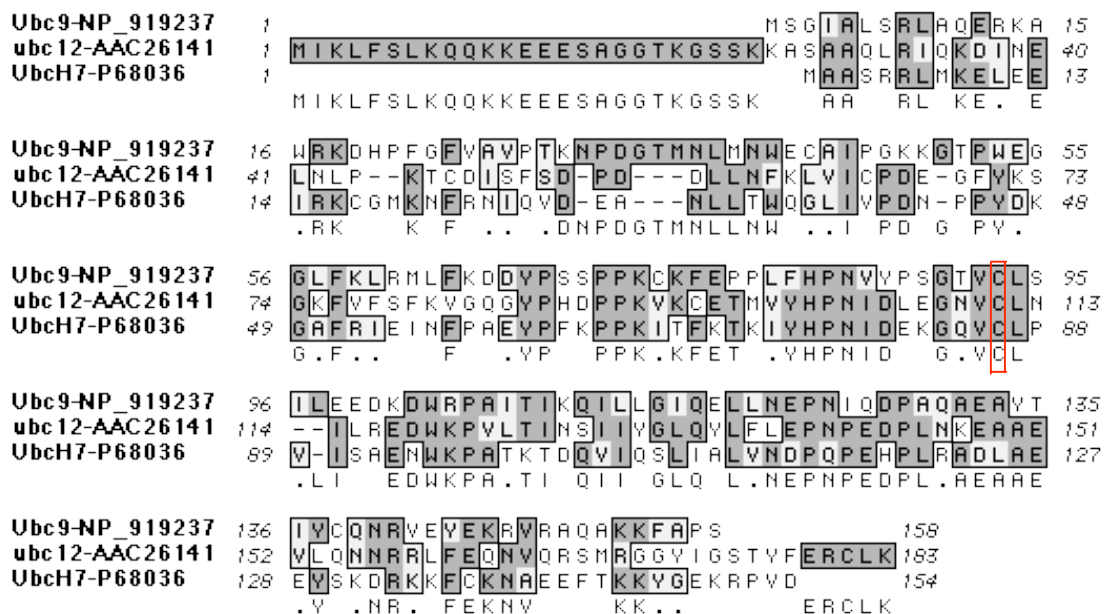


Figure 6. The alignment of conjugating E2 enzymes. All protein sequences are of Homo sapiens. Red box (AA93 for *ubc9*) indicates catalytic residues. *Ubc9*, *ubc12* and *ubcH7* are conjugating enzymes for sumo, Nedd8 and ubiquitin, respectively.

Most E2 enzymes, including *ubc9*, *ubc12*, *ubcH7* and some other ubiquitin E2s, contain a conserved 150-residue $\alpha\beta\beta\beta\beta(\beta\beta)\alpha\alpha$ motif named *ubc* superfold, and differ from one another only by N- and/or C-terminal extensions and/or small insertions within the *ubc* core (Jentsch, 1992; Tong et al., 1997; Bernier-Villamor et al., 2002). The superfold of *ubc9* is shown in Figure 7A. It contains four α -helices and six β -strands. $\alpha 1$, $\alpha 2$ and $\alpha 3/4$ cover three sides of the molecule, and the antiparallel β -sheet formed by $\beta 1-4$ strands cover another side. Still two sides are covered by loose strands, one surrounding the active residue Cys93 that is

situated close to the middle of a long extended stretch between the fourth β -strand and the second α -helix (Tong et al., 1997).

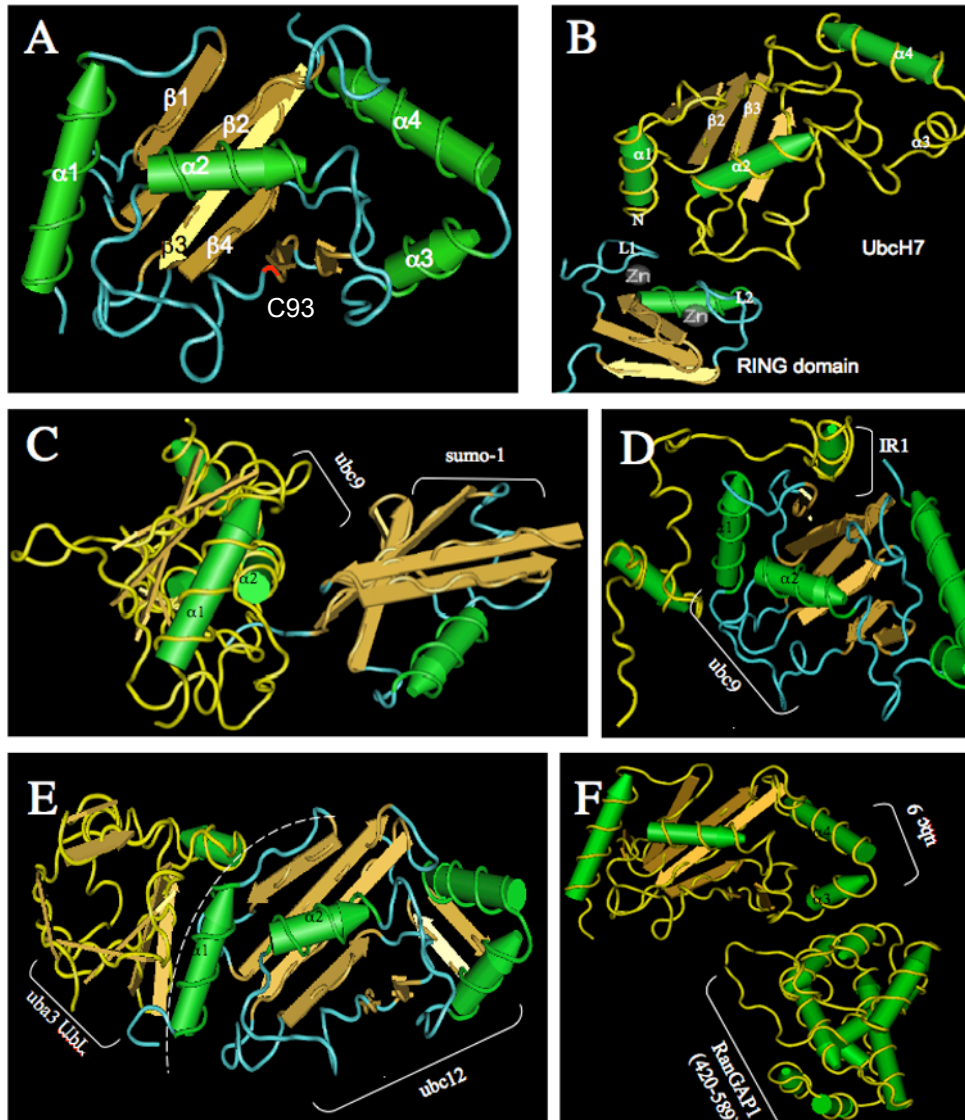


Figure 7. Structures of E2 conjugating enzymes with their binding partners. A. Ubc9, modified from 1U9A by Tong et al., (1997). It consists of $\alpha 1\beta 1-6\alpha 2-4$, the $\beta 1-4$ stretches form an antiparallel sheet, $\alpha 1-3$ are located on different sides. The catalytic Cys93 lies on a free loop in a crevice formed by L6 (the longest loop between $\beta 6$ and $\alpha 2$) and L7 (a long loop between $\alpha 2$ and $\alpha 3$). B. UbcH7 (yellow) bound with RING domain (blue) of Cbl, modified from 1FBV by Zheng et al. (2000). An interface is formed between UbcH7 $\alpha 1+L3+L6$ and cbl RING $L1+L2+a$. C. Ubc9 (yellow) and sumo-1 (blue) in the sumo-ubc9-RanBP2-RanGAP1 complex, with the sumo-1 β -sheet located near Ubc9 $\alpha 2$. Modified from Reverter and Lima (2005). Note that sumo-1 is not conjugated with Ubc9 in this complex, but with RanGAP1 as shown in figure 8. D. Ubc9 (blue) and RanBP2 (IR1 domain, yellow) in the sumo-ubc9-RanBP2-RanGAP1 complex. N-terminal IR1 contacts with L1 and β -sheet of Ubc9. E. Ubc12 (blue) bound with the ubiquitin-like (UbL) domain (yellow) of Uba3. Ubc12 $\alpha 1$ resides in a groove formed by $\alpha 13$ and the β -sheet of the Uba3 ubiquitin-like domain. Modified from Huang et al. (2004a). F. Ubc9 and RanGAP1 in the sumo-ubc9-RanBP2-RanGAP1 complex, the contact regions are around $\alpha 4$.

In the sumoylation pathway (Figure 1), E2 functions as an intermediate, thus it interacts with nearly all other proteins. It has at least 5 binding sites related to sumoylation:

1. The catalytic region that contains the catalytic site Cys93 and has a groove to hold the sumo-1 C-terminus (Figure 7C) (Liu et al., 1999). The binding of sumo at this site is the result of E2 interacting with E1. As modifiers and E1 interact specifically, ubiquitin or other UbIs cannot bind ubc9 at this site, and vice versa.
2. The $\alpha 1$ regions that contain the $\alpha 1$ -helix and the surrounding residues of the β -sheet. Similar regions in Nedd8's E2 (ubc12) are found bind the C-terminal ubiquitin-like domain of Nedd8's uba3 subunit in a firm and special way (Huang et al., 2005). Four of the five β -strands and the kinked α -13 helix of the uba3 ubiquitin-like domain form a W-shaped surface of two grooves, which cradles ubc12's long α -helix along its entire length and part of the ubc12 $\alpha 1\beta 1$ loop, respectively (Figure 7E) (Huang et al., 2005). The uba2 ubiquitin-like domain has also been shown to strongly interact with ubc9 (Lois and Lima, 2005). Although not proven, it is likely that ubc9 binds to the ubiquitin-like domain of uba2 in a similar way as ubc12 bind to uba3. Thus E1 and E2 may form a complex which acts as the core of the sumoylation machinery (See "SUMO COMPLEX").
3. The region below $\alpha 1$ that consists mainly of the N-terminal extension of $\alpha 1$ and the loop between $\beta 2$ and $\beta 3$, and between $\beta 6$ and $\alpha 2$ (Figure 7B). In the structures of ubiquitin conjugating enzymes, this is the region that interacts with both HECT- and RING-domains of ubiquitin E3 ligases (Huang et al., 1999; Zheng et al., 2000), and thus it seems to be a common site for E2-E3 binding. As no structure of the Pias RING domain is available, we take the structure of ubcH7-Cbl⁵ as the model of E2-E3 binding, and suppose that ubc9 interacts with the RING domain of Pias proteins in a similar way. In the ubcH7-Cbl structure, the apexes of the ubcH7 L3 and L6 loops reside contain a shallow groove formed by the α -helix and the two zinc-chelating loops (L1 and L2) of the Ubl-RING domain (Figure 7B) (Zheng et al., 2000).
4. The four-stranded β -sheet. In the sumo-1-ubc9-RanBP2-RanGAP1 complex, the ubc9 β -sheet is the binding area for RanBP2 IR1 domain (Figure 7D) (Tatham et al., 2005).
5. The C-terminal $\alpha 3,4$ region that binds to the substrates. RanGAP1 is the only known substrate with a second binding site for ubc9 (Pichler et al., 2004), and binds ubc9 at the $\alpha 3$

⁵ Cbl, a ubiquitin E3 ligase containing a RING domain. It attenuates signaling by the activated PDGF, EGF, and CSF-1 receptor tyrosine kinases (RTKs) by inducing their ubiquitination and subsequent degradation by the proteasome.

region (Figure 7F) (Bernier-Villamor et al., 2002; Tatham et al., 2003; Reverter and Lima, 2005).

E3

After activation, sumo is transferred from E1 to E2, and is then ready to conjugate with the substrate. The last step is completed with the help of the E3 ligase. Initially there was some doubt about whether E3 is needed in the last step, because sumo conjugation can take place *in vitro* in the absence of the E3. However, the vast majority of sumoylation in yeast is E3-dependent, and E3 enhances sumo attachment *in vitro* to all substrates that have been tested (Johnson, 2004).

A common characteristic of E3 ligases from both the ubiquitin and sumo systems is the existence of a nonproductive automodification reaction whereby sumo (or ubiquitin) is ligated from the E2 onto a lysine within the E3 itself in preference to a substrate molecule (Tatham et al., 2005). The function of E3 auto-modification is unknown. It is possible that the autosumoylation of E3 is the prerequisite for E3 recruitment of the substrate.

E3 is the largest group of enzymes in the modification pathway. It is estimated that there are more than 100 E3 ligases in the human genome, but only a few E3 ligases have been characterized at the molecular level (Chin et al., 2002). About ten E3 ligases have been found to be involved in sumoylation, less is known for neddylation. Ubiquitin ligases can be broadly subdivided into two groups based on the presence of either a RING (really interesting new gene) or HECT (homologous to E6AP carboxyl terminus) structural motif. RING-containing E3 ligases bind both E2 and a particular target, whereas HECT-containing E3 form ubiquitin-thioester complexes before conjugation of ubiquitin to targets (Pickart, 2001). The sumoylation E3 ligases are divided into three groups. The biggest group, Pias proteins, also contain RING domains, whereas HECT domain-containing E3 ligases have not been identified for sumoylation. Two additional groups of sumo ligases, the polycomb protein Pc2 and the nucleoporin RanBP2, do not belong to either RING or HECT class ligases (Tatham et al., 2005). As discussed later, these three groups of ligase actually differ in sumoylation.

Pias proteins

Pias proteins are the largest group of sumo E3 ligases up to now. They were first identified as inhibitors of activated STAT (signal transducers and activators of transcription) (Chung et al., 1997). Later on, they were shown to interact with and modulate several other proteins, and

more importantly, act as E3 ligases in sumoylation (Melchior et al., 2003). Pias proteins act not only as sumoylation E3 enzymes, e.g., Piasx can coactivate Elk-1 in an E3 activity-independent manner (Yang and Sharrocks, 2005).

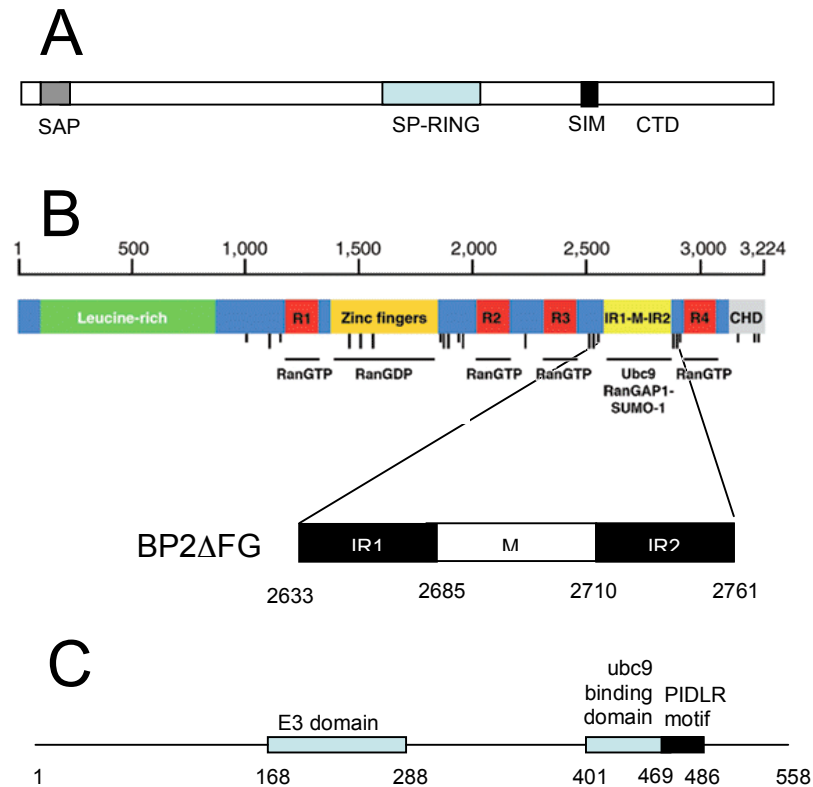


Figure 8. Schematic representation of the domains of sumoylation E3 ligases. A. Pias. A typical Pias protein contains a N-terminal SAP domain, a C-terminal domain (CTD), a sumo-interaction motif (SIM) and a SP-RING domain. B. RanBP2, modified from Matunis and Pichart, (2005). RanBP2 contains a leucine-rich domain, four RanBP1 homologues (RBD), a region containing eight Zinc-finger motifs and the sumo E3 ligase domain BPAFG, which consist of two internal repeats (IR) and a middle (M) domain. C. Pc2, drawn according to Kagey et al., (2005.) It contains three domains related to sumoylation of CtBP, an uncharacterized E3 domain, a PIDLR motif for CtBP binding, and a ubc binding domain in between.

Four mammalian genes encoding Pias proteins have been described: *Pias1* (also called *GuBP*), *Pias3*, *Piasx*, and *Piasy*. *Pias3* has a splice variant called KChaP, and *Piasx* also produces two isoforms derived from alternative splicing, designated *Piasx α* (ARIP3) and *Piasx β* (Miz1). *Pias1* and *Pias3* are ubiquitously expressed, whereas *Piasx* and *Piasy* appear to be found primarily in testis. All of the Pias proteins localize to intranuclear dots, and colocalize, at least in part, with PML nuclear bodies (Johnson, 2004). *Pias1* contains a N-

terminal SAP (SAR⁶, Acinus, Pias) domain, SP-RING domain (Siz/Pias-RING), SIM (sumo interaction motif), and a highly divergent C-terminal domain (Figure 8A). The SAP domain is known to bind DNA and some proteins, such as the tumor suppressor p53 (Okubo et al., 2004) and Lymphoid enhancer factor 1 (Sachdev et al., 2001). NMR spectroscopy showed that the NTD forms the four-helix SAP domain. One end of the four-helix bundle is the binding site for DNA and is thought to fit into the DNA minor groove (Okubo et al., 2004). The SIM domain has been implicated in directly binding sumo. It is an 11-amino acid motif that contains a central serine doublet separated by one amino acid, thus called SXS motif. On the N-terminal side, the SXS triplet is flanked by predominantly hydrophobic amino acids, and on the C-terminal side by acidic amino acids (D/E). Alanine replacement analysis shows that both the serines and the acidic C-terminal residues are crucial for interaction with sumo-1 (Minty et al., 2000). Deletion of the SIM domain has little effect on the ability of Pias proteins to promote sumo conjugation, but it can affect their localization and activity in transcriptions (Sachdev et al., 2001; Kotaja et al., 2002). The CTDs of Pias proteins are often found to interact with sumoylation substrates, e.g. the tumor suppressor homologue p73 α and interferon regulatory factor-1 (IRF-1) (Minty et al., 2000; Nakagawa and Yokosawa, 2002); so, it is generally considered to be a substrate specific domain (Johnson, 2004). A conspicuous feature of Pias proteins is the SP-RING finger domain that is located in the middle of the protein. RING fingers have been defined by the consensus sequence Cx2Cx(9–39)Cx(1–3)Hx(2–3)C/Hx2Cx(4–48)Cx2C, with the Cys and His side chains representing zinc binding sites (Figure 9A-B) (Pickart, 2001; Capili et al., 2004). It is known that SP-RING domains of Pias proteins interact with sumo conjugating enzyme E2 (Kahyo et al., 2001; Melchior et al., 2003; Johnson, 2004). But no structure of Pias protein RING domain has been identified. The ubiquitin E3 ligase Cbl RING domain structure consists of a three-stranded β -sheet, an α -helix, and two large zinc-chelating loops. The helix and the two loops form a groove, into which the L1 and L2 loops of the E2 protein ubcH7 can bind (Figure 9C) (Zheng et al., 2000).

Unlike Pias proteins that contain binding sites for both the substrates and E2, most ubiquitin E3 are complexes of several proteins, and the binding sites for E2s and substrates are separated in different subunits. For example, in the Rbx1-Cul1-Skp1-Skp2 E3 complex, Rbx1

6 SAR, scaffold-associating regions. Interphase chromatin is arranged into topologically separated domains comprising gene expression and replication units through genomic sequence elements, so-called SAR regions. SAR regions are located near the boundaries of actively transcribed genes and were shown to influence their activity.

binds E2, and Skp2 binds the substrate β -catenin (Wu et al., 2003). Recently, two other proteins have been found to function as sumo ligases. They form a large complex with other proteins, and may thus, similar to ubiquitin E3s, be functional in large E3 complexes. One is the yeast protein Mms21 and its human homolog NSE2a (Potts and Yu, 2005; Zhao and Blobel, 2005). The other is topors, a protein originally identified as cellular binding partner of DNA topoisomerase I and of p53, recently found to function as an ubiquitin E3 ligase for the sumoylation of p53 and a variety of other unidentified cellular proteins (Weger et al., 2005). Those newly found E3 ligases also contain RING domains, but at different positions. Both Mms21 and NSE2 have RING domains at their C-termini, topors has a RING domain at its N-terminus. As they do not show any homologue with any of the known Pias proteins, they might belong to new families of sumo E3 ligases.

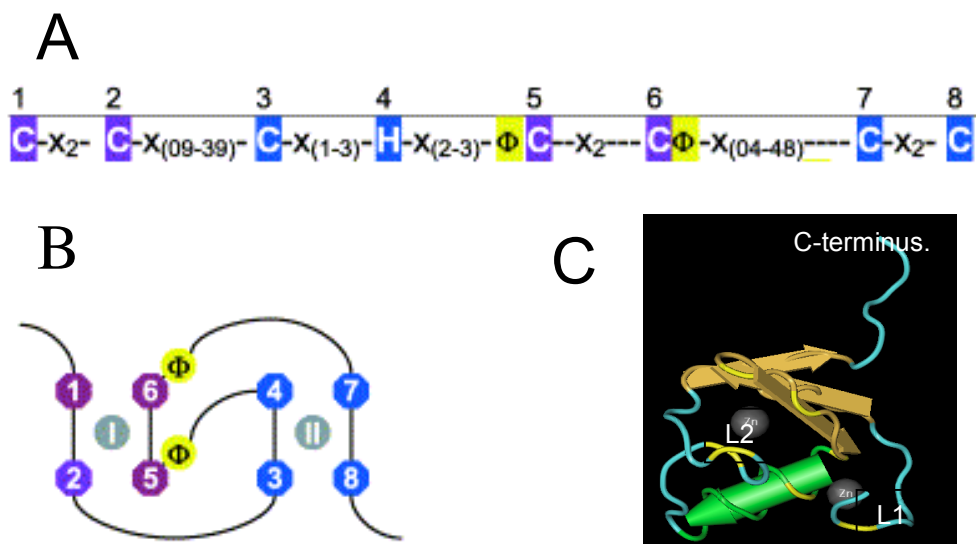


Figure 9. RING domain. A. The consensus sequences that define RING domains. B. Schematic representation of the cross-brace zinc ligation found in RING domains. C. Worm representations of the Cbl RING domain. A and B are taken from Capili et al. (2004). C is modified from PDB structure 1FBV by Zheng et al. (2000).

RanBP2

The nuclear pore complex protein Ran binding protein 2 (RanBP2) is neither a HECT- nor RING-type E3 ligase. It was previously found to catalytically enhance sumoylation of the nuclear body component (Pichler et al., 2002). RanBP2 directly interacts with the E2 enzyme ubc9 and strongly enhances sumo-1-transfer from ubc9 to the sumo-1 target Sp100 (Pichler et al., 2002). RanBP2 is a multidomain protein with interaction sites for proteins including

nuclear transport receptors, the GTPase Ran, ubc9, and sumoylated GTPase-activating protein RanGAP1 (Pichler et al., 2004) (Figure 7). The sumo E3 activity of the 358-kDa RanBP2 was mapped to a 33-kDa, 286-residue fragment termed BP2 Δ FG. This fragment contains two approx. 50-residue long internal repeats (IR1 and IR2) separated by a 25-residue middle domain (M) (Pichler et al., 2002; Matunis and Pickart, 2005) (Figure 8B). The IR1 is an ubiquitin-like protein binding domain. It mediates attachment of both sumo-1 and sumo-2 to their substrates (Tatham et al., 2005). It is interesting that IR2 is highly homologous to IR1, but it does not bind to ubc9. IR2 can mediate sumo-1, but not sumo-2 attachment. Thus, it is supposed to act in a sumo-1 specific manner mediated by direct interaction between sumo-1 and IR2 motif (Tatham et al., 2005). The M motif strongly enhances both IR1 and IR2 activity, but does not contain any catalytic activity itself (Pichler et al., 2004). In the sumo-1-RanGAP1(432-587)-ubc9-RanBP2(IR1) complex, the IR1 domain of RanBP2 adopts an extended structure. It binds the β -sheet of ubc9 with its C-terminal fragment that forms an α -helix. The middle free loop of IR1 extends across ubc9 α 1 (Figure 7D). Unlike Pias proteins, which interact with the substrate through their C-terminal domains, no direct connection has been found between RanBP2 and any of its substrates found up to now (discussed below). Thus, it is proposed that RanBP2 acts as an E3 by binding both sumo and ubc9 to position the sumo-E2-thioester in an optimal orientation, thereby enhancing conjugation (Reverter and Lima, 2005).

Pc2

Pc2 was identified as a sumo E3 for the transcriptional corepressors CtBP (C-terminal binding protein of adenovirus E1A) and CtBP2, both *in vivo* and *in vitro* (Kagey et al., 2003; Lin et al., 2003). It is a member of the polycomb group of proteins, which were first identified in *Drosophila* as regulators of segment identity (Simon et al., 1992; Simon and Tamkun, 2002). Human Pc2 shares only limited sequence similarity to *Drosophila* Pc, primarily in the amino-terminal chromodomain and a small region at the extreme carboxyl-terminus (Satijn et al., 1997). Pc2 has no obvious sequence similarity to other known E3, suggesting that it is a new group of sumo E3, with no apparent unifying structural features. However, the enhancement of CtBP sumoylation by Pc2 *in vitro* is very modest, and Pias1, Piasx, and RanBP2 can also promote CtBP sumoylation, suggesting that there may be multiple factors involved in CtBP sumoylation (Kagey et al., 2003; Johnson, 2004). In mammalian cells, various polycomb proteins, including Pc2, have a distinct subnuclear localization, forming discrete foci, termed polycomb bodies (Gerasimova and Corces, 1998). A CTD fragment of Pc2 (Figure 8C, amino

acids 401–558) interacts with both ubc9 and CtBP, and recruits both proteins to polycomb bodies. An E3 activity has been shown, not in the CTD *in vivo*, but a separate domain in the NTD, which has E3 activity on its own *in vitro*. *In vivo*, both the NTD and the CTD domains contribute to E3 activity (Kagey et al., 2005).

SUMOYLATION COMPLEX

The processes of ubiquitination, sumoylation and neddylation are quite similar, thus they probably share a common mechanism. With the available structures of proteins and complexes involved in different modification pathways, we here propose how and in which sequence the sumoylation machinery is assembled.

Sumoylation model

Figure 10 depicts all structures of the protein components of the sumoylation pathway. They are IR1 domain of RanBP2 (Figure 10A), ubc9 (Figure 10B), a cartoon of Pias1 bound with STAT1 (Figure 10C), sumo-1 in free, adenylated and activated states (Figure 10D), and the aos1/uba2 complex (Figure 10E).

Aos1-uba2 and ubc9 form a complex and serve as the core components of the machinery. Ubc9 resides in the upper part of the E1 cleft 1, with firm contact with the UbL domain of E1 as illustrated in Figure 11. It is not known whether there are any other interactions to strengthen the location of ubc9. Its catalytic site Cys93 should be near to Cys173 of uba2 (Huang et al., 2005). As discussed below, it is likely that RanBP2 is also a member of the core machinery. The C-terminus of RanBP2 IR1 domain binds to Ubc9; the N-terminus extends, crosses the E1 UbL domain, and extends to E1 cleft 1. It is also shown in the sumo-ubc9-RanBP2-RanGAP1 that the M domain, which follows C-terminal IR1, turns back and extends to the same direction as N-terminal IR1. Although not shown in the crystal structure of the complex, it can be imagined that the IR2 domain of RanBP2 also resides over E1 cleft 2, even extends further than IR1. Thus, it is speculated that IR2 domain plays some roles in recruiting the sumo molecule to the nucleotide-binding site and translocating to the E1 catalytic Cys site afterwards. One ATP molecule is bound in a pocket around the Gly-x-Gly-x-x-Gly nucleotide binding motif (Walden et al., 2003b), which is conserved among ubiquitin, sumo and Nedd8 activating enzymes. Of ubc9, the binding sites for Pias protein RING domain and for some substrates such as RanGAP1 are exposed.

For a sumoylation reaction, a sumo molecule is bound to the adenylation center. Contacts between the C-terminal carboxylate of sumo-1 Gly97 and the ATP α -phosphate place the C-

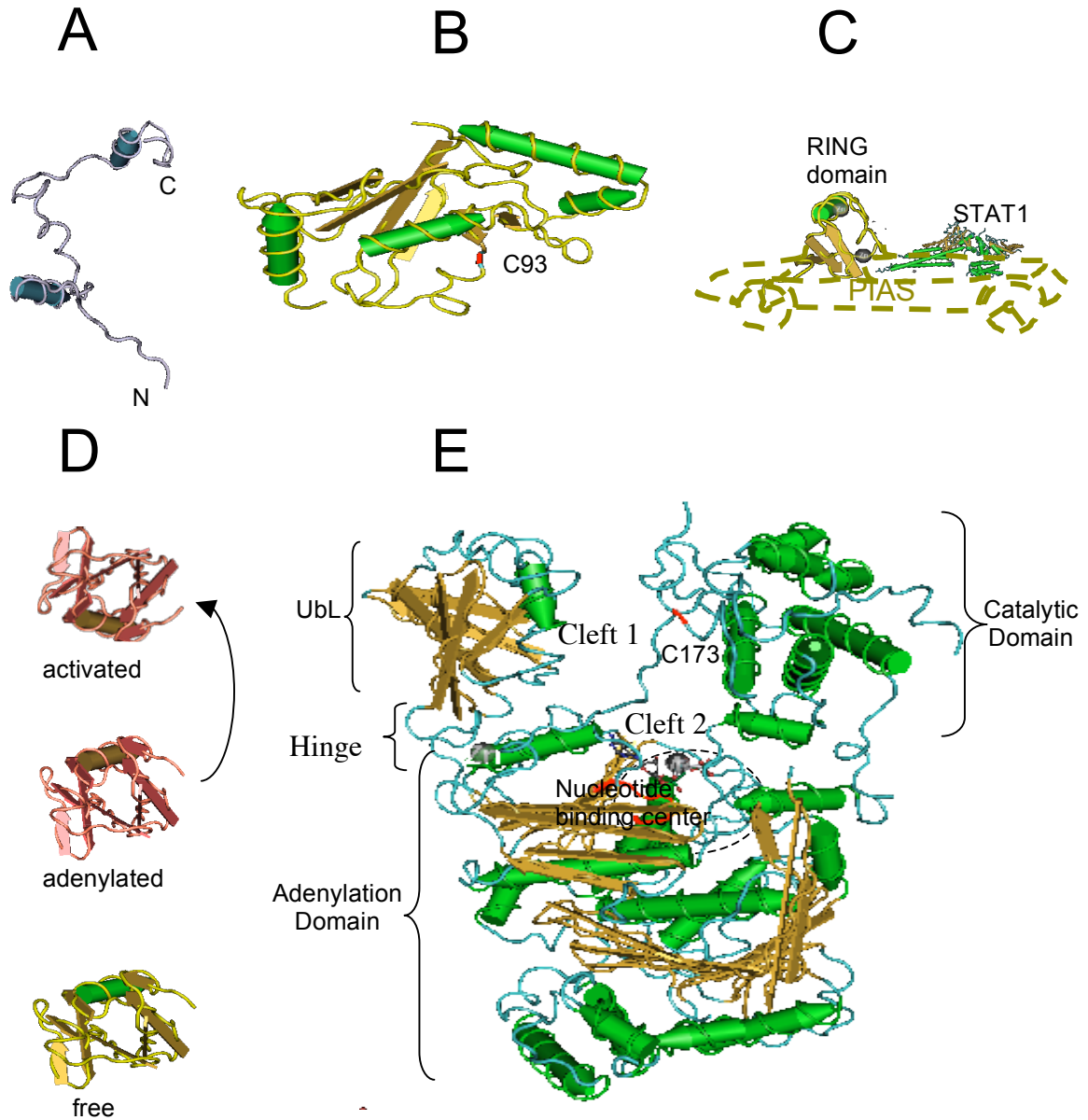


Figure 10. Components of the sumoylation machinery. A. RanBP2-IR1 (2,631-2,693). B. Ubc9 (2-157). C. PIAS protein loaded with a substrate STAT1. D. Sumo-1 (20-97). E. E1 complex aos1-uba2.

terminal sumo-1 glycine in an optimal orientation for attack at the ATP α -phosphate (Lois and Lima, 2005). Next, a thioester bond forms between E1 catalytic Cys173 and sumo. As the Cys173 is far from the adenylation domain, sumo-1 needs to translocate and probably make an 180° turn in order to get into the right position to form the thioester bond with E1, and later on with E2. This force may originate from M and/or IR2 domain of RanBP2 that are supposed to be in vicinity, or pushed by a new free sumo-1 that comes and binds with the ATP in the nucleotide binding motif. As the M-IR2 fragment of RanBP2, which contains both M and IR2 domains (Figure 8B), has been shown to interact with sumo-1 in GST pulldown assays in a ubc9 independent way (Tatham et al., 2005), thus make it possible that the M-IR2 fragments

play a role in recruiting and translocation sumo. The activated sumo is then transferred to E2 and later to the substrate through interactions between E1-E2 and E2-substrate, respectively.

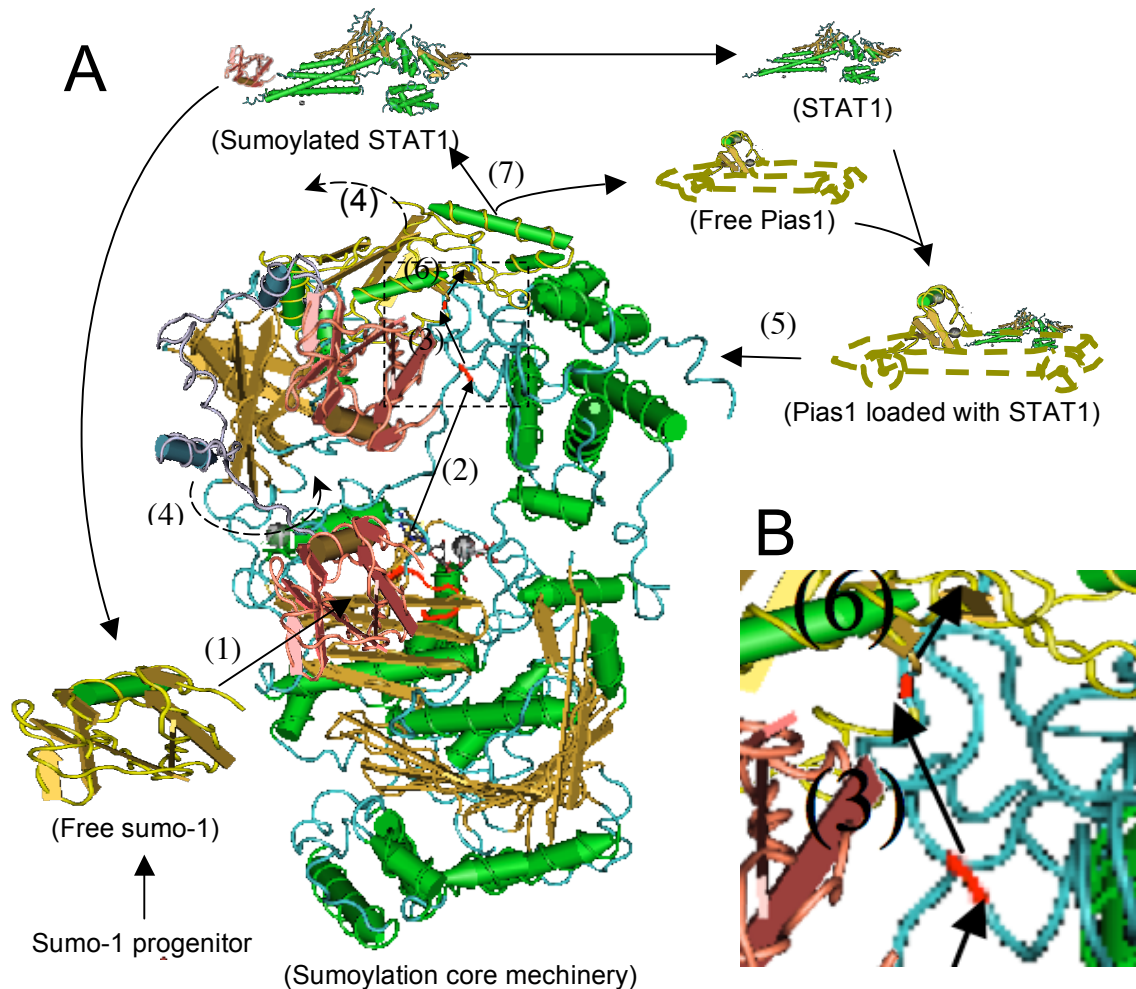


Figure 11. A. Proposed sequence of assembly of the sumoylation complex. B. Blow-up of the box in A.

1. One sumo enters into adenylation areas and is adenylated.
2. A second sumo enters into the adenylation areas and shifts the first sumo to E1 catalytic Cys173. During translocation, the first sumo undergoes a turn of 180°, and reaches the correct position to bind E2 and/or RanBP2.
3. Sumo is transferred to E2 catalytic site Cys93.
4. E2, together with UbL domain of E1, turn along UbL axis. Thus E2 and E3 catalytic sites detach.
5. A Pias protein bound with a substrate binds to E2. RanGAP1 binds E2 by itself. Both E2 and the substrate are ready to accept sumo.
6. Sumo is further transferred to the substrate.
7. The sumoylated substrate exits the complex.

After conjugation with a sumo molecule, the E2 protein makes a translocation, with the E1 UbL domain, along the rotation of the linkage between the UbL domain and the rest of the E1 protein (Huang et al., 2005. Figure 11). Thus the catalytic Cys sites of E1 and E2 proteins are

detached. E1 catalytic site again is available for another sumo conjugation. A substrate is recruited to the E2 by an E3 ligase, and is conjugated with the sumo. At last, the sumoylated substrate leaves the Pias protein and departs from the complex. The SIM of Pias protein may play a role for the dissociation of sumoylated substrate and Pias. Free Pias protein then associates with another unmodified substrate and is ready for another round of sumoylation.

Prospective of the Model

In the previous section, a model of the sumoylation complex was described under the assumption that aos1/uba2-ubc9-RanBP2 forms the core of the sumoylation machinery. Both RanBP2 and Pias proteins are needed for an efficient modification: RanBP2 is a component in the core machinery for all sumoylation reaction, and Pias proteins work as adaptors for recruiting substrates to the core. Of the three types of E3 ligases found so far, only Pc2 is not involved in the model. The only found Pc2 substrates for sumoylation are CtBP proteins, whose sumoylation was also enhanced by Pias proteins and RanBP2 (Kagey et al., 2003). The studies on Pc2 function were performed in cells (Kagey et al., 2003; Kagey et al., 2005), thus one cannot exclude the involvement of other cellular proteins in the sumoylation of CtBPs.

About 100 proteins have been found to be sumoylation substrates. Most of them were initially identified as interactors for Pias proteins and/or ubc9 by protein-protein interaction assays, such as yeast two-hybrid and/or GST pulldown, and confirmed later to be sumoylated by sumoylation and/or mutagenesis assays. For only four proteins, the sumoylation reactions have not been reported to be enhanced by Pias proteins. These are RanGAP1 (Matunis et al., 1996; Mahajan et al., 1997), Sp100 (Pichler et al., 2002), promyelocytic leukaemia protein (PML) (Tatham et al., 2005) and histone deacetylase 4 (HDAC4) (Kirsh et al., 2002). All these proteins were initially found to be endogenously sumoylated in cell extracts, which is an unusual observation as most sumoylated proteins are quickly desumoylated before analysis. For references, see Matunis et al., 1996; Mahajan et al., 1997; Sternsdorf et al., 1997; Kirsh et al., 2002. Actually, RanBP2 does not directly interact with either RanGAP1 or Sp100 in pulldown assays (Matunis et al., 1998; Pichler et al., 2002), and no direct interaction between RanBP2 and the other two substrates has been shown either.

As RanBP2 is located in the core of the sumoylation complex and thus does not interact with these four substrates, there must be some other interactions to recruit these substrates to the core. RanGAP1 has a second binding site for E2 (Pichler et al., 2004), which may help in the reaction. PML contains a RING domain (Borden et al., 1995), which may mediate direct

interactions between PML and ubc9. Once proven, it may be further deduced that PML may also work as an adaptor between ubc9 and other proteins in the PML-nuclear body, such as Sp100. Sp100 and HDAC1/4/6 have been shown to be sumoylated *in vitro*, and these sumoylations were enhanced by addition of RanBP2. But as these assays were performed with HeLa cell extracts (Kirsh et al., 2002; Pichler et al., 2002), there may have been additional factors in the cell extracts that aided in this reaction. Actually, HDAC6 has a RING domain, and it may work as an adaptor for other HDAC proteins. It has been shown that nuclear localization is a prerequisite for HDAC4 sumoylation (Kirsh et al., 2002).

According to the model, RanBP2 and Pias proteins enhance the recruitment of sumo and substrates, respectively, to the core. It suggests that both of them may be able to enhance sumoylation. Actually, it has been shown that both RanBP2 and some Pias proteins enhance sumoylation of the transcription corepressor CtBP (Lin et al., 2003) and Mdm2 (Miyachi et al., 2002) in *in vitro* sumoylation assays. In addition, the model also suggests that both RanBP2 and Pias proteins are needed for sumoylation. Of the numerous sumoylation assays, those performed *in vivo*, or *in vitro* but with cell extracts, can be considered to contain both RanBP2 and Pias proteins, or their homologues. The *in vitro* sumoylation assays with purified proteins are supposed to lack other protein contaminations. But obviously *in vitro* assays do not faithfully reproduce the physiological substrate selection mechanisms (Johnson, 2004). The intracellular space provides a highly compartmentalized system for sumoylation pathways (Gunning et al., 1998). In cells, E3 adaptors are needed to recruit the substrates to the core. But in the *in vitro* sumoylation system, as the reaction is performed in solution, different protein molecules will meet randomly with high frequency. That may be the reason for altered sumoylation levels observed without RanBP2 or Pias proteins in most *in vitro* sumoylation assays. It is interesting that in the functional assays of Pias proteins (without addition of RanBP2), the ratio of sumo: E1: E2: substrate was approximately 50: 1: 1: 8 (Kahyo et al., 2001; Kirsh et al., 2002), so sumo was 50-fold excess over E1-E2. Conversely, in the assay for RanBP2 (without addition of Pias proteins), the ratio of sumo: E1: E2 was 5: 1: 1 (Pichler et al., 2002). This difference suggests that high levels of sumo and substrates can compensate for deficiencies caused by the lack of RanBP2 and E3 adaptors, respectively.

REFERENCES:

- Baba D, Maita N, Jee JG, Uchimura Y, Saitoh H, Sugasawa K, Hanaoka F, Tochio H, Hiroaki H, Shirakawa M (2005) Crystal structure of thymine DNA glycosylase conjugated to SUMO-1. *Nature* 435:979-982.

- Bayer P, Arndt A, Metzger S, Mahajan R, Melchior F, Jaenicke R, Becker J (1998) Structure determination of the small ubiquitin-related modifier SUMO-1. *J Mol Biol* 280:275-286.
- Bernier-Villamor V, Sampson DA, Matunis MJ, Lima CD (2002) Structural basis for E2-mediated SUMO conjugation revealed by a complex between ubiquitin-conjugating enzyme Ubc9 and RanGAP1. *Cell* 108:345-356.
- Bohren KM, Nadkarni V, Song JH, Gabbay KH, Owerbach D (2004) A M55V polymorphism in a novel SUMO gene (SUMO-4) differentially activates heat shock transcription factors and is associated with susceptibility to type I diabetes mellitus. *J Biol Chem* 279:27233-27238.
- Borden KL, Boddy MN, Lally J, O'Reilly NJ, Martin S, Howe K, Solomon E, Freemont PS (1995) The solution structure of the RING finger domain from the acute promyelocytic leukaemia proto-oncoprotein PML. *Embo J* 14:1532-1541.
- Capili AD, Edghill EL, Wu K, Borden KL (2004) Structure of the C-terminal RING finger from a RING-IBR-RING/TRIAD motif reveals a novel zinc-binding domain distinct from a RING. *J Mol Biol* 340:1117-1129.
- Chin LS, Vavalle JP, Li L (2002) Staring, a novel E3 ubiquitin-protein ligase that targets syntaxin 1 for degradation. *J Biol Chem* 277:35071-35079.
- Chung CD, Liao J, Liu B, Rao X, Jay P, Berta P, Shuai K (1997) Specific inhibition of Stat3 signal transduction by PIAS3. *Science* 278:1803-1805.
- Ding H, Xu Y, Chen Q, Dai H, Tang Y, Wu J, Shi Y (2005) Solution structure of human SUMO-3 C47S and its binding surface for Ubc9. *Biochemistry* 44:2790-2799.
- Dohmen RJ (2004) SUMO protein modification. *Biochim Biophys Acta* 1695:113-131.
- Dohmen RJ, Stappen R, McGrath JP, Forrova H, Kolarov J, Goffeau A, Varshavsky A (1995) An essential yeast gene encoding a homolog of ubiquitin-activating enzyme. *J Biol Chem* 270:18099-18109.
- Gerasimova TI, Corces VG (1998) Polycomb and trithorax group proteins mediate the function of a chromatin insulator. *Cell* 92:511-521.
- Gill G (2004) SUMO and ubiquitin in the nucleus: different functions, similar mechanisms? *Genes Dev* 18:2046-2059.
- Gunning P, Weinberger R, Jeffrey P, Hardeman E (1998) Isoform sorting and the creation of intracellular compartments. *Annu Rev Cell Dev Biol* 14:339-372.
- Huang DT, Paydar A, Zhuang M, Waddell MB, Holton JM, Schulman BA (2005) Structural basis for recruitment of Ubc12 by an E2 binding domain in NEDD8's E1. *Mol Cell* 17:341-350.
- Huang L, Kinnucan E, Wang G, Beaudenon S, Howley PM, Huibregtse JM, Pavletich NP (1999) Structure of an E6AP-UbcH7 complex: insights into ubiquitination by the E2-E3 enzyme cascade. *Science* 286:1321-1326.
- Huang WC, Ko TP, Li SS, Wang AH (2004) Crystal structures of the human SUMO-2 protein at 1.6 Å and 1.2 Å resolution: implication on the functional differences of SUMO proteins. *Eur J Biochem* 271:4114-4122.
- Jentsch S (1992) The ubiquitin-conjugation system. *Annu Rev Genet* 26:179-207.
- Johnson ES (2004) Protein modification by SUMO. *Annu Rev Biochem* 73:355-382.
- Kagey MH, Melhuish TA, Wotton D (2003) The polycomb protein Pc2 is a SUMO E3. *Cell* 113:127-137.
- Kagey MH, Melhuish TA, Powers SE, Wotton D (2005) Multiple activities contribute to Pc2 E3 function. *Embo J* 24:108-119.
- Kahyo T, Nishida T, Yasuda H (2001) Involvement of PIAS1 in the sumoylation of tumor suppressor p53. *Mol Cell* 8:713-718.
- Kamitani T, Nguyen HP, Kito K, Fukuda-Kamitani T, Yeh ET (1998) Covalent modification of PML by the sentrin family of ubiquitin-like proteins. *J Biol Chem* 273:3117-3120.

- Kirsh O, Seeler JS, Pichler A, Gast A, Muller S, Miska E, Mathieu M, Harel-Bellan A, Kouzarides T, Melchior F, Dejean A (2002) The SUMO E3 ligase RanBP2 promotes modification of the HDAC4 deacetylase. *Embo J* 21:2682-2691.
- Kotaja N, Karvonen U, Janne OA, Palvimo JJ (2002) PIAS proteins modulate transcription factors by functioning as SUMO-1 ligases. *Mol Cell Biol* 22:5222-5234.
- Li Y, Wang H, Wang S, Quon D, Liu YW, Cordell B (2003) Positive and negative regulation of APP amyloidogenesis by sumoylation. *Proc Natl Acad Sci U S A* 100:259-264.
- Lin X, Sun B, Liang M, Liang YY, Gast A, Hildebrand J, Brunnicardi FC, Melchior F, Feng XH (2003) Opposed regulation of corepressor CtBP by SUMOylation and PDZ binding. *Mol Cell* 11:1389-1396.
- Liu Q, Jin C, Liao X, Shen Z, Chen DJ, Chen Y (1999) The binding interface between an E2 (UBC9) and a ubiquitin homologue (UBL1). *J Biol Chem* 274:16979-16987.
- Lois LM, Lima CD (2005) Structures of the SUMO E1 provide mechanistic insights into SUMO activation and E2 recruitment to E1. *Embo J* 24:439-451.
- Mahajan R, Delphin C, Guan T, Gerace L, Melchior F (1997) A small ubiquitin-related polypeptide involved in targeting RanGAP1 to nuclear pore complex protein RanBP2. *Cell* 88:97-107.
- Matunis MJ, Pickart CM (2005) Beginning at the end with SUMO. *Nat Struct Mol Biol* 12:565-566.
- Matunis MJ, Coutavas E, Blobel G (1996) A novel ubiquitin-like modification modulates the partitioning of the Ran-GTPase-activating protein RanGAP1 between the cytosol and the nuclear pore complex. *J Cell Biol* 135:1457-1470.
- Matunis MJ, Wu J, Blobel G (1998) SUMO-1 modification and its role in targeting the Ran GTPase-activating protein, RanGAP1, to the nuclear pore complex. *J Cell Biol* 140:499-509.
- Melchior F (2000) SUMO--nonclassical ubiquitin. *Annu Rev Cell Dev Biol* 16:591-626.
- Melchior F, Schergaut M, Pichler A (2003) SUMO: ligases, isopeptidases and nuclear pores. *Trends Biochem Sci* 28:612-618.
- Minty A, Dumont X, Kaghad M, Caput D (2000) Covalent modification of p73alpha by SUMO-1. Two-hybrid screening with p73 identifies novel SUMO-1-interacting proteins and a SUMO-1 interaction motif. *J Biol Chem* 275:36316-36323.
- Miyachi Y, Yogosawa S, Honda R, Nishida T, Yasuda H (2002) Sumoylation of Mdm2 by protein inhibitor of activated STAT (PIAS) and RanBP2 enzymes. *J Biol Chem* 277:50131-50136.
- Nakagawa K, Yokosawa H (2002) PIAS3 induces SUMO-1 modification and transcriptional repression of IRF-1. *FEBS Lett* 530:204-208.
- Okubo S, Hara F, Tsuchida Y, Shimotakahara S, Suzuki S, Hatanaka H, Yokoyama S, Tanaka H, Yasuda H, Shindo H (2004) NMR structure of the N-terminal domain of SUMO ligase PIAS1 and its interaction with tumor suppressor p53 and A/T-rich DNA oligomers. *J Biol Chem* 279:31455-31461.
- Pichler A, Gast A, Seeler JS, Dejean A, Melchior F (2002) The nucleoporin RanBP2 has SUMO1 E3 ligase activity. *Cell* 108:109-120.
- Pichler A, Knipscheer P, Saitoh H, Sixma TK, Melchior F (2004) The RanBP2 SUMO E3 ligase is neither HECT- nor RING-type. *Nat Struct Mol Biol* 11:984-991.
- Pichler A, Knipscheer P, Oberhofer E, van Dijk WJ, Korner R, Olsen JV, Jentsch S, Melchior F, Sixma TK (2005) SUMO modification of the ubiquitin-conjugating enzyme E2-25K. *Nat Struct Mol Biol* 12:264-269.
- Pickart CM (2001) Mechanisms underlying ubiquitination. *Annu Rev Biochem* 70:503-533.
- Potts PR, Yu H (2005) Human MMS21/NSE2 Is a SUMO Ligase Required for DNA Repair. *Mol Cell Biol* 25:7021-7032.

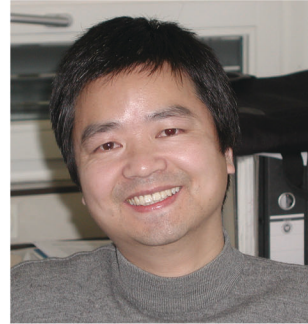
- Reverter D, Lima CD (2004) A basis for SUMO protease specificity provided by analysis of human Senp2 and a Senp2-SUMO complex. *Structure (Camb)* 12:1519-1531.
- Reverter D, Lima CD (2005) Insights into E3 ligase activity revealed by a SUMO-RanGAP1-Ubc9-Nup358 complex. *Nature* 435:687-692.
- Sachdev S, Bruhn L, Sieber H, Pichler A, Melchior F, Grosschedl R (2001) PIASy, a nuclear matrix-associated SUMO E3 ligase, represses LEF1 activity by sequestration into nuclear bodies. *Genes Dev* 15:3088-3103.
- Satijn DP, Olson DJ, van der Vlag J, Hamer KM, Lambrechts C, Masselink H, Gunster MJ, Sewalt RG, van Driel R, Otte AP (1997) Interference with the expression of a novel human polycomb protein, hPc2, results in cellular transformation and apoptosis. *Mol Cell Biol* 17:6076-6086.
- Shen LN, Liu H, Dong C, Xirodimas D, Naismith JH, Hay RT (2005) Structural basis of NEDD8 ubiquitin discrimination by the deNEDDylating enzyme NEDP1. *Embo J* 24:1341-1351.
- Simon J, Chiang A, Bender W (1992) Ten different Polycomb group genes are required for spatial control of the *abdA* and *AbdB* homeotic products. *Development* 114:493-505.
- Simon JA, Tamkun JW (2002) Programming off and on states in chromatin: mechanisms of Polycomb and trithorax group complexes. *Curr Opin Genet Dev* 12:210-218.
- Sternsdorf T, Jensen K, Will H (1997) Evidence for covalent modification of the nuclear dot-associated proteins PML and Sp100 by PIC1/SUMO-1. *J Cell Biol* 139:1621-1634.
- Su HL, Li SS (2002) Molecular features of human ubiquitin-like SUMO genes and their encoded proteins. *Gene* 296:65-73.
- Szczepanowski RH, Filipek R, Bochtler M (2005) Crystal structure of a fragment of mouse ubiquitin-activating enzyme. *J Biol Chem* 280:22006-22011.
- Tatham MH, Kim S, Jaffray E, Song J, Chen Y, Hay RT (2005) Unique binding interactions among Ubc9, SUMO and RanBP2 reveal a mechanism for SUMO paralogue selection. *Nat Struct Mol Biol* 12:67-74.
- Tatham MH, Jaffray E, Vaughan OA, Desterro JM, Botting CH, Naismith JH, Hay RT (2001) Polymeric chains of SUMO-2 and SUMO-3 are conjugated to protein substrates by SAE1/SAE2 and Ubc9. *J Biol Chem* 276:35368-35374.
- Tatham MH, Kim S, Yu B, Jaffray E, Song J, Zheng J, Rodriguez MS, Hay RT, Chen Y (2003) Role of an N-terminal site of Ubc9 in SUMO-1, -2, and -3 binding and conjugation. *Biochemistry* 42:9959-9969.
- Tong H, Hateboer G, Perrakis A, Bernards R, Sixma TK (1997) Crystal structure of murine/human Ubc9 provides insight into the variability of the ubiquitin-conjugating system. *J Biol Chem* 272:21381-21387.
- Walden H, Podgorski MS, Schulman BA (2003a) Insights into the ubiquitin transfer cascade from the structure of the activating enzyme for NEDD8. *Nature* 422:330-334.
- Walden H, Podgorski MS, Huang DT, Miller DW, Howard RJ, Minor DL, Jr., Holton JM, Schulman BA (2003b) The structure of the APPBP1-UBA3-NEDD8-ATP complex reveals the basis for selective ubiquitin-like protein activation by an E1. *Mol Cell* 12:1427-1437.
- Weger S, Hammer E, Heilbronn R (2005) Topors acts as a SUMO-1 E3 ligase for p53 in vitro and in vivo. *FEBS Lett*.
- Whitby FG, Xia G, Pickart CM, Hill CP (1998) Crystal structure of the human ubiquitin-like protein NEDD8 and interactions with ubiquitin pathway enzymes. *J Biol Chem* 273:34983-34991.
- Wu G, Xu G, Schulman BA, Jeffrey PD, Harper JW, Pavletich NP (2003) Structure of a beta-TrCP1-Skp1-beta-catenin complex: destruction motif binding and lysine specificity of the SCF(beta-TrCP1) ubiquitin ligase. *Mol Cell* 11:1445-1456.

- Yang SH, Sharrocks AD (2005) PIASx acts as an Elk-1 coactivator by facilitating derepression. *Embo J* 24:2161-2171.
- Zhao X, Blobel G (2005) A SUMO ligase is part of a nuclear multiprotein complex that affects DNA repair and chromosomal organization. *Proc Natl Acad Sci U S A* 102:4777-4782.
- Zheng N, Wang P, Jeffrey PD, Pavletich NP (2000) Structure of a c-Cbl-UbcH7 complex: RING domain function in ubiquitin-protein ligases. *Cell* 102:533-539.

CURRICULUM VITAE

Biographical

Name TANG, Zhongshu
Date of birth May, 03, 1969
Place of birth Anhui, China
Nationality Chinese
Family state Married



Education

Doctor of Philosophy
2001- Department of Neurochemistry
Max-Planck-Institute for Brain Research
Frankfurt am Main, Germany
Dissertation Advisor: Heinrich Betz, MD, Prof.

Master of Sciences
1995-1998 Shanghai Institute of Physiology,
Chinese Academy of Sciences
Shanghai, China
Dissertation Advisor: Changfu Zhou, Prof.

Bachelor of Sciences
1989-1993 Department of Biology
Anhui Normal University
Wuhu, China

Employment experience

Research Assistant
1998-2001 Shanghai Institute of Physiology,
Chinese Academy of Sciences
Shanghai, China

Teacher for Biochemistry
1993-1995 Huainan Normal University
Huainan, China

Publications

1. Tang Z, El Far O, Betz H, Scheschonka A. PIAS1 interaction and sumoylation of metabotropic glutamate receptor 8. J Biol Chem 280: 38153-38159.

2. Xu L, Sheng J, Tang Z, Wu X, Yu Y, Guo H, Shen Y, Zhou C, Paraoan L, Zhou J (2005) Cystatin C prevents degeneration of rat nigral dopaminergic neurons: in vitro and in vivo studies. *Neurobiol Dis* 18:152-165.
3. Guo H, Tang Z, Yu Y, Xu L, Jin G, Zhou J (2002) Apomorphine induces trophic factors that support fetal rat mesencephalic dopaminergic neurons in cultures. *Eur J Neurosci* 16:1861-1870.
4. Tang Z, Yu Y, Guo H, Zhou J (2002) Induction of tyrosine hydroxylase expression in rat fetal striatal precursor cells following transplantation. *Neurosci Lett* 324:13-16.
5. Shen Y, Yu Y, Guo H, Tang Z, Yu FS, Zhou J (2002) Identification and comparative analysis of differentially expressed proteins in rat striatum following 6-hydroxydopamine lesions of the nigrostriatal pathway: up-regulation of amyloid precursor-like protein 2 expression. *Eur J Neurosci* 16:896-906.
6. Xu H, Tang Z, Zhou C (2001) Schwann cells promote the survival and growth of cholinergic neurons both in co-culture and co-graft. *Chin J Neuroanat* 17:1-5.
7. Tang Z, Xu H, Zhou C (2000) Neurotrophic Effects of Primarily Cultured Schwann Cells Is Regulated By Their Interactions with Neural Cells. *Chin J Neurosci* 16: 228-231.
8. Zhou J, Shen Y, Tang Z, Xu L, Bradford HF, Yu Y (2000) Striatal extracts promote the survival and phenotypic expression of rat fetal dopaminergic neurons in vitro. *Neurosci Lett* 292:5-8.
9. Zhou J, Yu Y, Tang Z, Shen Y, Xu L (2000) Differential expression of mRNAs of GDNF family in the striatum following 6-OHDA-induced lesion. *Neuroreport* 11:3289-3293.